

**PEO/POLY(VINYL PHENOL-CO-STYRENE SULFONATE) AQUEOUS COMPLEX FORMATION**

By  
RONGJUAN CONG, M.S., B.S.

A Thesis  
Submitted to the School of Graduate Studies  
In Partial Fulfillment of the Requirements for the  
Degree of PhD

McMaster University  
©Copyright by Rongjuan Cong, May 2002

# **Aqueous PEO/Phenolic Polymer Complexes**

DOCTOR OF PHILOSOPHY (2002)

McMASTER UNIVERSITY

(Chemical Engineering)

Hamilton, Ontario, Canada

TITLE: PEO/poly(vinyl phenol-co-styrene sulfonate) aqueous complex  
formation

AUTHOR: Rongjuan Cong, M.S., B.S.

SUPERVISOR: Professor Robert H. Pelton

NUMBER OF PAGES: vii, 168

## **Abstract**

High molecular weight poly(ethylene oxide) (PEO) is an effective flocculant in the papermaking process. The performance of PEO can be greatly enhanced in the presence of second polymeric component. This second component is called cofactor in paper technology literature. In this thesis, poly(vinyl phenol-co-styrene sulfonate (PKS) is chosen as a model cofactor. The mechanism for complex formation between PEO and PKS, the transport properties of PEO/PKS complexes, the relationship between PEO/PKS complex formation and flocculation performance, and the effects of the surface properties of colloidal particles on flocculation are discussed. PEO mainly interacts with aromatic groups of PKS through hydrogen bonding and hydrophobic interactions. The widely proposed hydrogen bonding mechanism between phenolic hydroxyl group and ether oxygen is investigated by comparing the complex formation, flocculation performance between PEO/PKS and PEO/poly(styrene-co-styrene sulfonate). Phenolic content, salt, temperature and PEO molecular weight affect the complex formation and flocculation efficiency. A hydrophilic, sterically stabilized and negatively charged colloidal model, dextran sulfate modified precipitated calcium carbonate, is developed to mimic the solution properties of fillers in papermaking flocculation. This work gives a better understanding about PEO/cofactor flocculation mechanism.

## Acknowledgements

I am most grateful to Dr. Robert H. Pelton, my advisor. His encouragement and resourcefulness allowed me to stay with my family in Louisiana while working towards my degree.

My deepest thanks go to:

Dr. Paul S. Russo (Chemistry Department, Louisiana State University) for providing me a nice working environment in his lab, and constructive direction.

Mr. Doug Keller (the manager of Pulp and Paper Research Center, McMaster University) for generously offering his help.

Drs. Heather Sheardown, Alex Bain, Shiping Zhu, the committee members, for their support and productive discussions.

Dr. Truis Smith-Palm (Chemistry Department, St. Francis Xavier University), Dr. R. Ceuto (Chemistry Department, Louisiana State University), Dr. Dale Trevelon (College of Basic Science, Louisiana State University) for their critical discussions.

Mr. Shisei Goto (Nippon Paper Inc., Japan) for leading me to the entrance of the papermaking world.

Many thanks also go to my friends, Drs. Ju Zhang, Jin Zhang, Jun Liu, Xiaorong Zhao, Ms. Wei Chen, Mr. Chen Lu, Mr. Boxin Zhao in McMaster University, Ms. Sibel Turken, Mr. Garret Doucet and Ms. Nadia Edwin for sharing their care and friendship.

I wish to thank my parents for persistently reminding me of their dream on my career: "You can do it! You should do it!!"

Last but not least, I like to thank my husband Zhe and daughter Nijia, for their cheer and love that always keeping my spirit high.

## Table of contents

<b>ACKNOWLEDGEMENTS .....</b>	<b>III</b>
<b>ACKNOWLEDGEMENTS .....</b>	<b>IV</b>
<b>CHAPTER 1 INTRODUCTION .....</b>	<b>1</b>
<b>1. Conformation and complex formation in solid state .....</b>	<b>2</b>
<b>2. Properties of aqueous PEO solution.....</b>	<b>5</b>
<b>3. Background and objectives of this thesis .....</b>	<b>13</b>
<b>4. Outlines of this thesis .....</b>	<b>18</b>
<b>References.....</b>	<b>20</b>
<b>CHAPTER II BINDING MECHANISMS IN WATER-SOLUBLE POLY(VINYL PHENOL-CO-STYRENE SULFONATE) /POLY(ETHYLENE OXIDE) COMPLEXES .....</b>	<b>24</b>
<b>Abstract.....</b>	<b>24</b>
<b>Introduction.....</b>	<b>24</b>
<b>Introduction.....</b>	<b>25</b>
<b>Experimental .....</b>	<b>28</b>
<b>Results .....</b>	<b>32</b>

Discussion.....	39
Conclusions.....	41
References.....	53
<b>CHAPTER III FACTORS AFFECTING THE SIZE OF POLY(VINYL PHENOL-CO-STYRENE SULFONATE POTASSIUM SALT)/POLY(ETHYLENE OXIDE) COMPLEXES .....</b>	<b>55</b>
Abstract.....	55
Introduction.....	57
Experimental .....	61
Results .....	66
Discussion.....	74
Conclusions.....	79
<b>CHAPTER IV A MODEL COLLOID FOR FLOCCULANT TESTING ....</b>	<b>93</b>
Abstract.....	93
Introduction.....	94
Experimental .....	95
Results .....	101

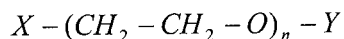
<b>Discussion.....</b>	<b>105</b>
<b>Conclusions.....</b>	<b>109</b>
<b>References.....</b>	<b>120</b>
<b>CHAPTER V THE INFLUENCE OF PEO/POLY (VINYL PHENOL-CO-STYRENE SULFONATE) AQUEOUS COMPLEX STRUCTURE ON FLOCCULATION .....</b>	<b>121</b>
<b>Abstract.....</b>	<b>121</b>
<b>Introduction.....</b>	<b>123</b>
<b>Experimental .....</b>	<b>126</b>
<b>Results .....</b>	<b>130</b>
<b>Discussion.....</b>	<b>139</b>
<b>Conclusions.....</b>	<b>146</b>
<b>References.....</b>	<b>163</b>
<b>CHAPTER VI CONCLUDING REMARKS.....</b>	<b>165</b>



## Chapter 1 Introduction

Water-soluble synthetic polymers have been widely used in waste-water treatment and papermaking processes. In this thesis, the mechanism of high molecular weight poly(ethylene oxide) as flocculant in papermaking is discussed.

Poly(ethylene oxide) (PEO or PEG) is a fascinating polymer. It is a crystalline, thermoplastic, water-soluble polymer with the general formula:



Polymers with molecular weight less than 6600 Dalton are generally called PEGs, although PEGs with molecular weight up to 20,000 Dalton are commercially available. PEGs have hydroxyl end groups because alcohol, ethylene glycol, or water is used as an initiator. By contrast, PEO is available in molecular weights ranging up to 10,000,000 Dalton. Both the patent and scientific literature contains thousands of applications and studies involving PEG and PEO. <sup>1</sup>

This chapter summarizes the solid state and solution properties of PEO, as well as the complex formation with phenolic compounds, peptides and proteins at microscopic and macroscopic levels. Then, the major unsolved problems in the study of PEO/cofactor flocculation mechanism, and the objectives of this thesis are introduced.

## ***1. Conformation and complex formation in solid state***

### *1.1 Conformation*

PEO crystallizes in a  $7/2$  helical conformation, that is, two helical turns per every 7 monomeric repeating units.<sup>1,2,3,4</sup> The  $7/2$  helix is constructed with a succession of *trans* (CCOC), *gauche* (OCCO) and *trans* (COCC) conformers along PEO chain. The degree of crystallinity in bulk is about 78%.<sup>5</sup>

### *1.2 Complex formation with phenolic compounds*

The widespread potential applications for solid polymer blends have led in recent years to an increased research effort in understanding and controlling polymer miscibility. The miscibility of PEO with various phenolic polymers at molecular level have been extensively discussed by Coleman et al..<sup>6</sup> The major results include: PEO is miscible with poly(vinyl phenol) (PVPh) or Novolac resin across the entire range of compositions.<sup>7,8</sup> IR and solid-state  $^{13}\text{C}$  NMR studies showed that the average strength of the intermolecular hydrogen bonding between hydroxyl groups of PVPh or Novolac resin and the ether oxygen of PEO is higher than the self-associated hydrogen-bonding in PVPh or Novolac resin.<sup>8,9,10,11</sup> The strong intermolecular interaction between PEO and phenolic hydroxyl group is widely accepted as the major reason for the miscibility of PEO/PVPh,<sup>8,10</sup> PEO/phenolic resin,<sup>12,13</sup> and for the complex formation between PEO and small aromatic compounds.<sup>14,15</sup>

### *1.3 Molecular structure of solid state PEO complexes*

An important feature of hydrogen bonding, compared with electrostatic or hydrophobic interactions, is that high electronegative elements (e.g., oxygen) and hydrogen atoms are involved. Furthermore, when oxygen acts as hydrogen bonding acceptor these atoms must be very close (i.e. <0.24 nm) with an appropriate angle of 107 degrees. These requirements constrain the complex formation. In some cases, only a portion of ether oxygens in PEO may be involved in complex formation. This phenomenon was called structural specificity by several groups.<sup>13,15</sup> Four molecular models predicting the structures for PEO/phenolic compounds complexes have been proposed.

McManus et al. measured the heat of interaction between PEO and simple phenolic compounds.<sup>15</sup> Resorcinol showed a much stronger interaction with PEO than catechol because two hydrogen-bonding sites of resorcinol cooperatively stabilized the establishment of an ordered helical structure of PEO.

Stack et al. used molecular modeling to simulate the complex structure for PEO/phenolic resin complexes in 1991.<sup>13</sup> It was proposed that PEO adopted a zigzag conformation. Structural specificity resulted in that every other ether oxygen forming hydrogen bonding with phenolic OH group.

Pelton et al. simulated the complex structures for PEO/PVPh oligomers in 1996. Molecular mechanics calculations of relative energies of PEO/PVPh complexes with varying hydrogen bonding sequences indicated that hydrogen bonding with adjacent or

alternating polyether oxygen along the PEO chain was less favorable than that for complexes with bonding of every fourth or fifth oxygen atom.<sup>16</sup>

Zhong et al. proposed that PEO adopted a zig-zag structure in Novolac resin/PEO complexes based on experimental results.<sup>8</sup> The frequency shift of hydroxyl absorption on IR spectrum was regarded as a measure of the strength of hydrogen bonding. The maximum shift was found when each phenolic OH group was surrounded by one ether oxygen.

Lannelli et al. reported in 1999 the structure for PEO/resorcinol complexes determined with X-ray diffraction technique.<sup>17</sup> Stable complexes were formed at PEO monomeric unit-to-resorcinol molecule ratio of 2:1. More interestingly, adding methyl group to resorcinol resulted in an increased distance between adjacent polymer layers.

The main conclusion is that due to the ordered structure of PEO in solid state, when PEO form molecular complexes with phenolic compounds, only part of the ether oxygen may be involved in hydrogen bonding, the presence of substituent groups on the phenolic ring may affect complex structures.

PEO also forms complexes with cations, e.g.,  $\text{Li}^+$ ,  $\text{K}^+$  or  $\text{Hg}^{2+}$  through the ion-dipolar interactions between ether oxygen and cationic ions.<sup>1,18,19</sup> The complex formation process disturbs the PEO ordered helix. Depending on PEO/salt mixing ratio, an amorphous, quite rubbery and elastic materials can be obtained.<sup>19,20,21,22,23</sup>

## ***2. Properties of aqueous PEO solution***

The properties of PEO in solution reflect the balance between hydrophobic ethylene group and hydrophilic ether oxygen. The hydrophilic oxygen in PEO results in a strong interaction between PEO and water.

PEO is soluble both in water and a number of common organic solvents such as acetonitrile, anisole, chloroform, ethylene dichloride and dimethylformamide. PEO has a reverse solubility in water, that is, PEO loses its solubility at elevated temperature above 100°C.<sup>1</sup> PEG depresses the freezing point of water<sup>24</sup> by forming a PEO-rich phase at a temperature as low as -15°C.<sup>46</sup>

The ordered helical structure of PEO in aqueous solution is largely lost at PEO concentrations of below 50 wt%, although the band at  $\sim 1060\text{ cm}^{-1}$  in the Raman spectrum indicated that the *tgt* conformation is present in aqueous solution, suggesting some retention of ordering.<sup>3</sup> Single molecule force spectroscopy indicates the existence of helical structure for PEO in water.<sup>25</sup> Nevertheless, the commonly accepted view is that PEO adopts random coil conformation in dilute aqueous solution.<sup>26,27</sup>

The hydrophilic oxygen in PEO results in a strong interaction between PEO and water. There are three different kinds of water molecules in PEO aqueous solution: hydration water (another name is bound water), interstitial water and bulk water.<sup>28</sup> This unique property makes PEO or PEG a widely used biocompatible water-soluble polymer, commonly used in the biomedical field.<sup>28,29</sup>

Because of its strong interaction with water, PEO coils in water are larger than those found for typical polymer coils in good solvents. For example, the radius gyration,  $R_g$ , of polystyrene sulfonate sodium salt Mw at  $10^6$  Dalton in 0.5 M NaCl solution is  $\sim 40$  nm,<sup>30</sup> while the same molecular weight PEO has a  $R_g$  of 67 nm. The unusually large size and long range of PEO coil-coil interactions in water are proposed due to the unusual ability of water molecules to "pack" so efficiently in the coil's interior that they swell PEO to a size substantially larger than would normally be possible in a solution where such solvent packing is not possible.<sup>26</sup>

### *2.1 Intrinsic aggregation*

The large coil size and strong long-range PEO-PEO attractions make high molecular weight PEO display drag reduction behavior.<sup>1,31</sup> On the other hand, the unusually large size of PEO coils in water causes difficulties when using light scattering technique to investigate PEO properties in solution. Extreme care must be paid to obtain true scattering from PEO to avoid the scattering from dust that can have particle sizes in the same range as PEO coils.

There have been reports about the existence of large-size PEO aggregates, commonly named as "slow-mode behavior" observed by dynamic light scattering at PEO concentration below/or higher than critical coil overlap concentration ( $C^*$ )<sup>32</sup>

$$C^* = \frac{2.5}{\eta} \quad (1)$$

$$[\eta] = 1.25 \times 10^{-5} [M_w]^{0.78} (m^3 kg^{-1}) \quad (2)$$

where  $[\eta]$  is intrinsic viscosity,<sup>1</sup>The light scattering behavior is often interpreted as the onset of semi-dilute behavior and/or aggregation (clustering).<sup>33,34,35,36</sup> On the other hand, it was proposed that PEO does not necessarily aggregate in aqueous solution.<sup>26,27,37,38</sup> The major arguments for the presence of impurities are:

1. The aggregation was related to the presence of an impurity at very low concentration level (several parts per million, ppm). The impurity can be collected within samples at the ppm level during the whole history of synthesis. It may be conveniently described as micro-droplets or compact microparticles, stabilized by adsorbed PEO chains, and increasingly soluble in methanol. Heptane, a model hydrophobic impurity, was deliberately added to impurity-free PEO solution. DLS elucidated that the effect of heptane on PEO dynamic light scattering was basically similar to PEO before proper filtering.<sup>37</sup>

2. The impurity was originated from the water. By using high quality water with reducing organic impurities as much as possible, with proper care, a well-behaved PEO solution was obtained. No obvious change in the size of PEO 17 months after being properly filtered with hydrophobic filter unambiguously indicated a long-time stability of PEO solution. Both static and dynamic light scattering measurement of single-chain behavior reveal that PEO with molecular weight  $10^{5-6}$  Dalton exhibits asymptotic good

solvent behavior. The size of PEO coil is proportional to  $M_w^{0.583}$ , close to the theoretical prediction of  $M_w^{0.6}$ .<sup>26</sup>

$$\begin{aligned} R_g &= 0.0215 M_w^{0.583 \pm 0.031} \text{ nm} \\ R_h &= 0.0145 M_w^{0.571 \pm 0.009} \text{ nm} \end{aligned} \quad (3)$$

## 2.2 Salt

PEO does not interact with cationic ions in water, which is quite different from the cases in solid state<sup>1,18,19</sup> or in methanol.<sup>39</sup> Salt addition can lower the phase separation temperature of PEO aqueous solution.<sup>40,41,42</sup> The phase separation temperature decreases linearly with salt concentration.<sup>1</sup> This salting-out process can be understood according to the Flory-Huggins model. An additive stabilizes the one-phase region if

$$-0.5 < \chi_{sa} - \chi_{pa} < 1.5 \quad (4)$$

where  $s$  denotes solvent,  $p$  is polymer and  $a$  is the additive and  $\chi$  is the interaction parameter.<sup>43</sup> The addition of the substances that are more polar than water, or less polar than PEO will decrease phase separation temperature.<sup>40</sup> Interestingly, the effectiveness of salt does not follow ionic strength principle.<sup>44</sup> In other words, the magnitude of the effect is not proportional to the charge of cationic ions. Instead, it is determined by the nature of the anions. Depending on the nature of anion and concentration, phase separation may occur at room temperature.<sup>1,40</sup> No obvious change in PEO hydrodynamic radius at KCl



concentration up to 0.1 M was observed.<sup>45</sup> This indicates that the effect on PEO coil size can be minor at moderate salt concentration up to 0.1 M KCl.

The properties of PEO solution are related to the molecular weight. The polydispersity increases up to 15~20 with the increase in molecular weight of PEO,<sup>1,36</sup> which is much broader than a random distribution with polydispersity at 2. As the molecular weight rises, PEO chain begins to fold in on itself, forming segment-segment interactions as it traps additional, more loosely bound water between the segments.<sup>46</sup> The number of the bound water molecules increases with the molecular weight of PEO.<sup>47</sup> Two water molecules bind with each repeating unit for PEG with molecular weight 600 Dalton; while the number of binding water molecules increased to 2.7 for PEG molecular weight 6000 Dalton. Thus, the complex formation of PEO with other compounds, such as aromatic polymers, is expected to be related to the molecular weight of PEO.

### *2.3 Aqueous PEO Complexes*

The complex formation between PEO and various water-soluble polymers have attracted great attention in the polymer science literature. For example, PEO binds strongly to some ionic surfactants such as sodium dodecyl sulfate.<sup>48</sup> Neutron scattering results suggest that the bound surfactant is present as micelles with the bound PEO segments concentrated amongst the sulfate head groups.<sup>49</sup> PEO forms aqueous complexes with poly(acrylic acid) and poly(methacrylic acid) at low pH where the protonated carboxylate groups hydrogen bond with the polyether oxygens on PEO.<sup>50, 51, 52, 53, 54, 55, 56</sup> The complex formation of PEO/poly(carboxylic acid) has been extensively

reviewed by Tsuchida and Abe in 1982.<sup>57</sup> The complex formation seems to be a cooperative process of weak hydrogen bonding and the minimum chain lengths of PEO for binding onto high molecular weight polymethacrylic and polyacrylic acid are 40 and 200, respectively. Complex formation in water is enhanced by raising the temperature suggesting a hydrophobic contribution.<sup>16</sup> Computer modeling of PAA and PEO oligomer showed a stereo-regularity, stoichiometric 1:1 complex could be formed only between atactic PAA and PEO.<sup>53</sup> A recent study also showed that PEO forms complexes with poly(vinyl alcohol)(PVA) and polyacrylamide (PAM) based on viscosity measurements. PVA/PEO or PAM/PEO complexes were more shear-sensitive than PEO itself. The interaction was presumed to be mainly driven by hydrogen bonding with ether oxygen of PEO without experimental proof.<sup>58</sup>

Recent studies showed that PEO formed water-soluble complexes with various peptides and proteins. The knowledge and techniques used to study the complex formation between PEO and biopolymers were very helpful for this thesis. Thus, the complex formation of PEO with biopolymers is summarized below.

#### *2.4 PEO complex formation with peptides*

In a broader context, PEO is not a strongly interacting polymer. Indeed, its inertness explains its popularity as a surface treatment for biocompatibility<sup>29</sup> and as the hydrophilic component of nonionic surfactants.<sup>48</sup> PEG or PEO is widely used in modification of biomedical surfaces. Both the amount of protein adsorption and the magnitude of other biochemical events, such as platelet adhesion, rapidly decline as the

PEG molecular weight rises. This decline is most apparent at molecular weights up to 1000, after which the biointeractions gradually level out.<sup>29</sup>

Nevertheless, recent studies showed that PEO forms complexes with poly( $\alpha$ , L-glutamate)<sup>59</sup> and poly(L-lysine).<sup>60</sup> The interaction sites were proposed to be the hydrophobic interaction between ethylene group of PEO and  $\gamma$ -CH<sub>2</sub>-of poly( $\alpha$ , L-glutamate)<sup>60</sup> or  $\gamma$ -CH<sub>2</sub> of poly(L-lysine),<sup>60</sup> and ion dipolar interaction between ether oxygen—Na<sup>+</sup>.<sup>59</sup> The amount of sodium ion involved in the ion dipole interaction sites and the number of contact points interacting through hydrophobic interactions were reduced significantly or diminished in dilution solutions both for aqueous and nonaqueous cases. The complex formation resulted in a change in the conformation of poly( $\alpha$ , L- glutamate),<sup>59</sup> poly( $\beta$ -benzyl L-asparatate) segment and poly(L-lysine)<sup>60</sup> from extended conformation to more compact helical conformation.

### *2.5 PEO complex formation with proteins*

Dubin et al. investigated the water-soluble complexes of PEO (14,000 to 19,800 Dalton) with human serum albumin (absolute molecular weight of 66, 436 Dalton with 98 carboxyl and 18 phenolic OH),<sup>45,61</sup> and pepsin (absolute molecular weight of 34,542 Dalton with 43 carboxyl and 16 phenolic OH)<sup>62</sup> at macroscopic levels with light scattering techniques. Interestingly, flexible PEO chains did not adsorb and flatten on the surface of human serum albumin or pepsin globules in a similar way as the adsorption of PEO on spherical polystyrene latex.<sup>63,64,65</sup> Instead, cooperative complex formation was

proposed, in which several human serum albumin or pepsin globules bind with each PEO chain. Complexes seem to have a conformation like a necklace. An extended structure of PEO/ human serum albumin complexes appeared to be due to “steric” rather than “electrostatic” repulsion among charged PEO-bound human serum albumin globules. The size of the complexes increased with PEO molecular weight, but decreased with ionic strength. Hydrogen bonding between carboxylic /or phenolic OH and ether oxygen of PEO was attributed to the complex formation at acidic condition,<sup>45,62</sup> while the hydrogen bonding between basic NH<sub>2</sub> groups and ether oxygen of PEO caused the complex formation at pH 8.<sup>45</sup>

In summary, PEO adopts a helical structure in the solid state and forms hydrogen bonds with phenolic polymers. In aqueous solution, due to hydrophilic oxygen part, PEO interacts strongly with water by forming unusually large random coils. Although hydrogen bonding has been widely accepted as a major driving force for the complex formation between PEO and poly(carboxylic acid), it is not obvious that hydrogen bonding should occur between PEO and phenolic groups in water. Compared with water, the PEO oxygen atoms should be rather weak hydrogen bond acceptors. Besides, the interactions between PEO and peptide suggest that hydrophobic interactions between aromatic rings and ethylene groups of PEO may be the major driving force for the complex formation between PEO and peptide.

### ***3. Background and objectives of this thesis***

#### *3.1 Background*

Our interest in PEO/aromatic compound complexes is because very high molecular weight PEO (i.e., 2,000,000 Dalton) is an effective flocculant for the papermaking process when mixed with water-borne phenolic polymers. In the paper technology literature the phenolic polymers are called cofactors.<sup>66, 67, 68</sup> A variety of polymers act as cofactors by aiding colloidal flocculation by complex formation with PEO. These include phenolic resins,<sup>1, 69, 70</sup> tannic acid,<sup>71</sup> lignin derivatives,<sup>72</sup> calixarenes,<sup>73</sup> poly(vinylphenol).<sup>16, 74</sup> Except for poly (sodium naphthalene sulphonate),<sup>5</sup> all the other cofactors contain phenolic groups in their structures. The reason for that is unclear.

There is much circumstantial evidence suggesting that PEO forms complexes with phenolic compounds both in the bulk<sup>8, 10, 11, 14</sup> and in aqueous solution.<sup>13, 77</sup> Hydrogen bonding between phenolic OH and polyether oxygen has been proposed by many researchers to be the main driving force for the complex formation.<sup>6, 13, 16</sup> On the other hand, hydrogen bonding seems not the only reason for phenolic polymers to work as effective cofactors, as there are polymers forming complexes with PEO through hydrogen bonding but do not enhance PEO flocculation performance, e.g. PAA and PMAA.<sup>75</sup>

Stack et al. compared the behavior of PEO complex formation with Resoles and Novolacs, They proposed that hydrophobic interaction between the hemiformyl groups of

Resoles and ethylene groups of PEO chains may be another factor for the complex formation of PEO with aromatic cofactors.<sup>76</sup>

Most of flocculation mechanisms have been proposed on the basis of the complex formation.<sup>6, 64, 75, 77</sup> Therefore, complex structure at a large size scale may provide valuable information for a better understanding about PEO and for a further development of the application of PEO.

The majority of PEO/cofactor complexes readily phase separate from aqueous solution. Therefore, many difficulties arise in the characterization of an intrapolymer or interpolymer PEO/cofactor complex by means of light scattering techniques. Hydrophilic phenolic polymers form gel when mixed with PEO. Examples include poly(vinyl phenol-co-styrene sulfonate sodium salt),<sup>78</sup> poly(vinyl phenol-co-acrylate sodium salt)<sup>79</sup> and modified phenol-formaldehyde or poly (sodium naphthalene) in the absence of salt.

Carignan et al. pioneered the use of dynamic light scattering to estimate the size of aqueous complexes formed between PEO and modified phenol-formaldehyde resin or poly (sodium naphthalene) in the absence of salt.<sup>70</sup> They found that modified phenol-formaldehyde resin or poly (sodium naphthalene) promoted the aggregation of PEO chains, however, the apparent hydrodynamic radius of PEO contracted upon forming complexes, the extent of shrinkage depended on the structure of cofactors.

The relationship between PEO/cofactor complex formation and the PEO flocculation mechanism have been investigated by using well-defined, highly

hydrophobic and negatively charged polystyrene latex<sup>6,77</sup> and positively charged precipitated calcium carbonate (PCC)<sup>80</sup>. The reality is that mechanical pulping processes produce high concentrations of a mixture of dissolved and colloidal substances in the pulp suspension. Dissolved and colloidal substances (DCS) are sometimes referred to as anionic trash, mostly because of high cationic demand.<sup>81, 82, 83</sup> Some of them interfere with the flocculation of fillers, for example by adsorbing onto the filler surfaces. This changes the surface properties of the particles involved, sterically stabilizing them and making them more difficult to be flocculated. Research using these colloidal models is invaluable for determining mechanisms, but has a very limited ability to predict the behavior of retention aids in commercial mechanical pulp suspensions.

In order to narrow the gap between the laboratory and the commercial process, some research groups have used mill water containing dissolved colloidal substance to dilute fillers.<sup>84</sup> Although effective, white waters are continuously changing in composition so it is impossible to compare results from day to day. Therefore, there is a need for a more realistic colloidal model for flocculation studies.

### *3.2 Objectives of this thesis*

The work described in this thesis aims at a better understanding of the PEO/cofactor flocculation mechanisms both at microscopic and macroscopic levels. The specific objectives are:

1. **To specify the major interaction sites when PEO complexes with a cofactor.** The requirement of aromatic groups in cofactor structures, especially in most cases, the requirement of phenolic hydroxyl groups, may suggest a connection with hydrogen bonding. Poly(vinyl phenol-co-styrene sulfonate) (PKS) was chosen as a model cofactor to study the complex formation with PEO. With high resolution NMR techniques, the interaction between PKS and PEO at very low concentration (several parts per million, close to the concentrations used in PEO/cofactor flocculation) was studied.
2. **To determine the importance of hydrogen bonding in PEO/cofactor complex formation by using  $^1\text{H}$  and  $^{13}\text{C}$  NMR measurements as functions of pH and temperature.**
3. **To explore the mechanism for the complex formation in the absence of hydrogen bonding.** Poly(styrene-co-styrene sulfonate) (PS-co-SSS) was employed as a model cofactor. In this case, hydrogen bonding with PEO was impossible. Comparison between PS-co-SSS/PEO complex formation and PKS/PEO complex formation provided information about the role of hydrogen bonding and the requirement for aromatic groups in cofactors.
4. **To investigate the role of cationic ions in complex formation by using multiple-quantum filtered  $^{23}\text{Na}$  NMR.**



5. **To study the effect of PEO molecular weight on complex formation.**

Molecular weight of PEO affects the interaction between PEO and water.

Only very high molecular weight PEO is an effective flocculant.

Fluorescence photobleaching recovery and viscosity measurements were used to investigate the effect of PEO molecular weight on the size and shear-sensitiveness of formed complexes.

6. **To determine the effect of salt addition on viscosity of the complexes.**

van de Van et al. proposed that PEO chain expanded upon forming complexes with cofactors, and the complexes may behave like polyelectrolytes.<sup>5</sup> By investigating the effect of salt on viscosity, the difference between usual synthetic polyelectrolytes and PEO/PKS complexes were determined.

7. **To develop a realistic colloidal model for flocculation.**

In order to narrow the gap between lab fundamental research and real flocculation in the papermaking process, an ideal colloidal model is hydrophilic, negatively charged, electro-sterically stabilized, easily prepared, and contains adjustable amounts of anionic substances to mimic the contaminants in a range of pulp suspensions

8. **To link the hydrogen bonding with flocculation efficiency.**

By using PKS and hydroxyl-free PS-co-SSS as cofactors, the role of hydrogen bonding on flocculation efficiency is addressed.

9. **To explore the relationships between the complex formation and flocculation efficiency.** Flocculation at different ionic strength, PEO/cofactors with various phenolic content, and temperature was evaluated.
  
10. **To evaluate the effect of properties of colloidal particles on flocculation performance.** Four different types of colloidal particles, positively charged precipitated calcium carbonate (PCC), negatively charged PCC treated with dextran sulfate, hydrophobic polystyrene latex and poly (N-isopropylacrylamide) grafted polystyrene latex were chosen as colloidal targets. The effects of surface-charge sign, hydrophobicity and the presence of  $\text{Ca}^{2+}$  are examined.

#### ***4. Outlines of this thesis***

There are four parts in this thesis prepared as manuscripts for publication. The contents of each chapter are briefly described as follows:

Chapter II discusses the mechanism of PEO/PKS complexes at microscopic level probed by various NMR techniques. In addition to the widely proposed hydrogen bonding between phenolic OH and ether oxygen, the hydrophobic interaction between aromatic rings of phenolic polymers and ethylene group of PEO is proposed to be another important driving force for complex formation. This chapter has accepted by *Colloid and*

*Polymer Science* for publication. Some of the results were published in *Journal of Polymer Science*, 38, 1276 (2000)

Chapter III investigates PEO/ PKS complex formation at macroscopic level by fluorescence photobleaching recovery (FPR) and diffusion-ordered NMR. Effects of temperature, ionic strength, mixing ratio of PKS/PEO, PEO molecular weight and phenolic molar content of PKS on the transport properties of PEO/PKS complexes are discussed. This chapter was submitted for publication in *Macromolecules*.

Chapter IV describes the characterization of the surface properties of a new colloidal model produced by the adsorption of dextran sulfate (DS) onto PCC, and the flocculation behavior of the model system with a variety of flocculants. This well-defined new model is shown to have similar surface properties to PCC suspended in actual pulp furnish. This chapter was published in *Journal of Pulp Paper Science* 27, 379 (2001).

Chapter V reports the result of a series of flocculation experiments using PKS/PEO and PS-co-SSS/PEO as flocculants. Flocculation was measured as a function of temperature and ionic strength to extract the relationships between cofactor/PEO size and flocculation performance. This chapter was submitted for publication in *Journal of Colloid and Interfacial Science*.

## References

---

- <sup>1</sup> Bailey, F.E.; Koleske, J.V. Poly (ethylene oxide), Academic Press, New York, **1976**.
- <sup>2</sup> Yang, R.; Yang, X.P.; Evans, D.F.; Hendrickson, W.A.; Baker, J. *J. Phys. Chem.*, **1990**, *94*, 6123
- <sup>3</sup> Maxfield, J.; Shepherd, I.W. *Polymer* **1975**, *16*, 505.
- <sup>4</sup> Jaeger, R.; Schoenherr, H. and Vancso, G.J. *Macromolecules*, **1996**, *29*, 7634.
- <sup>5</sup> Pedrosa P.; Pomposo, J.A.; Calahorra, E.; Cortazar, M. *Polymer* **1995**, *36*, 3889.
- <sup>6</sup> Coleman, M.M.; Graf, J.F.; Painter, P.C. Specific interactions and the miscibility of polymer blends, Technomic Publishing Company, Lancaster, PA, 1991.
- <sup>7</sup> Jack, K.S.; Whittaker, A. K. *Macromolecules* **1997**, *30*, 3560.
- <sup>8</sup> Zhong, Z.; Guo, Q. *J. Poly. Sci. Part A* **1998**, *36*, 401.
- <sup>9</sup> Moskala, E.E.J.; Varnell, D.F.; Coleman, M.M. *Polymer* **1985**, *26*, 228.
- <sup>10</sup> Zhang, X.; Takegoshi, K.; Hikichi, K. *Macromolecules* **1992**, *25*, 2336.
- <sup>11</sup> Zhang, X.; Takegoshi, K.; Hikichi, K. *Macromolecules* **1993**, *26*, 2198.
- <sup>12</sup> Stack, K.R.; Dunn, L.A.; Roberts, N.K. *Appita* **1990**, *43*, 125.
- <sup>13</sup> Stack K.R.; Dunn, L.A.; Roberts, N.K. *Colloids and Surfaces* **1991**, *61*, 205.
- <sup>14</sup> Point, J.J.; Damman, P. *Macromolecules* **1991**, *24*, 2019.
- <sup>15</sup> McManus, J.P.; Davis, K.G.; Beart, J.E.; Gaffney, S.H; Lilley, H.T; Haslam, E. *J. Chem. Soc. Perkin Trans. II* , **1985**, 1429.
- <sup>16</sup> Pelton ,R.H.; Xiao, H.; Brook, M.A.; Hamielec, A. *Langmuir* **1996**, *12*, 5756.
- <sup>17</sup> Lannelli, P.; Dosiere, M.; Moulin, J.F. *Macromolecules* **1999**, *32*, 2293.
- <sup>18</sup> Videira, A.L.L.; Carlos, L.D. *J. Chem. Phys.* **1996**, *105*, 8878.
- <sup>19</sup> MacGlashan, G.S.; Andreev, Y.G.; Bruce, P.G. *Nature*, **1999**, *398*, 792.
- <sup>20</sup> Lundberg, R.D.; Bailey, F.E.; Callard, R.W. *J. Polym. Sci*, **1966**, *4*, 1563.
- <sup>21</sup> Li, J; Pratt, L.M.; Khan, I.M. *J. Poly. Sci: Part A*. **1995**, *33*, 1657.
- <sup>22</sup> Blumberg, A. A.; Pollack, S.S. *J. Poly. Sci. Part A* **1964**, *2*, 2499.
- <sup>23</sup> Wright, P.V. *J. Mater. Chem.*, **1995**, *5*, 1275.
- <sup>24</sup> Hager, S.L.; Macrury, T.B. *J. Appl. Poly Sci*, **1980**, *25*, 1559.

- 
- <sup>25</sup> Oesterhelt, R.; Rief, M.; Gaub, H.E. *New J. Phy.* **1999**, *1998*, 1.
- <sup>26</sup> Devanand, K.; Selser, J.C. *Macromolecules* **1991**, *24*, 5943.
- <sup>27</sup> Devanand, K.; Selser, J.C. *Nature* **1990**, *343*, 739.
- <sup>28</sup> Kitano, H.; Sudo, K.; Ichikawa, K.; Ide, M.; Ishihara, K. *J. Phys. Chem.* **2000**, *104*, 11425.
- <sup>29</sup> Harris, J.M. *Poly(ethylene Glycol) Chemistry: Biotechnical and Biomedical Applications*; Plenum Press: New York, **1992**
- <sup>30</sup> Borochoy, N.; Eisenberg, H. *Macromolecules*, **1994**, *27*, 1440.
- <sup>31</sup> Cowan, M.E.; Hester, R.D.; McCormick, C.L. *J Appl. Poly Sci* **2001**, *82*, 1211.
- <sup>32</sup> Brown, W.; Stilbs, P.; Johnsen, R.M. *J. Poly. Sci. Polym Phys* **1983**, *21*, 1029.
- <sup>33</sup> Brown, W. *Macromolecules* **1984**, *17*, 66.
- <sup>34</sup> Zhou, P; Brown, W. *Macromolecules* **1990**, *23*, 1131.
- <sup>35</sup> Duval, M. *Macromolecules* **2000**, *33*, 7862.
- <sup>36</sup> Polverari, M.; van de Ven, T.G.M. *J. Phys. Chem.* **1996**, *100*, 13687.
- <sup>37</sup> Porsch, B.; Sundelöf, L.O. *Macromolecules* **1995**, *28*, 7265.
- <sup>38</sup> Kinugasa, S.; Nakahara, H.; Fudagawa, N.; Koga, Y. *Macromolecules* **1994**, *27*, 6889.
- <sup>39</sup> Ono, K.; Honda, H.; Murakami, K. *J. Macromol. Sci., Chem.* **1998**, *A26*, 567.
- <sup>40</sup> Kenkare, P.U.; Hall, C.L.K. *AIChE J.* **1996**, *42*, 3508.
- <sup>41</sup> Khoultaev, K.H.; Kerekes, R.J.; Englezos, P. *AIChE J.* **1997**, *43*, 2353.
- <sup>42</sup> Pang, P.; Englezos, P. *Fluid Phase Equil.* **2002**, *194-197*, 1059.
- <sup>43</sup> Johansson, H.; Karlström, G.; Tjerneld, F. *Macromolecules*, **1993**, *26*, 4478.
- <sup>44</sup> Harned, H. S.; Owen, B. *The Physical Chemistry of Electrolytic Solutions*, ACS series, Reinhold Publishing Corp.; New York, **1958**, PP 80.
- <sup>45</sup> Azegami, S.; Tsuboi, A.; Izumi, T.; Hirata, M.; Dubin, P.L.; Wang, B.; Kokufuta, E. *Langmuir* **1999**, *15*, 940.
- <sup>46</sup> Antonsen, K.P.; Hoffman In, A.S. *Poly(ethylene glycol) Chemistry. Biotechnical and Biomedical Applications*; Harris, J.M., Ed.; Plenum Press: New York and London, **1992**; pp 15.
- <sup>47</sup> Tilcock, C. P. S.; Fisher, D. *Biochim Biophys Acta*, **1982**, *688*, 645.
- <sup>48</sup> Goddard, E. D. *Colloids Surf.* **1986**, *19*, 255.

- 
- <sup>49</sup> Cabane, B.; Duplessix, R. *J. Phys.* **1982**, *43*, 1529.
- <sup>50</sup> Tsuchida, E.; Osada, Y.; Ohno, H. *J. Macromol. Sci.-Phy.* **1980**, *B17*, 683.
- <sup>51</sup> Bailey, F. E.; Lundberg, R. D.; Callard, R.W. *J. Polym. Sci. Part A* **1964**, *2*, 845.
- <sup>52</sup> Iliopoulos, I.; Halary, J. H.; Audebert, R. *J. Polym. Sci. Part A*: **1988**, *26*, 275.
- <sup>53</sup> Iliopoulos, I.; Audebert, R. *Macromolecules* **1991**, *24*, 2566.
- <sup>54</sup> Smith, L.; Winslow, A. E.; Petersen, D.E. *Ind. Eng. Chem.* **1959**, *51*, 1361.
- <sup>55</sup> Osada, Y.; Sato, M. *Polym. Lett. Edi.* **1976**, *14*, 129.
- <sup>56</sup> Miyoshi, T.; Takegoshi, K.; Hikichi, K. *Polymer* **1997**, *38*, 2315.
- <sup>57</sup> Tsuchida, E.; Abe, K. *Adv. Polym. Sci.* **1982**, *45*, 2.
- <sup>58</sup> Dan, Y.; Chen, S.Y.; Zhang, Y.F.; Xiang, F.R. *J. Polym. Sci. Part B*. **2000**, *38*, 1069.
- <sup>59</sup> Pemawansa, K. P.; Thakur, A.; Karikari, E. K.; Khan, I. M. *Macromolecules* **1999**, *32*, 1910.
- <sup>60</sup> Harada, A.; Cammas, S.; Kataoka, K. *Macromolecules* **1996**, *29*, 6183.
- <sup>61</sup> Xia, J.; Dubin, P. L. *Macromolecules* **1993**, *26*, 6688.
- <sup>62</sup> Kokufuta, E. *Polym. Bull.*, **1991**, *26*, 277.
- <sup>63</sup> Couture, L.; van de Ven, T.G.M. *Colloid. Surfaces* **1991**, *54*, 260.
- <sup>64</sup> van de Ven, T.G.M. *Advances in Colloid and Interface Science* **1994**, *48*, 121.
- <sup>65</sup> Lu, C.; Pelton, R.H. *Langmuir* **2001** *17*, 7770.
- <sup>66</sup> Carrard, J. P.; Pummer, H. *US Patent* 4,070,236, **1975**.
- <sup>67</sup> Pelton, R.H., Allen, L.H.; Nugent, H.M. *Tappi* **1981**, *64*, 89.
- <sup>68</sup> Gibbs, A.; Pelton, R. H.; Cong, R. *Colloids Surf.* **1999**, *159*, 31.
- <sup>69</sup> Stockwell, J. O. *WO Patent* 95/21296, **1995**
- <sup>70</sup> Carignan, A.; Garnier, G.; van de Ven, T. G. M. *J. Pulp Paper Sci* **1998**, *24*, 94.
- <sup>71</sup> Lindström, T.; Glad-Nordmark, G. *Colloids Surfaces* **1984**, *8*, 337.
- <sup>72</sup> Pelton, R.H.; Allen, L.; Nugent, H. *US Patent* 4,313,790, **1980**.
- <sup>73</sup> Goto, S.; Miyanishi, T.; Pelton, R.H. *Nord. Pulp Pap. Res. J.* **2000**, *15*, 395.
- <sup>74</sup> Ech, E. *US Patent* 5,472,570, **1995**
- <sup>75</sup> Xiao, H.; Pelton, R.H.; Hamielec, A. *J. Pulp Paper Sci.* **1996**, *22*, J475.
- <sup>76</sup> Stack, K.R., Dunn, L.A.; Roberts, R.K. *J. Wood Chem. Tech.* **1993**, *13*, 283.

- 
- <sup>77</sup> van de Ven, T.G.M. ; Allice, B. *J. Pulp Paper Sci.* **1996**, *22*, J257.
- <sup>78</sup> Cong, R.; Bain, A. D.; Pelton, R.H. *J. Poly .Sci. Part B* **2000**, *38*, 1276.
- <sup>79</sup> Gibbs, A.; Zhou, Y.; Xiao, H.; Pelton, R.H. *Transactions of the 11th fundamental research symposium in papermaking*. C.F.Baker. 2, 1135, **1997** Cambridge, UK.
- <sup>80</sup> Gibbs, A.; Xiao, H.; Pelton, R. H. *Tappi J.* **1997**, *80*, 163.
- <sup>81</sup> Penniman, J. G. *Pap. Trade J.* **1978**, April, 36.
- <sup>82</sup> Pelton, R. H.; Allen, L. H.; Nugent, H. M. *Svensk Papperstidning*, **1980**, *83*, 251.
- <sup>83</sup> Sundberg, K.; Thornton, J.; Holmbom, B.; Ekman, R. *J. Pulp Paper Sci*, **1996**, *22*, ssJ226.
- <sup>84</sup> Allen, L.; Polverari, M.; Levesque, B.; Francis, W. *Tappi J.* **1999**, *82*,188.

## **Chapter II Binding Mechanisms in Water-soluble Poly(vinyl phenol-co-styrene sulfonate) /poly(ethylene oxide) Complexes**

### ***Abstract***

Macromolecular complexes of poly (vinyl phenol-co-styrene sulfonate) (PKS) /poly(ethylene oxide) (PEO) in aqueous solution were studied by multiple quantum filtered (MQF)  $^{23}\text{Na}$  NMR and  $^1\text{H}$  NMR. The upfield shift of  $^1\text{H}$  chemical shift for PEO ethylene group and the existence of strong NOE cross peaks between aromatic rings of PKS and ethylene proton of PEO indicated that aromatic rings interacted with the PEO ethylene groups. Temperature sensitivities were consistent with hydrophobic interactions.

It was concluded that hydrogen bonding was not necessary for complex formation because the spectra of poly(styrene-co-styrene sulfonate) (PS-co-SSS) /PEO mixtures revealed complexes with structures similar to those formed with the phenolic copolymers. Also, complex formation was observed with PKS/PEO at pH 12 where there should be few phenolic protons available for hydrogen bond formation. PKS/PEO complex gave a MQF  $^{23}\text{Na}$  signal whereas PKS or PEO alone did not. It is postulated that this reflects a collapse in the PKS conformation upon complex formation.



## *Introduction*

This chapter describes the results of a NMR investigation of the binding mechanisms in aqueous complexes of high molecular weight, polyethylene oxide (PEO) and poly(vinylphenol-co-potassium styrene sulfonate) (PKS). Our interest in these complexes is because very high molecular weight PEO is an effective flocculant for the papermaking process when mixed with water-borne phenolic polymers. In the paper technology literature the phenolic polymers are called cofactors.<sup>1,2,3</sup> In addition to PKS, a variety of polymers act as cofactors by aiding colloidal flocculation by complex formation with PEO. These include phenolic resins,<sup>1,4,5</sup> tannic acid,<sup>6</sup> lignin derivatives<sup>7</sup>, calixarenes,<sup>8</sup> poly(vinylphenol).<sup>9,10</sup> Since the presence of phenolic groups is a common feature in these cofactor structures, it is widely proposed in literature that hydrogen bonding between phenolic hydroxyl and polyether oxygens is the driving force for PEO/cofactor complex formation.<sup>5,6,11</sup> Our results presented herein suggest that hydrogen bonding is not the sole bonding mechanism for these complexes.

In general, aqueous PEO is not a strongly interacting polymer. Indeed, PEO has been referred “gold standard” in the surface treatment for biocompatibility.<sup>12</sup> Nevertheless, there are classic examples of aqueous PEO complexes.<sup>13</sup> For example, PEO strongly binds to some ionic surfactants such as sodium dodecyl sulfate.<sup>14</sup> Neutron scattering results suggests that the bound surfactant is present as micelles with the bound PEO segments concentrated amongst the sulfate head groups.<sup>15</sup>

PEO also forms aqueous complexes with poly(acrylic acid) and poly(methacrylic acid) at low pH where the protonated carboxylate groups hydrogen bond with the polyether oxygens on PEO.<sup>16, 17, 18, 19, 20, 21, 22</sup> This complex formation seems to be a cooperative process and the minimum chain lengths of PEO for binding onto high molecular weight polymethacrylic and polyacrylic acid are 40 and 200 respectively.<sup>23</sup> Complex formation in water is enhanced by raising temperature, suggesting a hydrophobic contribution.<sup>16</sup>

PEO forms complexes with some proteins including pepsin<sup>24, 25</sup> and human serum albumin.<sup>26</sup> It is generally accepted that hydrogen bonding is the main complex formation interaction between proteins and PEO although there is little direct evidence.

Perhaps the most structural information has come from studies of PEO interactions with simple polypeptides and their block copolymers. 2D NOESY NMR has proven to be particularly powerful at predicting the local environment for complexed PEO segments. Harada et al. have shown that some PEO segments in poly(L-lysine-block-PEO) are closely associated with side chain methylene groups on lysine suggesting hydrophobic interactions.<sup>27</sup> NOESY has also revealed that in PEO/poly( $\alpha$ ,L-glutamate),<sup>28</sup> bound PEO protons interacted with  $\gamma$ -CH<sub>2</sub> on the peptide. Thus, although hydrogen bonding seems to be the primary driving force for complex formation in water, hydrophobic interactions may also be important.

Unlike PEO/surfactant or PEO/polyacid complexes, the interaction mechanisms in PEO/cofactor complexes are not fully elucidated. The commercially important

phenolic resins are polydisperse in structure and molecular weight and thus are difficult to characterize. Stack and coworkers studied complex formation between PEO and water-borne phenolic resins.<sup>29</sup> They showed that low molecular weight resins did not form complexes – the critical molecular weight for complex formation was between 500 and 3000 Da. Elementary molecular mechanics calculations indicated that, unlike PEO complexes with polyacid, PEO complex formation with phenolic polymers is restricted by the difficulty in obtaining a high degree of registration between PEO ether oxygens and phenolic hydroxyls.<sup>9</sup>

A number of flocculation studies have given indirect information about the PEO/cofactor structure. The optimum cofactor to PEO ratio for flocculation is close to 1:1 (wt/wt) for a wide variety of cofactor structures. Flocculation is less efficient at alkaline pH whereas it is rather insensitive to ionic strength.<sup>30</sup> Complexes formed with hydrophobic cofactors undergo coacervation, a process which competes with flocculation when colloids are present. Finally, PEO/cofactor/calcium carbonate flocs show substantial elasticity, suggesting the complex is a crosslinked network.<sup>31</sup>

In this work we report the properties of aqueous mixtures of high molecular weight PEO and well-defined phenolic polymers. Emphasized is the nature of the interactions between complexing polymer segments. This work follows an initial study which showed that PKS-type molecules are effective flocculant cofactors<sup>33</sup> and that NMR and particularly NOESY gives structural information about PEO/cofactor complexes.<sup>32</sup>

## ***Experimental***

### *Materials*

PEO (Polyox 309 and 303) with MW  $8 \times 10^6$  Da and  $7 \times 10^6$  Da were gifts from Union Carbide Corp. Styrene, 3-(trimethylsilyl) propionic 2,2,3,3-d<sub>4</sub> sodium salt (TSP), bovine serum albumin, sodium 4-styrene sulfonate were purchased from Sigma-Aldrich. Deuterium oxide (D<sub>2</sub>O) and dimethyl-d<sub>6</sub> sulfoxide (DMSO-d<sub>6</sub>) were purchased from Cambridge Isotope Laboratories. 2,2'-Azobis-(2-methylpropanenitrile) (VAZO-64) was purchased from Dupont. Poly (styrene sulfonate sodium salt) with MW  $7 \times 10^4$  Da was purchased from Scientific Polymer Products, Inc. Except for styrene that was purified by vacuum distillation; all the other materials were used as received.

### *Synthesis of poly(vinyl phenol-co-potassium styrene sulfonate) (PKS)*

PKS with phenolic molar content 0.48 was synthesized by free radical polymerization of 4-acetoxystyrene with sodium 4-styrene sulfonate followed by extensive hydrolysis in 1M KOH solution.<sup>33</sup> The detailed procedure for purification and characterization was reported previously.<sup>32</sup> The weight-averaged molecular weight was  $158,000 \pm 5000$  and the polydispersity =  $1.6 \pm 0.1$ . Details about MW measurement are given below.

### *Molecular weight measurement of PKS*

The molecular weight distribution was obtained by GPC/LS using a Waters 401 differential refractive index detector and light scattering detectors (at 16 different angles, wavelength 632.8 nm). For this, the specific refractive index increment,  $dn/dc$ , for PKS in water was measured at 23.0°C with a Brice-Phoenix differential refractometer which was calibrated by 5 standard KCl aqueous solutions.<sup>34</sup> The measurement was performed at three different wavelengths ( $\lambda$ ), 589 nm, 514.4 nm and 488 nm. The  $dn/dc$  value at 632.8 nm was 0.172 ml/g which was extrapolated from the linear relationship between  $dn/dc$  with  $\lambda^{-2}$  (correlation constant  $R= 0.999$ ). The GPC column used was PL aquagel-OH mixed 8  $\mu\text{m}$ . Water was used as solvent with a flow rate of 0.5 ml/min. The injection volume was 0.050 ml. The standard deviation of the weight average molecular weight was calculated from five duplicate measurements.

### *Synthesis of poly(styrene-co-styrene sulfonate) sodium salt (PS-co-SSS)*

The free radical copolymerization of styrene with sodium 4-styrene sulfonate in dimethylsulfoxide (DMSO) was reported in the early 1950's in the preparation of ion exchange resins.<sup>35,36</sup> However, the early recipes gave irreproducible results of the adsorption of polar sodium 4-styrene sulfonate, in varying amounts, on the precipitating copolymer PS-co-SSS, especially at low styrene feed ratio.<sup>36</sup> In order to circumvent this problem, DMSO/methanol solvent mixtures were employed.

Into a 250 mL 3-necked round-bottomed flask at room temperature were added 6.05g distilled styrene and 8.0 g sodium 4-styrene sulfonate (styrene/sodium 4-styrene sulfonate (molar ratio) =3:2), 0.070 g VAZO-64, 40.0 g DMSO and 5.0 g methanol. The contents were purged with ultra pure nitrogen and temperature was gradually increased to 70°C. After 24 hours the reaction was cooled and the product was precipitated with acetone and ice water. The precipitated PS-co-SSS was completely re-dissolved in water at 60°C. The product was extensively dialyzed against milli-Q water for 100 hours using cellulose dialysis tubing with molecular weight cut-off of 15,000. After the dialysis, a white powder was obtained by freeze-drying. The apparent solubility of PS-co-SSS in water decreased after freeze-drying. An elevated temperature (about ~60°C) was necessary to dissolve PS-co-SSS in water.  $^1\text{H}$  NMR in DMSO- $d_6$  was used to analyze the composition of the copolymer. The weight-averaged molecular weight was  $(127 \pm 3) \times 10^3$  Da, and polydispersity (PD) was  $2.7 \pm 0.1$

#### *Sample preparation for NMR*

0.005 wt % the stock solutions of PEO ( $M_w$   $7 \times 10^6$  Da and  $8 \times 10^6$  Da), PKS and PS-co-SSS were prepared with  $D_2O$  48 hours before the NMR experiments. Solutions for NMR analysis were prepared from appropriate mixtures of the stock solutions 1 to 3 hours before the NMR experiment in order to obtain steady-state behavior. The samples for 2D NOESY were prepared in the same way except that the PEO concentrations were 0.89 ~1.0 g/L. When PEO and PKS/or PS-co-SSS solutions were mixed together at this concentration, a viscous solution formed instantaneously, indicating the complex

formation.<sup>37</sup> The sample was sonicated for 3 minutes at room temperature to remove air bubbles caused by mixing.

### *NMR experiments*

A Bruker DPX400 NMR spectrometer operating at 105.8 MHz for <sup>23</sup>Na was used. The 5-mm broadband inverse probe was maintained at 25.0±0.1°C. Double and triple-quantum filtered <sup>23</sup>Na NMR spectra were acquired using the pulse sequence reported by Chung et al.<sup>38</sup> and Perkar et al.<sup>39</sup> and our experiments were set up by using 40% (w/w) solution of bovine serum albumin in 2M NaCl according to the literature. The experimental conditions were: acquisition time 642 ms, repetition rate 500 ms, evolution time 5 ms, number of acquisition 34800, the  $\pi/2$  pulse 23  $\mu$ s, and the sweep width 6372.52 Hz.

All proton NMR spectra were recorded on Bruker DRX 500, DPX 400 and ARX300 spectrometers. <sup>1</sup>H NMR spectra were measured at a temperature range from 293 to 333K with a 5-mm broadband inverse probe equipped with Z-axis gradient capability. A 30° pulse width was used and a 5.0 s delay time was inserted between successive acquisitions. A 10-minute incubation time was employed after every temperature change to achieve thermal equilibrium.

It was confirmed that under these experimental conditions all the important proton magnetizations were fully relaxed. Therefore quantitative results could be extracted. All

the chemical shifts were measured with respect to sodium salt of 3-(trimethylsilyl) propionic 2,2,3,3-d<sub>4</sub> acid (TSP) (0 ppm).

2D NOESY spectra were acquired in the phase-sensitive mode using the pulse sequence (90°-t<sub>1</sub>-90°-τ-90°-ACQ) (t<sub>1</sub> and τ stand for incremented delay time and mixing time, respectively). Two mixing times, 300 and 500 ms were used. The details for NMR experiment were reported previously.<sup>32</sup>

#### *Differential scanning calorimeter (DSC)*

DSC experiments were run on a Universal V2.6 DTA Instruments Calorimeter. Samples were sealed in a stainless steel pans. The heating and cooling programs were:

$$5^{\circ} C \xrightarrow{0.25^{\circ} C / \text{min}} 85^{\circ} C \xrightarrow{0.25^{\circ} C / \text{min}} 5^{\circ} C \xrightarrow{0.25^{\circ} C / \text{min}} 85^{\circ} C$$

Sample preparation: 1.542 g/L PEO solution (Mw 8×10<sup>6</sup> Da) and 2.088 g/L PKS were prepared separately in nanopure water 72 hours before DSC experiments. Two solutions were well mixed together at certain PEO/PKS mixing ratio. The mixture was kept at room temperature 24 hours before adding to DSC sample pan.

#### **Results**

Poly(vinyl phenol-co-potassium styrene sulfate) (PKS) containing 48 mole percent phenolic groups and a weight-averaged molecular weight of 158,000 Da was prepared by free radical polymerization. PKS forms stable, water-soluble complexes with very high molecular weight PEO – at concentrations greater than 0.2 g/L, the



complex forms transparent, stable gel. DSC was used to detect any phase transitions in the aqueous complex over the temperature range 5°C to 85°C. Within the sensitivity of the DSC instrument, no heat effects were detected for complexes based on mixing ratios ranging from 0.2 to 4 with PEO concentration ranging from 0.2 g/L to 3 g/L.

Conventional proton NMR, NOESY, and multiple quantum filtered  $^{23}\text{Na}$  NMR were employed to probe the complex structure as functions of temperature and pH as well as  $\text{Na}^+$  binding. In order to probe the importance of hydrogen bonding measurements were also made with mixtures of PEO and poly (styrene-co-sodium styrene sulfate), PS-co-SSS, an analogue of PKS without hydroxyl groups. The results are summarized in the following sections.

#### *Proton NMR of PKS/PEO complexes*

The chemical shift of the PEO ethylene protons is distinct from the PKS protons, making the ethylene proton signals an excellent probe of complex structure. Figure 1 shows the  $^1\text{H}$  NMR spectra of PEO in the presence of PKS. Pure PEO only had one  $^1\text{H}$  signal with the chemical shift ( $\delta$ ) at 3.704 ppm (with respect to TSP) at 25 °C.<sup>32</sup> Upon addition of PKS, PEO  $^1\text{H}$  signal split into two. The upfield signal was assigned as the complexed PEO signal, which represented those PEO segments involved in the complex formation. The upfield shift of chemical shift was due to the ring current effect.<sup>40</sup> The lowfield signal had the same chemical shift as pure PEO, and was assigned as the free PEO segments which were not involved in the complex formation.<sup>32</sup> The subsequent dilution of the PKS/PEO mixture until PEO concentration of 3.1 mg/L caused the integral

of the complexed PEO signal to decrease about 50% while the free PEO signal increased, suggesting the complex formation was partially reversible at the segmental level.

Temperature sensitivity can give information about the binding mechanisms.

Figure 2 shows the temperature effect on  $^1\text{H}$  NMR spectra of the mixed PKS/PEO solution at PKS/PEO (w/w)=0.2 and pH 6.4. The chemical shift of the signal, corresponding to uncomplexed PEO segments, decreased with temperature exactly as the behavior of pure PEO. The chemical shift of the complexed PEO segments shifted to lower field with increasing temperature. Furthermore, the fraction of PEO present as complex increased with increasing temperature.

In order to study the reversibility of temperature effects, PEO/PKS mixtures were heated to 333K and then cooled to 303K. No hysteresis in the  $^1\text{H}$  spectrum was observed before and after the heating/cooling cycles.

#### *NOESY spectrum for PKS/PEO mixed solution*

NOESY measurements, which can identify non-covalently bonded protons in close proximity,<sup>40</sup> were used to identify the domains in the PKS chains interacting with the PEO protons. Figure 3 shows the NOESY spectrum of PKS/PEO=2 (w/w) at 333K. Only the complexed PEO signal was observed at this high PKS/PEO mixing ratio. There were four kinds of cross peaks: the cross peaks between protons  $\text{H}_{\text{b-g}}$  and PEO; the cross peak between  $\text{H}_{\text{h,i}}$  protons and PEO; the cross peaks between aromatic protons  $\text{H}_{\text{b-g}}$  and  $\text{H}_{\text{h,i}}$ ; the cross peaks between aromatic protons  $\text{H}_{\text{b,i}}$  and backbone of PKS. The existence

of the strong NOE cross peaks between the PEO protons and the aromatic rings of PKS indicated that the complexed PEO ethylene groups were within 5 Å of the aromatic groups at least for part of the time.

The relative intensities of cross peaks are proportional to the strength of the interactions of interacting protons and the number of the protons. Taking account of the number of the protons contributing to NOE, the intensities of the cross peaks between H<sub>h,i</sub> and PEO were weaker than the cross peaks between phenolic ring and PEO. Thus, the interaction between phenolic ring/PEO was stronger than the interaction between styrene sulfonate group/PEO.

#### *Multiple quantum filtered <sup>23</sup>Na NMR*

Although PKS was synthesized with the potassium salt of styrene sulfonate, most of the experiments were conducted in dilute NaCl solutions so Na<sup>+</sup> is the most abundant counterion. The binding of sodium to PKS was probed with multiple quantum filtered <sup>23</sup>Na NMR. Figure 4 shows the single quantum filtered (SQF) and triple quantum filtered (TQF) <sup>23</sup>Na spectra of PKS in the presence and absence of PEO. Conventional Na NMR (i.e. the SQF results) showed so little influence of PEO addition. By contrast, no TQF <sup>23</sup>Na signals were detected without PEO whereas in the presence of PEO, significant TQF <sup>23</sup>Na signals were observed. Double quantum filtered <sup>23</sup>Na NMR showed similar results as TQF (spectra were not shown here). Also not shown is the TQF spectrum of PEO in the same salt solution that gave no Na<sup>+</sup> TQF signal.

The occurrence of a TQF sodium signal in the complex means that the exchange rate between sodium ions, bound to PKS, and those free in solution was slow in the NMR time scale. Without PEO the exchange rate was too fast to give a signal in the TQF spectra. One explanation is that upon complexing with PEO the conformation of the PKS cofactor is more compact giving a high local density of sulfonate groups which in turn gives stronger counterion binding and a lower exchange rate.

#### *The role of hydrogen bonding in complex formation*

The hydrogen bonding between phenolic hydroxyls and polyether oxygens is usually proposed to be the main driving force for PEO/cofactor complex formation. Two types of experiments were employed to determine the role of hydrogen bonding. In the first set of experiments the influence of pH on the extent of complex formation between PEO and PKS was probed. If hydrogen bonding is significant, the amount of complex formation should diminish at high pH because of the dissociation of phenolic groups. Figure 5 shows that at pH 6.4, most of the PEO segments were present in the complexed state, whereas at pH 12 the fraction of complexed PEO was 35% lower. Also, the chemical shift of the complexed signal shifted from 3.626 ppm at pH 6.4 to 3.656 ppm at pH 12. Based on  $pK_a=9.7$  for phenolic resins,<sup>29</sup> we estimate that at pH 12 only 1% of the phenolic groups are protonated. Therefore, this result suggests that mechanisms other than hydrogen bonding may be important in complex formation. Finally, the ionic strength was not constant in the pH results shown in Figure 5. The increase in ionic strength should promote the complex formation (Chapter III).

In the second type of experiments probing the role of hydrogen bonding, poly(styrene-co-sodium styrene sulfate), PS-co-SSS, was prepared with a monomer molar ratio of 3:2.  $^1\text{H}$  NMR was used to probe the composition of PS-co-SSS. The upper spectrum (a) in Figure 6 shows the  $^1\text{H}$  NMR spectrum of PS-co-SSS in DMSO- $d_6$ . PS-co-SSS had three peaks for aromatic protons with the chemical shifts ( $\delta$ ) at 7.404, 7.057, 6.485 ppm, which were assigned as  $\text{H}_{g, h}$ ,  $\text{H}_{b, c, d}$ ,  $\text{H}_{a, c, f, i}$  respectively, based on the work of Dickson et al.<sup>41</sup> The backbone protons were at 1.788~1.444 ppm. The other two peaks were from residual water and solvent DMSO- $d_6$ . From the corresponding peak areas, the composition of PS-co-SSS was calculated to be styrene /styrene sulfonate salt =0.71:0.29 (mole: mole). Figure 6c was obtained with the mixed PS-co-SSS and PEO at PS-co-SSS /PEO weight ratio of 4. In comparison with the pure PEO solution with a signal at 3.704 ppm (Figure 6b), the PEO proton signal in PS-co-SSS/PEO mixed solution shifted to 3.446 ppm. The resolution of the signals from the aromatic protons of PS-co-SSS degraded; it was difficult to observe the change in chemical shifts of PS-co-SSS in the presence of PEO. The separation of aromatic protons,  $\text{H}_{g, h}$ ,  $\text{H}_{b, c, d}$ ,  $\text{H}_{a, c, f, i}$ , was much less in water than in DMSO- $d_6$  at 25°C (Data were not shown), indicating that the mobility of aromatic groups was higher in DMSO- $d_6$  than in  $\text{D}_2\text{O}$ .

The influence of PS-co-SSS on the PEO  $^1\text{H}$  spectra is shown in Figure 7. The presence of PS-co-SSS caused the splitting of ethylene PEO  $^1\text{H}$  signal similar to that observed with the PKS/PEO complexes (e.g. Figure 5). There we concluded that complex formation occurred under conditions when hydrogen bonding was impossible.

NOESY was used to probe the PS-co-SSS/PEO complex structure and the results are shown in Figure 8. Two kinds of cross peaks were observed, one between aromatic protons of PS-co-SSS with ethylene protons of PEO and, the other, between aromatic protons of PS-co-SSS with backbone of PS-co-SSS. As with the PKS/PEO NOESY results, the existence of the intense NOE cross peaks between aromatic protons of PS-co-SSS with ethylene protons of PEO indicates that PS-co-SSS and PEO chain segments separated by less than 5 Å for part of the time. Unfortunately, due to the poor resolution of proton signals between aromatic protons, it was impossible to determine if the PEO was interacting with styrene and/or styrene sulfonate moieties.

Mixing poly (styrene sulfonate sodium salt) with PEO yielded no detectable change both in the half width and chemical shift for PEO  $^1\text{H}$  signal. Therefore, it was concluded that the complex formation between PEO and PS-co-SSS was mainly due to the existence of styrene group in its structure.

The PS-co-SSS/PEO complexes showed a similar response to increasing temperature as did the PKS/PEO complexes. While the bound PEO proton signals in the phenolic PKS based complex shifted to high values upon heating (see Figure 2), the free and bound signals merged together upon heating the PS-co-SSS/PEO complex (see Figure 9). Thus heating seemed to cause a more rapid exchange between free and complexed PEO segments in the PS-co-SSS/PEO complex. Note, the spectra before and after a heating cycle were similar indicating the changes in complex structure were reversible.

The tendency for the PS-co-SSS/PEO complex to increase mobility with heating was also observed in the NOESY spectra. Figure 10 shows NOESY spectra for the mixed PS-co-SSS/PEO (w/w)=4 at 50°C. The cross peaks between aromatic rings of PS-co-SSS and PEO became much less intense, compared with the strong NOE cross peaks at 25°C (Figure 8).

### ***Discussion***

The interactions between aqueous PEO and PKS or PS-co-SSS are accessible by NMR. Our results address two issues – the structure of the PEO/cofactor complex at the NMR distance scale and the role of hydrogen bonding.

Hydrogen bonding between phenolic hydroxyl groups and ether oxygens on PEO is usually proposed to be the main driving force for the complex formation of PEO with cofactors.<sup>6,11,29</sup> There is no doubt that H-bonding is operative. Our earlier work showed that PEO induced a 0.4ppm <sup>13</sup>C chemical shift for phenolic C-OH.<sup>32</sup> This effect was attributed to H-bonding based on similar shifts (1.3 ~2.3 ppm) observed in solid state H-bonding complexes in PEO/polyvinylphenol mixtures.<sup>42,43</sup>

Nevertheless, this work has added to a growing body of evidence that PEO/cofactor complex formation also occurs in the absence of hydrogen bonding. Firstly, a substantial amount of complexed PEO signal existed at pH 12 where most of the phenolic hydroxyl groups were dissociated and thus unable to form hydrogen bonds (Figure 5). Secondly, PS-co-SSS/PEO complexes are a clear example of H-bond free complexes. Additional evidence of H-bonding free complexes is the existence of a

commercial cofactors based on (sodium naphthalene sulfonate) which do not appear to have hydroxyl groups.<sup>5</sup>

Hints about the relative orientation of interacting PEO and PKS segments are given by the PEO proton NMR results. Strong NOE interactions between phenolic and PEO protons were observed (Figure 3) and the chemical shift of the PEO protons were shifted to upfield in the presence of PKS (Figure 1, Figure 2, and Figure 5), due to the ring current effect. These results indicate that the complexed PEO segments reside on the top or bottom of the aromatic rings within a distance less than 5 Å. Furthermore, the PKS/PEO NOESY results and the absence of complex formation with poly(styrene sulfonate) homopolymer suggest that the styrene sulfonate moieties were not directly involved in complex formation.

The observation of the <sup>23</sup>Na TQF spectra for PKS only in the presence of PEO is an intriguing result. Increased sodium binding with complex formation could reflect counterion condensation<sup>44</sup> due to increased local sulfonate charge density resulting from a collapse of PKS chain. More hydrophobic cofactors are known to undergo syneresis to a coacervate phase when exposed to PEO,<sup>30</sup> so it seems reasonable that PKS adopts a more compact conformation upon complex formation.

Finally, it is noteworthy that aqueous PEO/cofactor complexes, particularly those based on PS-co-SSS, were weak. Evidence for this is the fact that the PEO/PKS complex was partially disrupted by dilution by a factor of 4 (Figure 1). Other evidence for weak complex formation was the absence of syneresis and formation of a coacervate phase.



Polyelectrolyte complexes and some hydrogen bonding complexes often phase separate in water.<sup>23</sup> The mobility of PS-co-SSS segments increased with temperature, as evidenced by the increase in the sharpness of PS-co-SSS proton signals and that the exchange rate of complexed PEO and free PEO increased with increasing temperature. Indirect evidence supporting the hypothesis that PS-co-SSS/PEO complexes are weak is that colloidal flocs formed in the presence of this complex are extremely shear-sensitive (Chapter V).

A broader implication of this work is that PEO has been shown to interact with aromatic moieties on aqueous polymers. Thus peptides with high tyrosine, phenylalanine and tryptophan contents are likely to interact with PEO in water. This may impact the utility of PEO surface treatments on biomaterials for implant applications and the selection of ideal cofactors in the future.

### ***Conclusions***

The main conclusions of this chapter are:

1. Hydrogen bonding between phenol protons and polyether oxygens is not the sole binding interaction in PEO/PKS complexes. Evidence includes: a) complexes form between PEO and poly(styrene-co-styrene sulfonate) where hydrogen bonding is impossible; b) complexes form at pH 12 where most phenolic hydroxyls are dissociated; and, c) NOESY indicated close interaction between the PEO ethylene groups and the aromatic rings.

2. The contact of PEO bound segments with the aromatic rings and temperature sensitivity suggest that hydrophobic interactions are important in PEO/cofactor complex formation.
3. Complex formation between PEO and cofactor is irreversible in the macroscopic sense – that is, they are not destroyed by dilution or temperature change. By contrast, NMR indicates that at a microscopic scale, PEO/cofactor binding is reversible. This behavior is analogous to that of high molecular weight polymers adsorbed on a solid – the adsorption of individual segments is usually reversible whereas desorption does not occur with dilution.
4. The conformation of the phenolic cofactors is more collapsed after complex formation as evidenced by the increased sodium counterion binding.

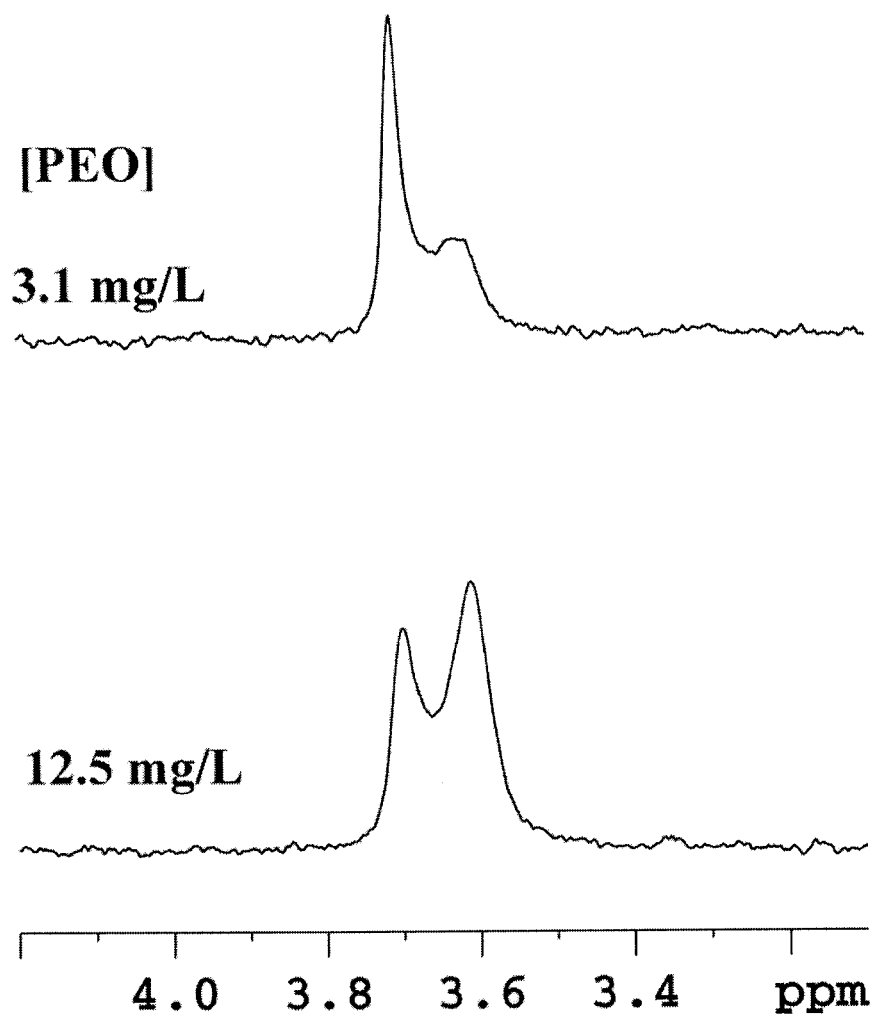


Figure 1. The effect of dilution on the  $^1\text{H}$  NMR spectra of PKS/PEO mixture. PEO Mw  $8 \times 10^6$  Da.

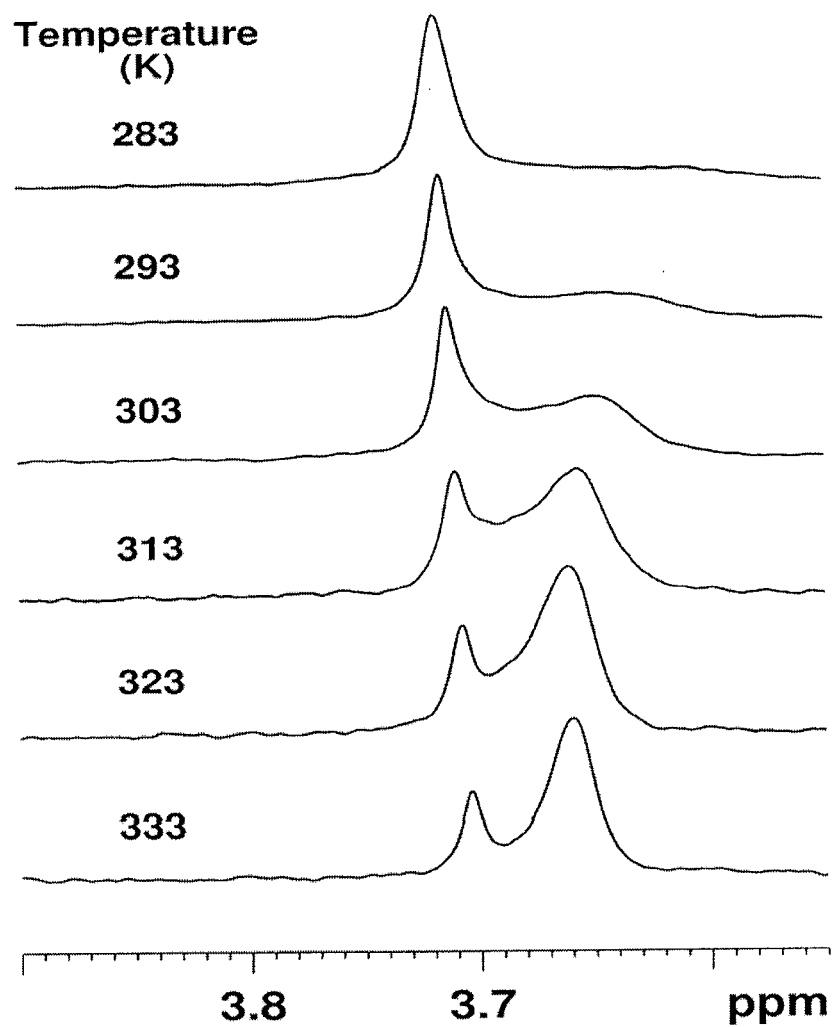


Figure 2. The  $^1\text{H}$  NMR spectra for the mixed PKS/PEO solutions as functions of temperature. [PEO]:12.5 mg/L; PEO Mw:  $8 \times 10^6$  Da; PKS/PEO (w/w)=0.2.

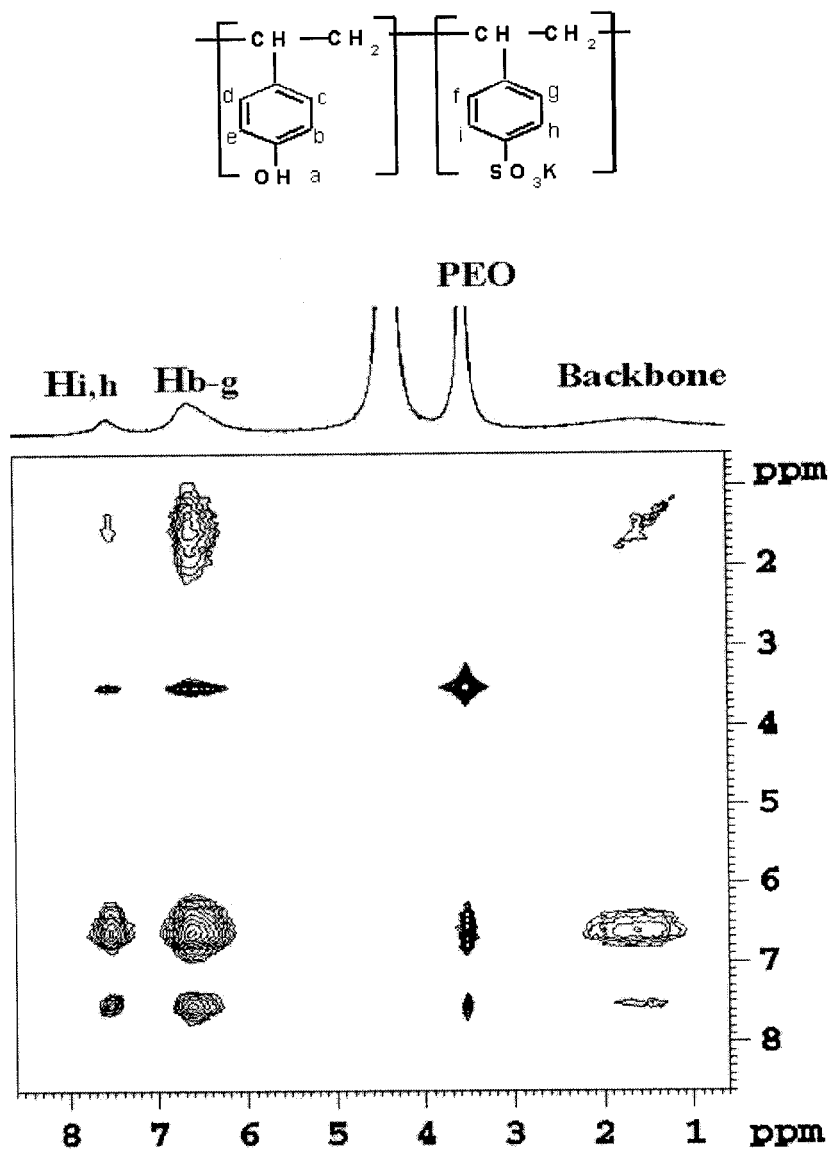


Figure 3. NOESY Spectrum of PKS.48/PEO mixture at 333K. The experimental conditions: PKS/PEO (w/w) =2; PEO Mw  $8 \times 10^6$  Dalton; [PEO]=0.5 g/L in D<sub>2</sub>O.

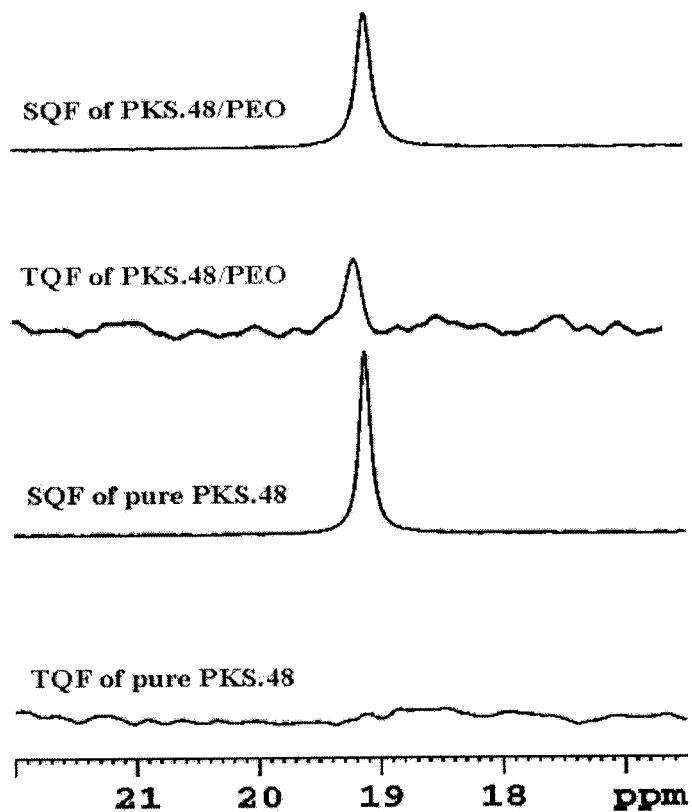
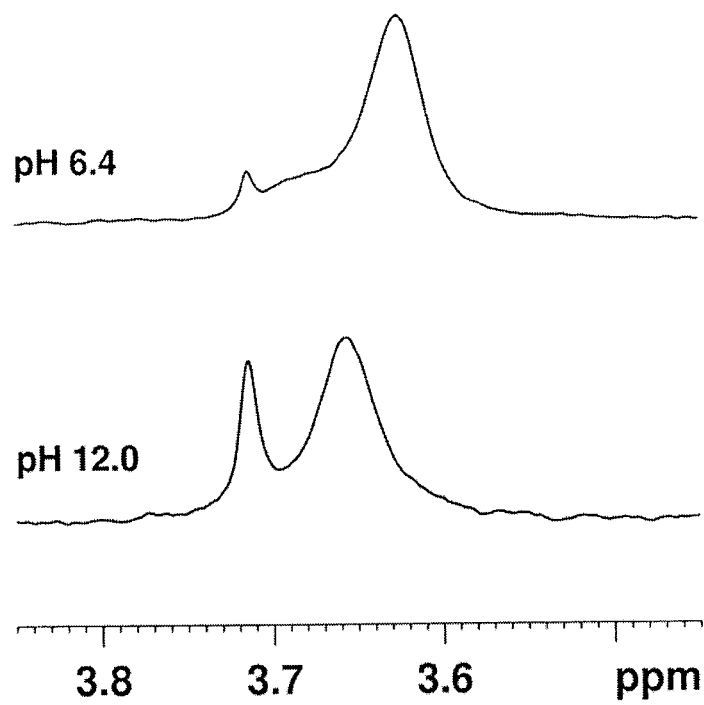


Figure 4. Single quantum filtered (SQF) and triple quantum filtered (TQF)  $^{23}\text{Na}$  NMR spectra for PKS in 10 mM NaCl in the presence or absence of PEO at 25°C. PEO Mw  $8 \times 10^6$  Da, PKS/PEO (w/w)=1, [PKS]=0.80 g/L in  $\text{D}_2\text{O}$ .



**Figure 5. The <sup>1</sup>H NMR spectra of PKS/PEO at pH 6.4 and 12.0. PEO Mw  $8 \times 10^6$  Da. [PEO]=12.5 mg/L, PKS/PEO=0.8 (w/w), 303K.**

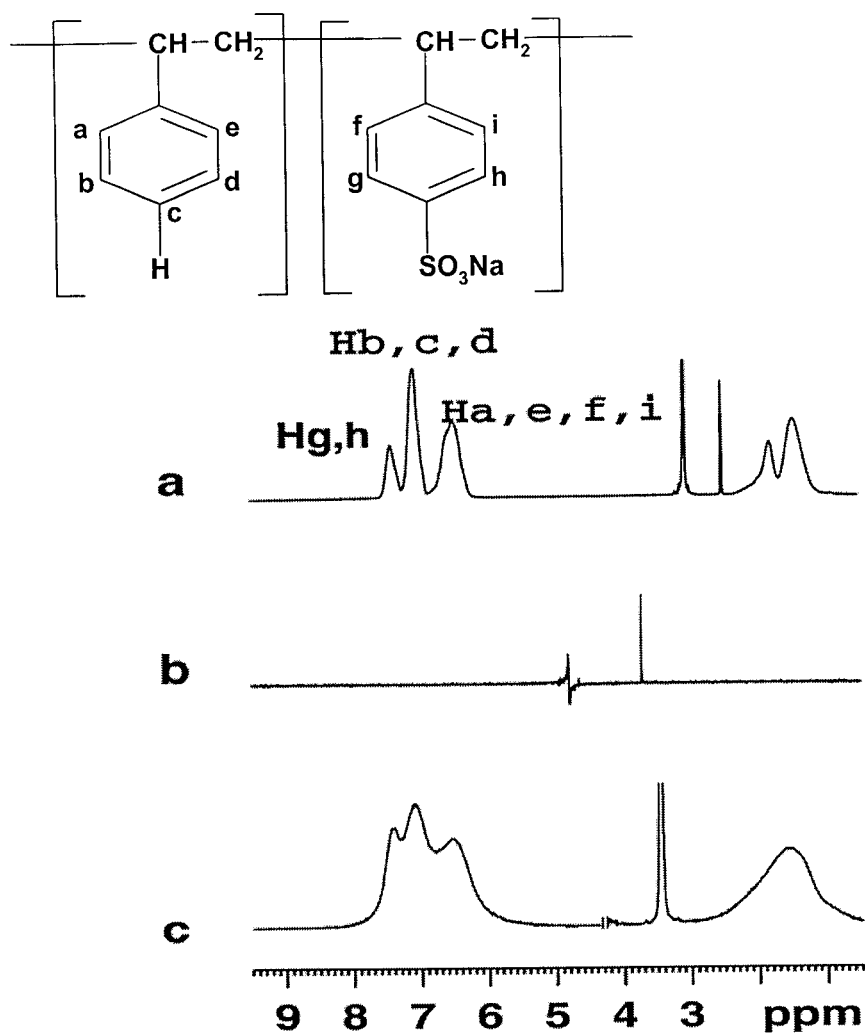


Figure 6.  $^1\text{H}$  NMR spectra for PS-co-SSS and mixed PS-co-SSS/PEO a: PS-co-SSS in  $\text{d}_6\text{-DMSO}$  at  $70.0^\circ\text{C}$ ; b: PEO in  $\text{D}_2\text{O}$  at  $25.0^\circ\text{C}$ ; c: PS-co-SSS/PEO in  $\text{D}_2\text{O}$  at  $25.0^\circ\text{C}$ . The spectra were obtained with Bruker ARX300 spectrometer.



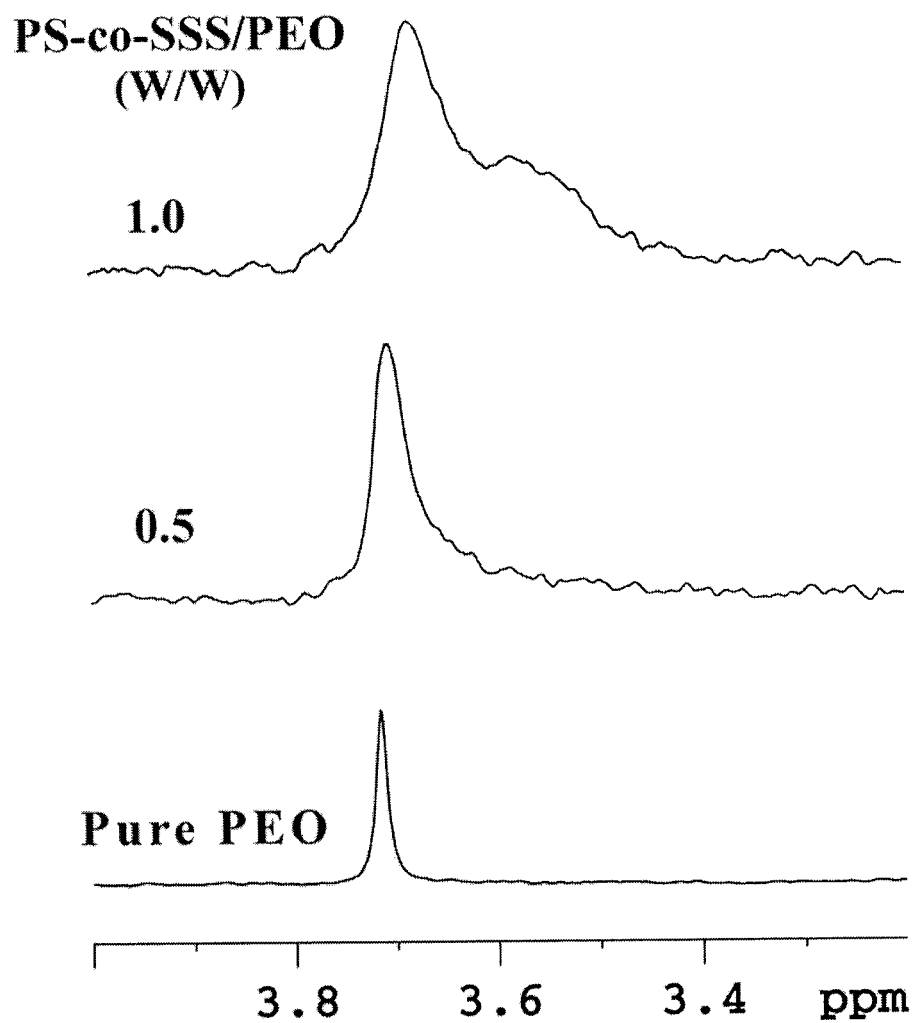


Figure 7.  $^1\text{H}$  NMR spectra for mixed PS-co-SSS/PEO in  $\text{D}_2\text{O}$  at different mixing ratio at  $25.0^\circ\text{C}$ .  $[\text{PEO}]=2.5\text{ mg/L}$ . The spectra were obtained with Bruker DPX400 spectrometer.

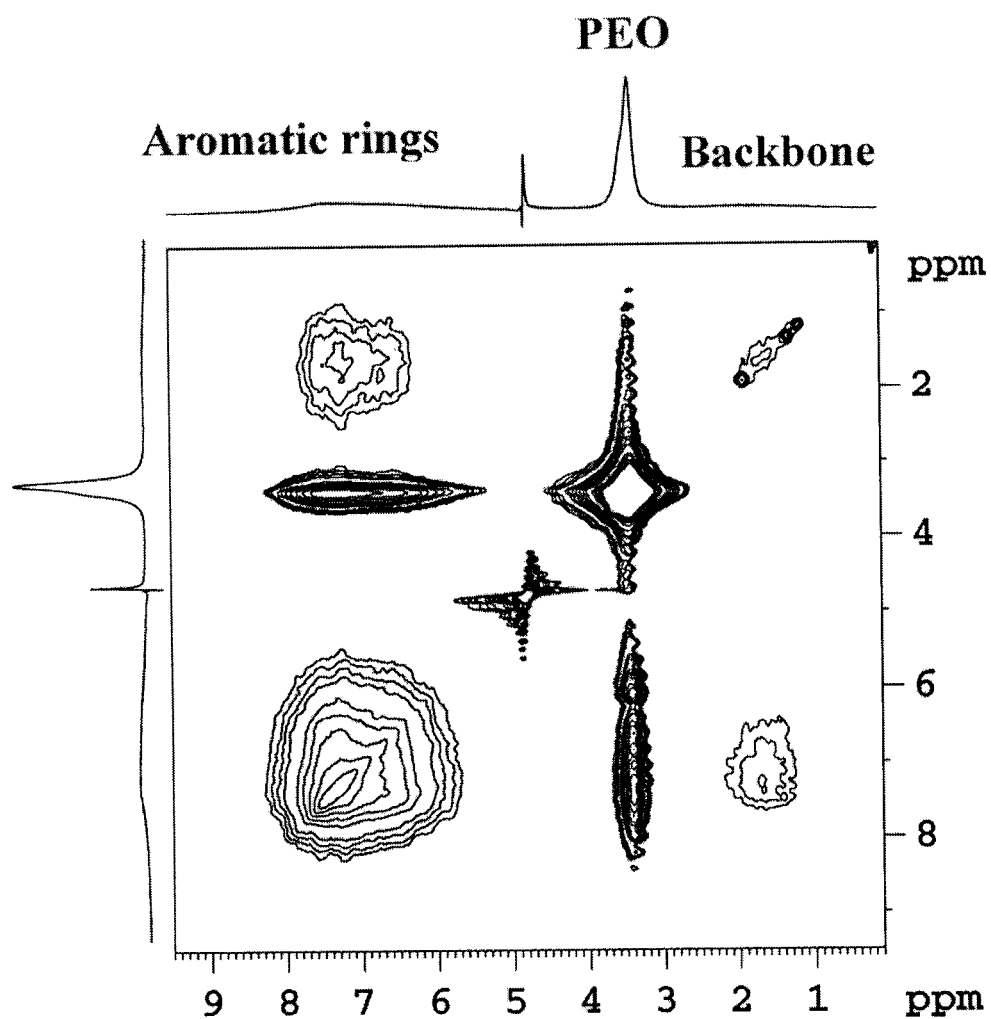


Figure 8. NOESY spectrum for mixed PS-co-SSS/PEO at 25°C. [PEO]=1g/L, mixing time 300 ms. The spectra were obtained with Bruker ARX300 spectrometer.

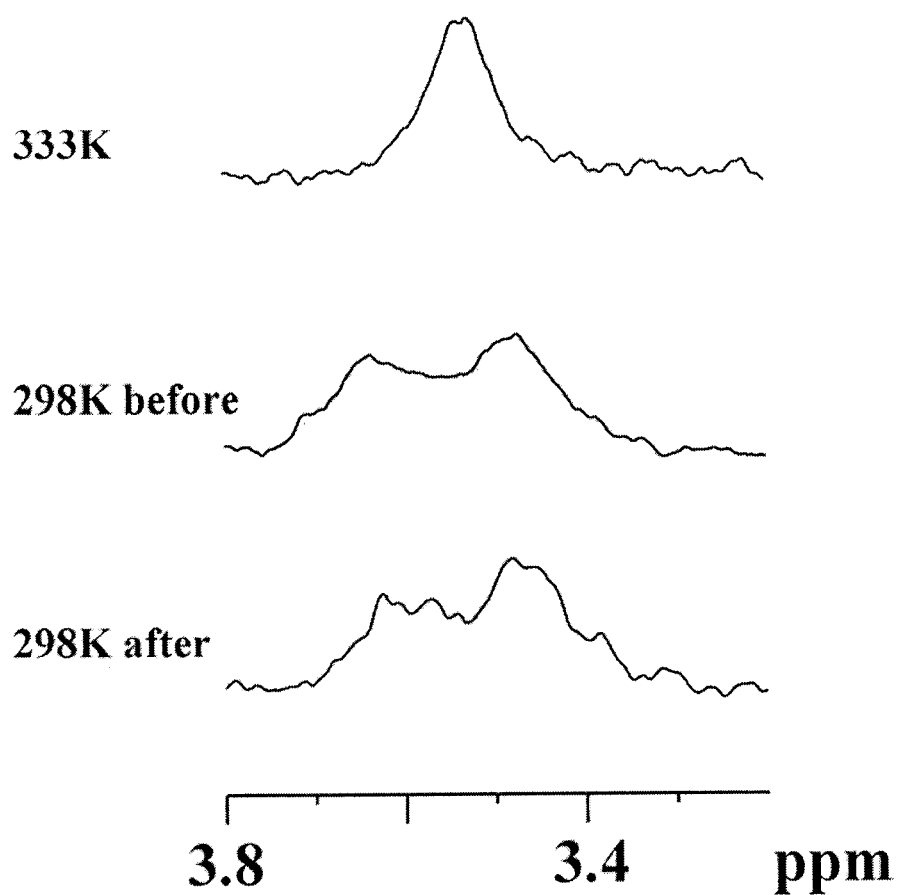


Figure 9.  $^1\text{H}$  NMR spectra for mixed PS-co-SSS/PEO at three temperatures. [PEO]: 12.5 mg/L. 298K before: spectrum was acquired before raising temperature to 333K. 298K after: spectrum was obtained after temperature was cooled from 333K to 298K. The spectra were obtained with Bruker ARX300 spectrometer.

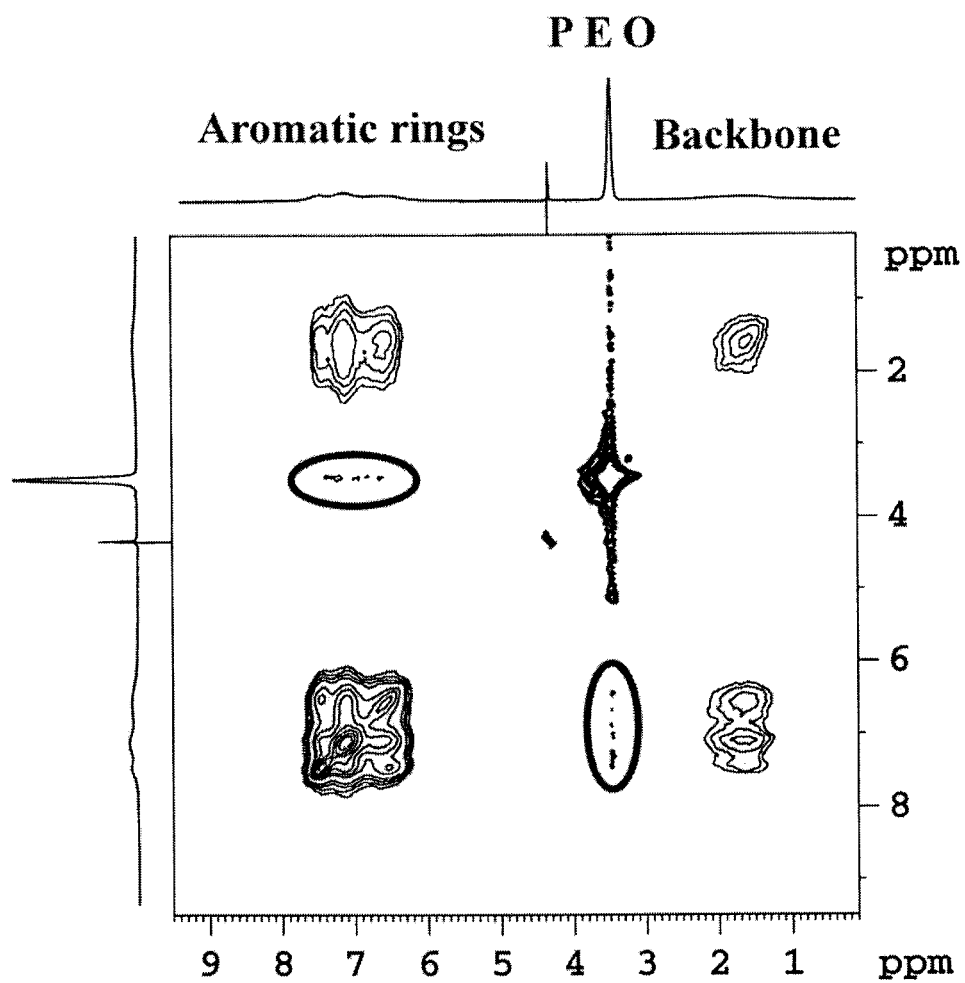


Figure 10. NOESY spectrum for mixed PS-co-SSS/PEO at 50°C. [PEO]=0.89 g/L, PS-co-SSS/PEO(w/w): 4, mixing time 300ms.

## References

---

- <sup>1</sup> Carrard, J. P.; Pummer, H. *US Patent* 4,070,236, **1975**.
- <sup>2</sup> Pelton, R.H., Allen, L.H., and Nugent, H. M. *Tappi* **1981**, 64, 89.
- <sup>3</sup> Gibbs, A.; Pelton, R. H.; Cong, R. *Colloids Surf.* **1999**, 159, 31.
- <sup>4</sup> Stockwell, J. O. *WO Patent* 95/21296, **1995**.
- <sup>5</sup> Carignan, A.; Garnier, G.; van de Ven, T. G. M. *JPPS* **1998**, 24, 94.
- <sup>6</sup> Lindström, T.; Glad-Nordmark, G. *Colloids Surf.* **1984**, 8, 337.
- <sup>7</sup> Pelton, R. H.; Allen, L.; Nugent, H *US Patent* 4,313,790, **1980**.
- <sup>8</sup> Goto, S.; Miyanishi, T.; Pelton, R. H. *Nord. Pulp Pap. Res. J.* **2000**, 15, 395.
- <sup>9</sup> Pelton, R. H; Xiao, H.; Brook, M. A.; Hamielec, A. *Langmuir* **1996**, 12, 5756.
- <sup>10</sup> Ech, E. *US Patent* 5,472,570, **1995**.
- <sup>11</sup> Pelton, R. H; Xiao, H.; Brook, M. A.; Hamielec, A. *J. Poly. Sci.* **1995**, 33, 2605.
- <sup>12</sup> Harris, J. M. *Poly(ethylene Glycol) Chemistry: Biotechnical and Biomedical Applications*; Plenum Press: New York, 1992
- <sup>13</sup> Bailey, F. E.; Koleske, J. V. *Poly(Ethylene Oxide)*; Academic Press: New York, 1976
- <sup>14</sup> Goddard, E. D. *Colloids Surf.* **1986**, 19, 255.
- <sup>15</sup> Cabane, B.; Duplessix, R. *J. Phys.* **1982**, 43, 1529.
- <sup>16</sup> Tsuchida, E.; Osada, Y.; Ohno, H. *J. Macromol .Sci.-Phy.* **1980**, B17, 683.
- <sup>17</sup> Bailey, F. E.; Lundberg, R. D.; Callard, R.W. *J. Polym. Sci .Part A* **1964**, 2, 845.
- <sup>18</sup> Iliopoulos, I.; Halary, J. H.; Audebert, R. *J. Polym .Sci. Part A:* **1988**, 26, 275.
- <sup>19</sup> Iliopoulos, I.; Audebert R. *Macromolecules* **1991**, 24, 2566.
- <sup>20</sup> Smith, L.; Winslow, A. E.; Petersen, D. E. *Ind. Eng. Chem.* **1959**, 51, 1361.
- <sup>21</sup> Osada, Y.; Sato, M. *Polym .Lett. Edi.* **1976**, 14, 129.
- <sup>22</sup> Miyoshi, T.; Takegoshi, K.; Hikichi, K. *Polymer* **1997**, 38, 2315.
- <sup>23</sup> Tsuchida, E.; Abe, K. *Adv. Polym. Sci.* **1982** 45, 2.
- <sup>24</sup> Kokufuta, E.; Nishimura, H. *Polymer. Bull.* **1991**, 26, 277.
- <sup>25</sup> Xia, J.; Dubin, P. L.; Kokufuta, E. *Macromolecules* **1993**, 26, 6688.

- 
- <sup>26</sup> Azegami, S.; Tsuboi, A.; Izumi, T.; Hirata, M.; Dubin, P.L.; Wang, B.; Kokufuta, E. *Langmuir* **1999**, *15*, 940.
- <sup>27</sup> Harada, A.; Cammas, S; Kataoka, K. *Macromolecules* **1996**, *29*, 6183.
- <sup>28</sup> Pemawansa, K. P.; Thakur, A.; Karikari, K. E.; Khan I. M. *Macromolecules* **1999**, *32*, 1910.
- <sup>29</sup> Stack, K. R.; Dunn, L. A.; Roberts, N. K. *Colloids Surf.* **1991**, *61*, 205.
- <sup>30</sup> Xiao, H.; Pelton, R.; Hamielec, A. *J. Pulp Paper Sci.* **1996**, *22*, 475.
- <sup>31</sup> Goto, S.; Pelton, R. *Colloids Surf. A* **1999**, *155*, 231.
- <sup>32</sup> Cong, R.; Bain, A. D.; Pelton, R. H. *J. Poly. Sci. Part B* **2000**, *38*, 1276.
- <sup>33</sup> Gibbs, A.; Yang, Z.; Xiao, H.; Pelton, R. H. *Transactions of 4th Fundamental Resource Conference, PIRA International, Leatherhead, UK* **1997**, 1135.
- <sup>34</sup> Kruis, A. *Ziet. Phys. Chem.* **1936**, 1936.
- <sup>35</sup> Wiley, R. H.; Trinley, W. A. *J. Poly. Sci.* **1958**, *28*, 163.
- <sup>36</sup> Wiley, R. H.; Trinley, W. A. *J. Amer. Chem. Soc.* **1955**, *78*, 2171.
- <sup>37</sup> Dan, Y.; Chen, S.; Zhang, Y.; Xiang, F. *J. Poly. Sci. Part B.* **2000**, *38*, 1069.
- <sup>38</sup> Chung, C. W.; Wimpers, S. *J. Magn. Reson.* **1990**, *88*, 440.
- <sup>39</sup> Pekar, J.; Leigh, J. S. *J. Magn. Reson.* **1986**, *69*, 582.
- <sup>40</sup> Friebolin, H. *Basic One- and Two-Dimensional NMR Spectroscopy*; VCH: New York, **1993**
- <sup>41</sup> Dickson, L. C.; Weiss, R. A.; Wnek, G. E. *Macromolecules* **2001**, *34*, 3108.
- <sup>42</sup> Zhang, X.; Takegoshi, K.; Hikichi, K. *Macromolecules* **1992**, *25*, 2336.
- <sup>43</sup> Zhang, X.; Takegoshi, K.; Hikichi, K. *Macromolecules* **1993**, *26*, 2198.
- <sup>44</sup> Manning, G. S. *J. Chem. Phys.* **1969**, *51*, 924.

### **Chapter III Factors affecting the size of poly(vinyl phenol-co-styrene sulfonate potassium salt)/poly(ethylene oxide) complexes**

#### *Abstract*

The transport properties of complexes formed between poly(ethylene oxide) (PEO) and poly (vinyl phenol-co-styrene sulfonate) (PKS) in aqueous medium were investigated by diffusion ordered NMR spectroscopy (DOSY), fluorescence photobleaching recovery (FPR) and viscosity measurements. The apparent self-diffusion coefficient ( $D_{app}$ ) was found to be related to PKS/PEO mixing ratio, phenolic molar content in PKS, temperature and ionic strength. The  $D_{app}$  of PKS/PEO mixtures changed with the mixing ratio of the components; maximum complex formation corresponded to each phenolic ring of PKS was surrounded by 5 PEO segments. These results suggested that steric registration dominates the number of PEO repeating units surrounding each phenolic group.  $D_{app}$  of PKS/PEO was up to 6 times smaller than pure PEO, indicating that PKS induced PEO aggregation with a few PEO coils in each complex. The phenolic groups were the main active component as proposed by many researchers. Increasing the phenolic molar content increased the attraction forces and decreased the electrostatic repulsion between charged styrene sulfonate groups, thus resulting in compact complexes. The  $D_{app}$  values of PKS/PEO mixtures increased with temperature and ionic strength. Temperature promoted complex formation as evidenced by an increase in the number of PEO segments involved in the complex. PKS/PEO complexes displayed synthetic

polyelectrolyte behavior with KCl addition. However, the complexes have a lower critical phase separation concentration of 50 mM KCl. The low solubility in electrolyte solutions indicated that complexes may have a much higher hydrophobicity than PEO and PKS.



### ***Introduction***

In recent years, the study of polymer-polymer interactions and formation of interpolymer complexes have evoked considerable interest in the polymer science literature. The size of interpolymer complexes is important for many fields. We are interested in the use of high molecular weight poly(ethylene oxide) (PEO) in conjunction with water-borne aromatic polymers, called cofactors in papermaking. These polymers act as flocculants which improve the deposition of inorganic fillers onto fiber surfaces.<sup>1,2</sup> The factors influencing the size of PEO/cofactor complexes are described in this chapter.

In 1998 Carignan et al. described the use of dynamic light scattering (DLS) to estimate the size of complexes formed between PEO and modified phenol-formaldehyde resin or poly (sodium naphthalene) in the absence of salt.<sup>3</sup> It was proposed that PEO aggregated in the presence of cofactors; and PEO coil contracted upon forming complexes, the extent of shrinkage depended on the structure of aromatic polymers.

Molecular modeling has been adapted to predict the conformation of the complexes.<sup>2,4</sup> The main conclusion is that due to the steric restrictions, only a portion of the ether oxygens of PEO could interact with phenolic hydroxyl groups.

Generally speaking, DLS is probably one of the most useful techniques for characterizing macromolecules. But, there are two major concerns associated with the

use of DLS in the study of the interaction between high molecular weight PEO and cofactors. The source of light scattering in a polymer solution originates from concentration fluctuations, which give rise to fluctuations in refractive index of the scattering medium. The diffusion coefficient is defined as the ratio of the driving force, e.g., the thermal energy  $kT$  for concentration fluctuation, to the hydrodynamic interaction between a moving particle and solvent ( $f$ ):

$$D = \frac{kT}{f} \equiv \frac{kT}{6\pi\eta R_h} \quad (1)$$

For a neutral polymer in the infinitive dilute regime, the hydrodynamic radius  $R_h$  can be calculated from the Stokes-Einstein equation. For polyelectrolyte solutions, the driving force for the concentration fluctuation not only comes from thermodynamic interaction  $kT$ , but also from electrostatic repulsion, which could be far stronger than  $kT$ . Therefore, it is a general procedure to add salt at the concentration high enough to suppress the non-thermodynamic interactions and /or “slow mode” terms.<sup>5</sup> Unfortunately, for mixed PEO/cofactors solution, the formed interpolymer complexes readily aggregate upon increasing the salt concentration or even may phase separate from solution.<sup>6</sup>

The second problem is associated with high molecular weight PEO. It has been reported that impurities accumulate during manufacture,<sup>10</sup> or improper handing of solution<sup>7</sup> or for some other reasons.<sup>8</sup> Furthermore, it has been proposed that the impurities cause PEO to form large aggregates consisting of a few hundred of PEO

free coils in aqueous solution.<sup>8,9,10</sup> These aggregates are reported to have the diameter of ~450 nm which is comparable to the wavelength of light commonly used in DLS. Theory shows that scattering and hydrodynamic interaction are strongly nonlinear functions of size. If the particles are composed of multiple subunits and if aggregates are comparable on size to the wavelength of scattered light, intraparticle interference will cause a diminution in the intensity of scattered light, as recently reviewed by Bloomfield.<sup>11</sup> Formation of irregularly shaped aggregates, even from regularly shaped small particles, can be very difficult for DLS to handle, which can lead to dramatic errors in the apparent size.

Fluorescence photobleaching recovery (FPR) offers a simpler alternative for studying the translational motion of specific components in a complex mixture. A FPR measurement is simple in concept.<sup>12,13</sup> The species of interest is labeled by covalent attachment of a fluorescent molecule. Therefore, only the fluorescently tagged diffuser is observed. Measurements begin when dye is erased (i.e. destroyed) from specific regions of the samples by a bright laser flash. The bleached area shows a recovery of fluorescence as unbleached molecules diffuse into and bleached molecules diffuse out of the irradiated region. The rate of recovery of the fluorescence signal can be used to obtain the self-diffusion coefficient. FPR responds to gradients in the intact dye concentration, not to gradients in overall polymer concentration like DLS. FPR offers advantages. For the polyelectrolytes with the aggregation, the most important ones are the less sensitivity to thermodynamic non-

ideality and different response to aggregation. The details about the comparison of DLS and FPR were given by Fong and Russo.<sup>14</sup>

Diffusion Ordered NMR Spectroscopy (DOSY) is another option for size measurement.<sup>15</sup> DOSY is based on pulsed field gradient (PFG) NMR that encodes the information about the translational motion into NMR data.<sup>16</sup> It combines the selectivity of high-resolution NMR with the hydrodynamic information provided by PFG NMR, it shows the information about chemical shift in one dimension and self-diffusion coefficient in the second dimension in a DOSY spectra. Most distinguishable features about DOSY include: 1) NMR active impurities are detected but do not interfere with measurements, and 2) it is non-destructive technique without covalent attachment fluorescence dye to target molecules. Therefore, there has been increasing interest in using DOSY to study polymer mixtures.<sup>17,18,19, 20</sup>

In this work linear poly(vinyl phenol-co-potassium styrene sulfonate) (PKS) has been used as a model cofactor (See Figure 1). PKS, together with high molecular weight PEO, is an effective flocculant for various colloidal particles.<sup>21</sup> Our recent NMR studies at microscopic level showed that PKS formed water-soluble complexes with high molecular weight PEO.<sup>22</sup> The main interaction sites were between aromatic rings of PKS and ethylene groups of PEO. Upon the complex formation, PEO bound segments resided on the top or bottom of aromatic rings.

This chapter describes results from a systematic study of the influence of phenolic content of PKS copolymers, PKS/PEO mixing ratio, ionic strength,

temperature and molecular weight of PEO on complex formation. DOSY, FPR together with dynamic viscosity measurements were used to characterize the transport properties of the complex.

## ***Experimental***

### *Materials*

5-(4,6-dichlorotriazinyl) aminofluorescein (5-DTAF) was purchased from Molecular Probes. Polyethylene oxide (PEO) (Polyox N-12K Mw=1×10<sup>6</sup> Da; Polyox N-3000 Mw=4×10<sup>5</sup> Da; Polyox N-750 Mw=3×10<sup>5</sup> Da; Polyox -10 Mw=1×10<sup>5</sup> Da) was gifts from Union Carbide (Danbury, CT). Poly (ethylene glycol) (PEO with Mw=8×10<sup>3</sup> Da) was purchased from Amresco, Ohio. All the chemicals were used without further purification.

### *Procedure*

#### *Synthesis of poly (vinyl phenol-co-potassium styrene sulfonate) (PKS)*

PKS was synthesized by free radical polymerization of 4-acetoxystyrene with sodium 4-styrene sulfonate followed by extensive hydrolysis in 1M KOH solution.<sup>21</sup> The detailed procedure for purification and characterization was reported previously.<sup>22</sup> PKS.48 was designated as PKS with phenolic content = 0.48 (mole: mole). The properties of five PKS copolymers are summarized in Table 1.

### *Viscosity measurement*

Viscosity was measured with ATS Rheosystems (Stresstech HR) at 25 °C and a shear rate of  $37.32 \text{ s}^{-1}$ . 1g/L PEO or PKS stock solutions were prepared 48 hours before the experiments. The stock solutions were diluted to the desired concentration 2 hours before the experiments. PEO and PKS solutions were well mixed 30 minutes before viscosity measurements, then kept at room temperature to allow the mixture to reach steady state behavior.

### *Fluorescein labeling*

PKS.48 was labeled with 5-(4,6-dichlorotriazinyl) aminofluorescein (5-DTAF) according to the literature.<sup>23</sup> The details are given below. 1.00 g of PKS was dissolved in 100 ml nano-pure water. pH of PKS solution was adjusted from pH 6 to pH 10~11 by adding 1.38g  $\text{K}_2\text{CO}_3$  solid. 17 mg 5-DTAF was dissolved in 10 ml acetone with stirring. The two solutions were mixed together at room temperature, giving the feed ratio of phenolic group in PKS.48/DTAF=100:1 (mole: mole). Soon after mixing, a clear bright yellow solution was obtained, indicating the start of labeling reaction. The mixture was gradually heated to 35°C for 5 minutes, and then kept in dark at room temperature for 26 hours to allow the labeling reaction to complete.

The mixture was poured directly into 1000 ml of isopropanol, and then heated to 40°C for 3 minutes. Yellowish PKS was precipitated out from isopropanol. Labeled

PKS was purified by dissolving in water followed by precipitation in isopropanol three times yielding colorless isopropanol supernatant. The product was air-dried, followed by vacuum drying for over 24 h at 40°C.

Fluorescence photobleaching recovery (FPR) was used to evaluate the purification efficiency. As a small molecule, 5-DTAF has a self-diffusion coefficient  $D$  of  $5.5 \times 10^{-9} \text{ m}^2/\text{s}$ .<sup>24</sup> After covalent bounding with DTAF, the apparent diffusion coefficient of labeled PKS.48 was measured at the order of  $10^{-12} \text{ m}^2/\text{s}$ , suggesting no free dye was in the labeled PKS.48 solutions.

#### *Fluorescence photobleaching recovery*

Instrumentation: A schematic diagram about FPR instrument is shown in Figure 2. A striped pattern was created by illuminating a coarse diffraction grating (Ronchi ruling) held in the rear focal plane of a standard epifluorescence microscope with an intense, brief laser flash. With the laser intensity greatly reduced, an electromechanical modulation detector system monitors the subsequent disappearance of the pattern due to exchange of molecules that were bleached (i.e. in the bright regions during the flash) and those that were not (i.e., molecules that were not illuminated during the flash). The ac amplitude from the modulation detector decays exponentially:

$$ac(t) = \exp(-K^2 D_{\text{app}} t) \quad (2)$$

Where the spatial frequency of the grating is  $K=2\pi/L$ ,  $L$  is the distance between stripes in Rochi Ruling, and  $D_{app}$  is the apparent self-diffusion coefficient of the labeled PKS.48. For the most of FPR experiments, two different  $K$  values each with 2~3 repeating measurements were conducted to ensure the absence of non-diffusive signal recovery. The detailed information about the instrument was described.<sup>25</sup>

Data analysis: Due to the broad distribution of PKS molecular weight, one-exponential model cannot fit the data well. Thus, two-exponential mode was used in FPR data analysis. The apparent diffusion coefficient  $D_{app}$  of the DTAF-bonded PKS was expressed as weight averaged value.

Sample preparation: PEO and PKS.48 were dissolved separately in a nanopure water at least 48 hours before FPR experiments. The two solutions were mixed at a specified ratio with shaking, and stored at room temperature for 3 hours with occasional shaking to obtain steady state behavior. The sample was loaded into a rectangular glass cell (Vitro Dynamics) having a path length of 100  $\mu\text{m}$  and frame sealed. The temperature of FPR sample deck was controlled by a NESLAB RTE-111 circulating water bath with a temperature control accuracy of  $\pm 0.02^\circ\text{C}$ . A 15-minute incubation time was employed after every change in temperature to achieve thermal equilibrium.

For the complex formation at different ionic strengths, KCl powder was added directly to the premixed PKS.48/PEO solution.



### *Fluorescence Spectroscopy*

Fluorescence emission spectra were recorded with Perkin Elmer Luminescence Spectrophotometer LIS 50B. A high-quality quartz cuvette with a 10 mm path length was employed.

### *DOSY experiments and data processing*

DOSY experiments were performed on Bruker DPX250 spectrometer. The strength of gradient field  $G$  was measured directly. The self-diffusion coefficient for residue HDO in  $D_2O$  was measured to be  $1.9 \times 10^{-9} \text{ m}^2/\text{s}$  at 298K, which was in a good agreement with the reported data.<sup>26</sup> The probe temperature was maintained at  $298 \pm 0.5 \text{ K}$ . Stimulated echo (STE) pulse sequence was employed.<sup>15</sup> Typical parameters of DOSY experiments: diffusion time ( $\Delta$ ) was 600 ms, the gradient pulse ( $\delta$ ) 10 ms, number of scans 8 to 32, dummy scans 120, number of sampled points in the gradient strength dimension was 8 and 16K in the spectral dimension (frequency resolution was not a critical factor), the relaxation delay was 3 s,  $90^\circ$  pulse ( $^1\text{H}$ ): 8  $\mu\text{s}$ . The apparent self-diffusion coefficient  $D_{\text{app}}$  was determined by fitting the decay of the echo amplitude.<sup>15</sup> The standard derivation for fitting was about 5%.

## **Results**

### *Viscosity of PKS/PEO mixture*

Viscosity measurements were used to study the complex formation between PEO and PKS. The structure and properties of PKS are summarized in Figure 1 and Table 1. Compared with the viscosity of pure polymer solutions, increased viscosity can be an indicator for interpolymer complex formation.<sup>27</sup> Furthermore, shear thinning is regarded as a criterion to evaluate the stability of formed complexes.

Figure 3 shows the relative viscosity ( $\eta_r$ ) of PEO in the absence or presence of five PKS samples with phenolic mole fractions ranging from 0.34 to 0.82 at [PEO]= 25 mg/L.  $\eta_r$  was herein defined as the viscosity of polymer solution with respect to pure water.  $\eta_r$  values of PEO/PKS mixtures were higher than the  $\eta_r$  for pure PEO solution (1.0 mPa.s), showing that PEO formed water-soluble complexes with PKS.

Neither  $\eta_r$  of pure PEO solution nor PEO/PKS mixtures changed with time at a shear rate of  $37.3 \text{ s}^{-1}$ , revealing that both PEO solution ( $M_w=1 \times 10^6 \text{ Da}$ ) and PEO/PKS complexes were stable, they did not degrade under the current experimental conditions.

The  $\eta_r$  values decreased with increasing phenolic content in PKS at a PEO/PKS mixing ratio (w/w) of 2 (see Figure 4). The decrease in  $\eta_r$  with phenolic

content suggested that the apparent size of PEO/PKS complexes depended on the phenolic content.

*The effect of phenolic content on size of PEO/PKS complexes*

Phenolic groups have been widely proposed in the literature as main interaction site for binding with PEO.<sup>1,2,4</sup> Our recent NMR studies demonstrated that both types of aromatic rings in PKS interacted with PEO,<sup>22</sup> although the interaction between phenolic group and PEO was stronger than the interaction between styrene sulfonate group and PEO (Chapter 2). Viscosity studies also suggested a possible relationship between phenolic content and size of complexes (Figure 4). Thus, DOSY was used to confirm the effect of phenolic content on the apparent size of PKS/PEO complexes.

The reliability of the DOSY measurements was confirmed by comparison with mutual diffusion coefficient determined by dynamic light scattering (Data was not shown here). By extrapolating into infinite dilution, both self-diffusion coefficient and mutual diffusion coefficient from DOSY and DLS gave the absolute diffusion coefficient ( $D_o$ ) as  $6.12 \pm 0.2 \times 10^{-12}$  m<sup>2</sup>/s at 25°C. This  $D_o$  value was within 2% error of the value calculated from the reference.<sup>7</sup>

Figure 4 shows that apparent self-diffusion coefficient ( $D_{app}$ ) of complexed PEO increased with phenolic molar content in PKS. The apparent self-diffusion coefficient was used to emphasize the effect of concentration. The overlap

concentration ( $C^*$ ) for PEO,  $C^* = 2.5/[\eta]$ ,<sup>28</sup> would be much higher than 1 g/L (i.e. approximately 4.4 g/L). PEO concentration used in this study was 1 g/L. In the dilution region, concentration decreases the self-diffusion coefficient simply by the increase in the viscosity.<sup>29</sup> It seems reasonable to assume the effect of concentration on self-diffusion coefficient to be the same both in pure PEO solutions and PKS/PEO solutions at same PEO concentration,  $D_{app}$  was inversely proportional to the apparent size of macromolecules. The increase in  $D_{app}$  value with phenolic content was thus interpreted as decreased size of complexes. That is to say, large complexes formed at low phenolic content.

The effect of phenolic content was proposed to be not due to the different molecular weight of PKS; as there was no clear trend in molecular weight for these five PKS copolymers (See Table 1).

The  $D_{app}$  of 1g/L PEO ( $M_w 1 \times 10^6$  Da) was  $4.9 \times 10^{-12}$  m<sup>2</sup>/s. The substantial decrease in  $D_{app}$  of PKS/PEO mixture, compared with free PEO, suggested that multiple PEO chains were involved in the complex formation. In other words, the presence of phenolic polymer greatly increased the apparent size of the PEO.

#### *The effect of mixing ratio on the apparent size of the complexes*

Molecular modeling studies predicted that steric restriction between PEO and cofactor prevents perfect registration of two polymers in complexes.<sup>2,6</sup> Our recent NMR studies suggested that bound PEO segments resided on the top or bottom of

aromatic rings of cofactor.<sup>22</sup> If the prediction is correct, maximum complex formation should be expected when the monomeric ratio of PEO/aromatic ring of PKS greater than 1. Thus, PKS .48 was labeled with fluorescence dye 5-DTAF, and fluorescence photobleaching recovery was used to study the effect of mixing ratio on transport properties.

Figure 5 shows the apparent self-diffusion coefficient ( $D_{app}$ ) for 5-DTAF labeled PKS.48 as a function of PEO/PKS.48 mixing ratios that were expressed as monomeric ratio of PEO/aromatic ring of PKS used. The concentration of PKS.48 was kept constant. By adding different amounts of PEO into labeled PKS.48,  $D_{app}$  decreased first to reach the minimum value when monomeric ratio= 1.8 to 2.9, then increased with further addition of PEO.

FPR measurement gives  $D_{app}$  as weight averaged self-diffusion coefficient of all the diffusers, including the uncomplexed free PKS.48 and all the complexed PKS.48. Therefore, the minimum  $D_{app}$  corresponded to the maximum complex formation. Taking into the consideration that most of PEO and PKS were involved in complex formation at this mixing ratio, it is concluded that the maximum complexes were formed when monomeric ratio of PEO/aromatic ring was 2.5.

The  $D_{app}$  for PKS.48/PEO (w/w)=2 measured by FPR was  $8.7 \times 10^{-13} \text{ m}^2/\text{s}$  while DOSY yielded  $9.1 \times 10^{-13} \text{ m}^2/\text{s}$  which was in a good agreement.

The decrease in  $D_{app}$  cannot be attributed to the viscosity of PEO, as the viscosity of PEO with  $M_w 1.0 \times 10^6$  Da was 1.0 mPa.s, only slightly larger than pure water, which would not be able to cause such profound decrease in  $D_{app}$ . Also, if the viscosity of PEO played important role here,  $D_{app}$  would have simply decreased with the addition of PEO.

#### *The effect of temperature on the size of complexes*

In general, increasing temperature increases the diffusion coefficient of macromolecules in two ways: by increasing thermal energy  $kT$  and reducing the hydrodynamic interaction by reducing fluid viscosity (see Equation 1). Heating promotes the complex formation between PEO and cofactor, as shown by our recent NMR studies,<sup>22</sup> the size of complexes should decrease. On the other hand, an increase in temperature promoted self-aggregation of PEO,<sup>30</sup> thus it would be possible to have large complexes when raising temperature.

Figure 6 shows  $D_{app}$  values for PEO/PKS.48 complexes as a function of temperature. The hydrodynamic radius of a random coil PEO in a dilute regime did not change with temperature at range from room temperature to 43°C.<sup>30</sup> Theoretical calculation according to the Stokes-Einstein equation shows that the diffusion coefficient exponentially increases with temperature. The different slopes of  $\log(D_{app})$  versus  $\frac{1}{T}$  revealed that temperature affected the self-diffusion coefficient for PKS.48/PEO complexes in a complicated fashion.

In order to study the reversibility of temperature effects, PEO/PKS.48 complexes were heating to 50°C and then cooled to 27°C. No hysteresis in  $D_{app}$  value was observed. This reversibility was in a good consistence with the results obtained by  $^1\text{H}$  NMR.<sup>22</sup>

*The effect of ionic strength on the size of the complexes*

Ions screen the electrostatic repulsion between charged styrene sulfonate groups. Therefore, the apparent self-diffusion should increase with ionic strength.

Figure 7 shows the effect of KCl on  $D_{app}$  of PKS.48/PEO mixture at 25°C. Except for the KCl concentration, all the other experimental conditions were constant. With increasing KCl concentration,  $D_{app}$  increased by about 6 times until the concentration of KCl reached 15 mM. Increasing the KCl concentration to 50 mM, resulted in phase separation. By contrast, PEO does not phase separate from 50 mM KCl at temperatures below 97°C. Pure PKS cannot be salted out by 50 mM KCl at the temperature studied. The salting out of PKS/PEO complexes suggests that the hydrophobicity of PKS/PEO complexes was higher than both of pure PEO and pure PKS, although our surface tension measurements showed that PEO/PKS aqueous solution had a almost same surface tension as water at 25°C, indicating that PEO/PKS complexes were not surface-active.

Phase-separated complexes were obtained by decanting from 100 mM KCl supernatant. They could be re-dissolved completely in pure water indicating that the salting out was a reversible process.

Viscosity measurement was also used to monitor  $\eta_r$  for PKS/PEO at different ionic strength values. As shown in Figure 7, the relative viscosity  $\eta_r$  decreased with increasing KCl concentration.

Cox proposed that the decrease of the viscosity of polyelectrolytes with added salt obeyed the following equation.<sup>31</sup>

$$\eta = \eta_o \left( \frac{C_s}{C_s^o} \right)^{-m} \quad (3)$$

Where  $C_s$  is the salt concentration,  $\eta_o$  is the viscosity at arbitrary salt concentration  $C_s^o$ .

Dividing by the viscosity of water gives

$$\eta_r = \eta_{ro} \left( \frac{C_s}{C_s^o} \right)^{-m} \quad (4)$$

Equation 4 was applied to our results by plotting  $\ln(\eta_r)$  versus  $\ln(C_s)$  which yielded a straight line, with  $m=0.57$  which is very close to 0.6 for synthetic polyelectrolytes<sup>31</sup>. The correlation constant R was 0.98.



### *Effect of PEO molecular weight on the complex formation*

The molecular weight of polymers is important if complex formation is a cooperative process. Five PEO samples with molecular weight ranging from  $8 \times 10^3$  to  $1 \times 10^6$  Da were used to investigate the importance of PEO molecular weight in complex formation. Figure 8 showed that up to  $1 \times 10^5$  Da, there was no obvious change in  $D_{app}$ , suggesting no substantial complexes were formed. Therefore,  $1 \times 10^5$  Da was regarded as the critical molecular weight for PEO to form complex with PKS.

### *The effect of low Mw PEO on fluorescence emission intensity*

The FPR study on the effect of PEO molecular weight showed that a substantial decrease in  $D_{app}$  was observed when the PEO molecular weight was higher than  $1 \times 10^5$  Da. Therefore it was of interest to investigate with fluorescence spectroscopy if low molecular weight PEO interacts with PEO.

Figure 9 shows that the change of emission intensity of labeled PKS.48 at 498 nm with the addition of PEG. The relative intensity was herein defined as the emission intensity of labeled PKS.48 in the presence of PEO /the emission intensity of PKS in the absence of PEO. PEO greatly enhanced the relative emission intensity of PKS. This result suggested that PEO also interact with labeled PKS.48.

## ***Discussion***

Water-soluble poly(vinyl phenol-co-styrene sulfonate potassium) (PKS) forms water-soluble complexes with high molecular weight PEO. By investigating the transport phenomena of PKS/PEO complexes at different PEO molecular weight, phenolic contents (molar fractions), PKS/PEO mixing ratios, temperatures and ionic strengths, we obtained the information about the factors affecting the apparent size of PKS/PEO complexes. The macroscopic properties are now discussed in terms of the microscopic interactions.

The apparent diffusion coefficient ( $D_{app}$ ) of PKS/PEO complexes changes with PEO concentration. Maximum amount of the complexes were formed when monomeric ratio of PEO/aromatic ring reached 2.5 (Figure 5). Our earlier work showed that upon complex formation, PEO segments reside above or below the phenolic ring of PKS.<sup>22</sup> Thus, it is proposed that the maximum number of PEO/phenolic ring in the complexes is limited by the space around phenolic rings. This result supports the molecular modeling study by Pelton et al. that steric restriction between PEO and poly(vinyl phenol) oligomers prevents the perfect registration of two polymer when forming complexes.<sup>2</sup>

The  $D_{app}$  values of complexes were up to 6 times smaller than that of the pure PEO coil. Thus, the hydrodynamic radius ( $R_h$ ) of PKS/PEO complexes could be 6 times larger than that of pure PEO. This can be explained by two extreme cases. One is that upon binding with PKS, the PEO chain may be expanded due to the short-

range electrostatic repulsion between charged styrene sulfonate groups. The hydrodynamic radius of variable ionized acrylamide/sodium acrylate copolymers was independent on the degree of ionization at infinite dilution.<sup>32</sup> Thus, it is unlikely that the decrease in  $D_{app}$  with complex formation was solely due to the chain expansion. The second is that PEO aggregated in the presence of PKS. Based on the increased scattering intensity, Carignan et al. proposed the aggregation of PEO in the presence of phenolic resin. This aggregation of PEO could be one of the reasons that PEO worked more efficiently as flocculants in the presence of phenolic resin.<sup>33,34,35</sup>

It is important to estimate the maximum degree of PEO aggregation, i.e., the number of PEO chains within one complex. It is difficult to isolate an "intact" complex from PEO/PKS mixture. The analytical approach developed by Dubin et al. was employed to calculate the weight-average molecular weight of complex ( $\overline{M}_x$ ):<sup>36</sup>

$$\overline{M}_x = \alpha \overline{M}_w (1 + \beta) \quad (5)$$

where  $\beta$  represents the mass ratio of bound PKS to PEO and  $\alpha$  is degree of PEO aggregation. At the maximum formation of complexes,  $\beta=2$ . The  $\overline{M}_w$  of the PEO used in our study was  $1 \times 10^6$  Da. The  $D_{app}$  of complex was  $9.0 \times 10^{-13}$  m<sup>2</sup>/s at [PEO]=1 g/L with FPR and DOSY.  $D_{app}$  of 1g/L PEO was  $4.9 \times 10^{-12}$  m<sup>2</sup>/s by DOSY. It is assumed that the relationship between the diffusion coefficient and molecular weight of PEO<sup>7</sup> is valid in the presence of PKS,

$$D \propto \frac{1}{M_w^{0.571}} \quad (6)$$

Therefore, the maximum  $\alpha$  was calculated to be 6. The importance of this number is that it shows the low possibility to form gel-like complexes for PEO with  $M_w 1 \times 10^6$  Da.

The degree of aggregation depends on PKS/PEO mixing ratio. At the highest PEO/PKS ratio (the right side of Figure 5), all of PKS are assumed to be bound with PEO. A similar calculation with Equation 5 shows that  $\alpha = 1$ . There was little PEO aggregation probably because each PEO has many unoccupied binding sites, PKS is likely to bind with single PEO chain.

The apparent size of PEO/PKS complexes depends on the phenolic content in PKS. Both DOSY and viscosity measurements showed that large complexes formed at low phenolic content while compact complexes formed at high phenolic content (Figure 4). It is generally accepted that phenolic groups are the active agents for the hydrogen bonded complex formation between cofactors and PEO<sup>1,2,6,22</sup> as well as for hydrophobic interaction.<sup>22</sup> The interactions between PKS and PEO became stronger with increasing phenolic content. Also, the low charge content decreases the short-range electrostatic repulsion between charged styrene sulfonate groups decreases. PEO and PKS chains were pulled ever closer, resulting in compact complexes,  $D_{app}$  of the complexes increased.

PKS/PEO complexes respond to added salt in a similar way as synthetic polyelectrolytes except that the complexes have a very low critical phase separation concentration (ca. 50 mM KCl). Added salt decreases the short-range electrostatic repulsion between charged styrene sulfonate groups, thus the attractions between PKS and PEO pull polymer chains ever closer. The low KCl phase separation concentration suggests that PKS/PEO complexes are more hydrophobic than PEO and PKS although the surface tension of PKS/PEO complexes did not show that the complexes are surface-active.

The  $D_{app}$  of PKS/PEO is closely related to the molecular weight of PEO. Molecular weight values higher than  $1.0 \times 10^5$  Da were required to observe a substantial decrease in  $D_{app}$  (Figure 8). One possibility is that low Mw PEO does not bind with PKS. This is unlikely because PEO increased fluorescent emission intensity of labeled PKS (Figure 9). A second possibility is that low Mw PEO binds with PKS in same way as high Mw PEO: upon complex formation ethylene groups of PEO reside on the top or bottom of aromatic rings. Our diffusion measurements are not sensitive enough to monitor the slight change in  $D_{app}$ .  $^1\text{H}$  NMR study on the complex formation showed that no upfield shift in ethylene  $^1\text{H}$  peaks from low Mw PEO, indicating that even if low Mw PEO binds with PKS, the PEO bound segments do not reside on the top or the bottom of the aromatic rings.

A third possibility is that PKS/PEO complex formation only occurs above a critical molecular weight of PEO. This critical molecular weight of PEO would be

much higher if compared with the complex formation of PEO with poly(carboxylic acid). Examples are PEO/poly(acrylic acid)(PAA)<sup>37,38,39</sup> or PEO/poly(methylacrylic acid) (PMAA),<sup>38,39</sup> in both cases the critical molecular weight of PEO was less than 7500. The difference in critical MW of PEO may be attributed to the different conformation of formed complexes. The ether oxygen of PEO hydrogen bonded with carboxylic group, resulting in a good registration between these two polymer chains, therefore forming the complexes with nearly 1:1 (mole: mole) stoichiometry. For PEO/cofactors, poor registration resulted in that several PEO segments resided above or below aromatic rings.<sup>22</sup>

Increasing temperature causes an increase in  $D_{app}$ . This behavior is opposite to that of PEO alone where increasing temperature promotes the aggregation of PEO coils,<sup>30</sup> and in a more dramatic way than just by increasing thermal energy  $kT$  and reducing viscosity (see Figure 6). Increasing temperature promoted the interaction between PEO and aromatic rings of PKS as evidenced by an increase in the number of PEO segments involved in complex formation (Chapter II).<sup>22</sup> Therefore, stronger interactions at elevated temperature pulled the polymer chains further closer to form compact complexes, thus  $D_{app}$  increased. This result suggests the existence of hydrophobic interactions.

A broader implication of this work is that the size of PEO/cofactor complexes has been shown to be closely related to mixing ratio, temperature, ionic strength and

phenolic molar content. Thus, the flocculation efficiency of PEO/cofactor as flocculants will likely be affected by these factors.

### ***Conclusions***

The main conclusions of this chapter are:

1. FPR measurements showed that PEO molecular weights higher than  $1.0 \times 10^5$  Da are required to obtain complex formation. PEO molecular weight  $8.0 \times 10^3$  Da interacts with dye labeled PKS probably as surfactants.
2. The maximum number of PEO segments residing around each phenolic ring is proposed to be limited by the space of aromatic ring of PKS. The minimum apparent self-diffusion coefficient ( $D_{app}$ ) of PKS/PEO complexes, corresponding to the maximum size, was formed by PEO/PKS (w/w)=0.45 ~0.73, which corresponds to ca 5 PEO repeating units per phenolic ring.
3. The phenolic group is the most active component for the complex formation. Increasing the phenolic molar content in PKS, increased the attraction forces and decreased electrostatic repulsions between charged styrene sulfonate groups leading to compact complexes.
4. Increasing temperature resulted in compact complexes, suggesting hydrophobic interactions contributed to the complex formation.

5. The relative viscosity decreases with salt addition, indicating that PKS/PEO complexes behave as synthetic polyelectrolytes except that the complexes phase separate from water at very low KCl concentration.



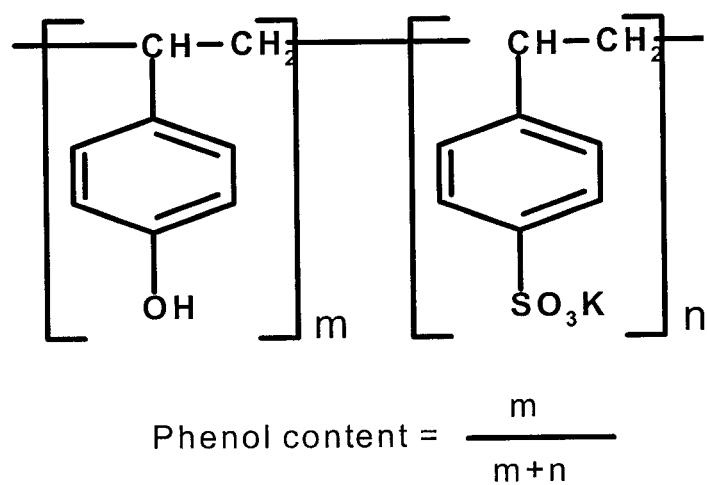


**Figure 1.** Structure of poly (vinyl phenol-co-styrene sulfonate potassium salt) (PKS)

**Table 1. Properties of poly(vinyl phenol-co-styrene sulfonate ) potassium salt**

<b>Sample</b>	<b>Phenolic Content<sup>*</sup> (Molar fraction)</b>	<b>Mw<sup>**</sup>(Da)</b>	<b>Polydispersity<sup>**</sup></b>
<b>PKS.34</b>	<b>0.34</b>	<b>141,000 ± 8, 000</b>	<b>1.4 ± 0.1</b>
<b>PKS.48</b>	<b>0.48</b>	<b>158,000 ± 5, 000</b>	<b>1.6 ± 0.1</b>
<b>PKS.67</b>	<b>0.67</b>	<b>210,000 ± 7, 000</b>	<b>1.6 ± 0.1</b>
<b>PKS.74</b>	<b>0.74</b>	<b>41,000 ± 1, 000</b>	<b>1.9 ± 0.1</b>
<b>PKS.82</b>	<b>0.82</b>	<b>127,000 ± 3,000</b>	<b>1.9 ± 0.1</b>

<sup>\*</sup>Measured by <sup>1</sup>H NMR in d<sub>6</sub>-DMSO.

<sup>\*\*</sup>*Measured by GPC-LS. The standard deviation was calculated by 3 ~5 repeat measurements.*

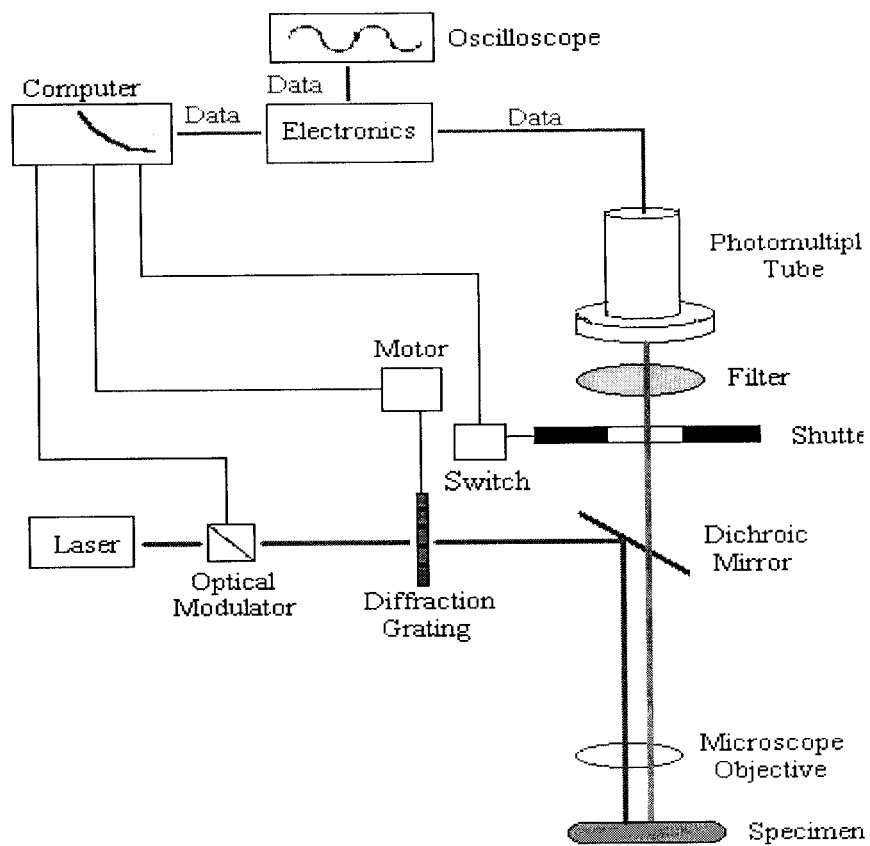


**Figure 2. A schematic diagram for fluorescence photobleaching recovery apparatus.**

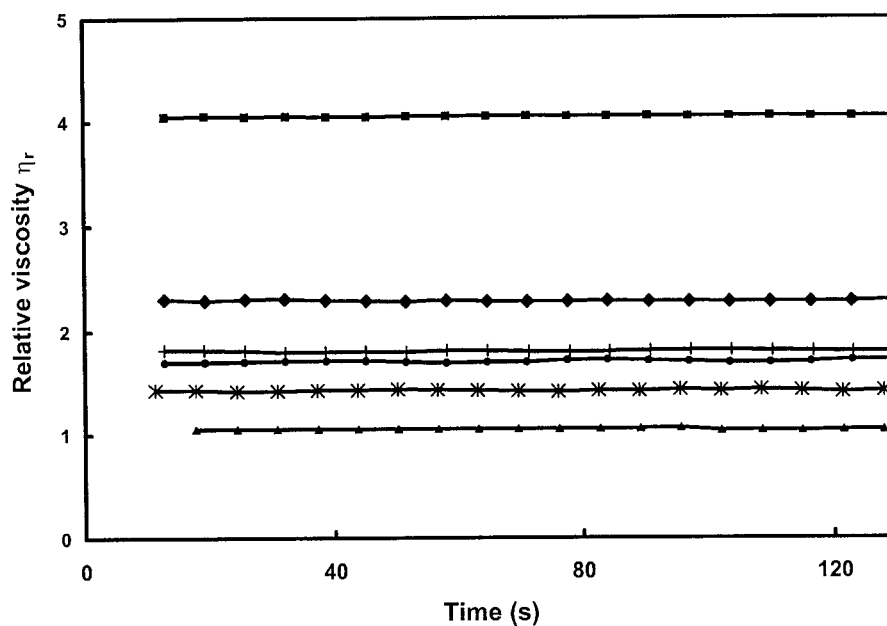
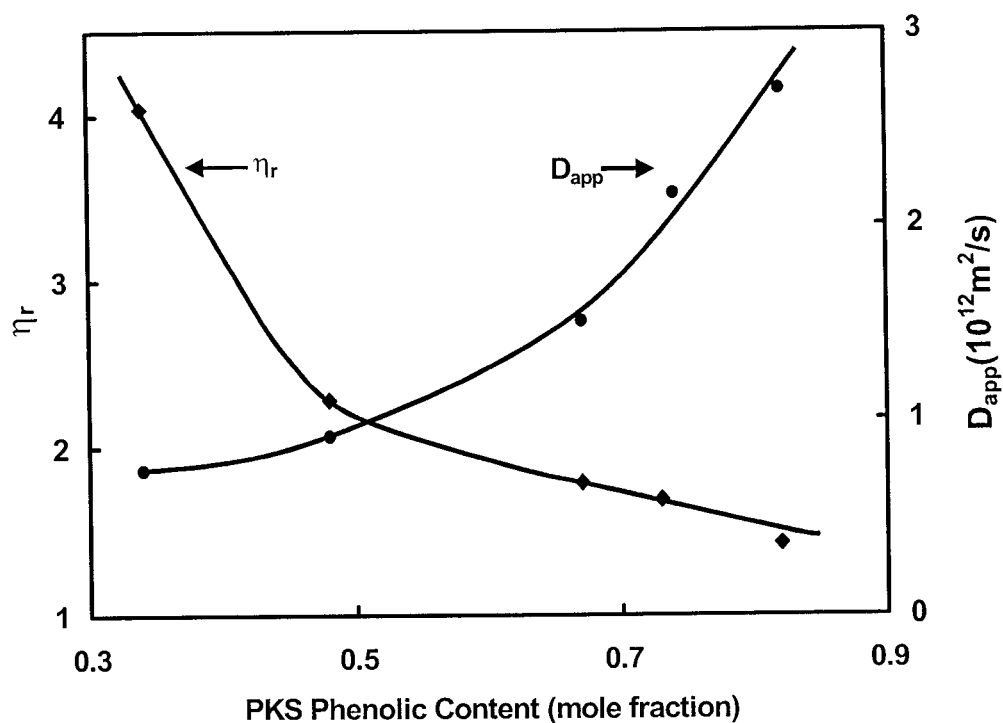
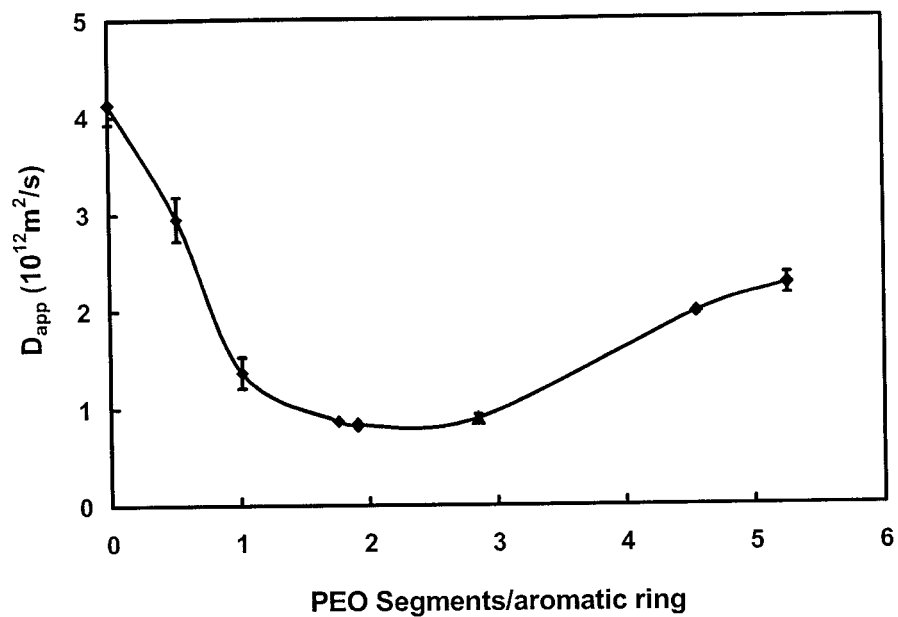


Figure 3. Relative viscosity ( $\eta_r$ ) of PKS/PEO mixtures at 25 °C. Experimental conditions: [PEO]: 24 mg/L; PEO Mw:  $1 \times 10^6$  Da; PKS/PEO (w/w): 2; shear rate:  $37.32 \text{ s}^{-1}$ . (▲) Pure PEO; (■) PKS.34/PEO; (◆) PKS.48/PEO; (+) PKS.67/PEO; (•) PKS.74/PEO; (×) PKS.82/PEO.



**Figure 4. Relative viscosity ( $\eta_r$ ) and apparent self-diffusion coefficient ( $D_{app}$ ) of PEO in the presence of PKS with different phenolic molar content. Experimental conditions: [PEO] for viscosity: 24 mg/L; PEO: Mw  $1 \times 10^6$  Da; PKS/PEO (w/w): 2; shear rate  $37.32 s^{-1}$ .**



**Figure 5.** Effect of mixing ratio of PKS.48/PEO on the apparent diffusion coefficient ( $D_{app}$ ) at 25°C. PEO  $M_w$ :  $1 \times 10^6$  Da; the concentration of PKS.48 was kept constant 1.07 g/L; no additional salt was added. The error was calculated by three repeating measurements at different parts of FPR cells by using same sample.

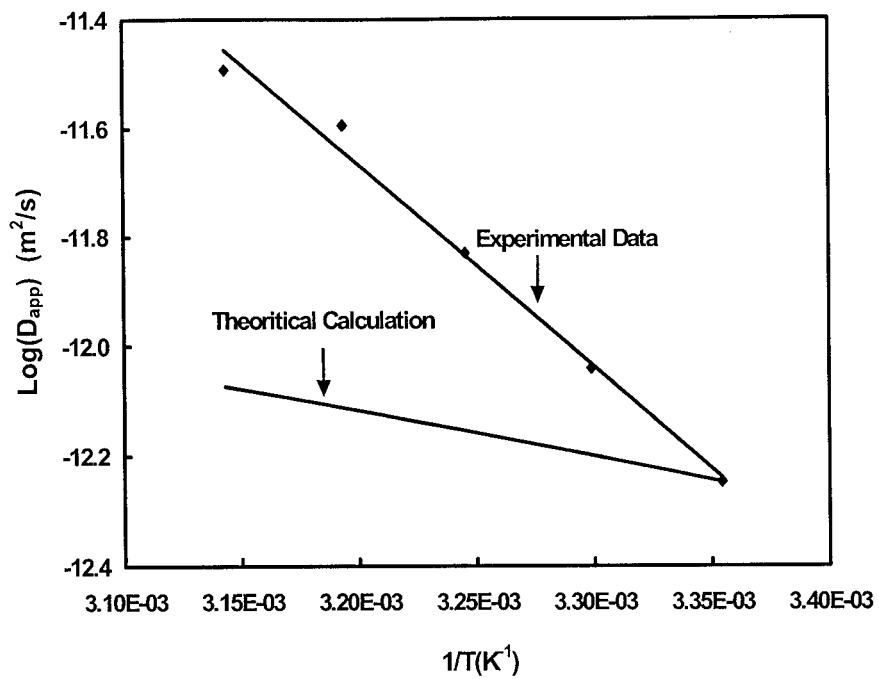


Figure 6. Apparent self-diffusion coefficient of PKS.48/PEO mixture at different temperature. PKS.48 concentration: 1.06 g/L; PKS.48/PEO (w/w)=1; PEO MW  $1 \times 10^6$  Da.

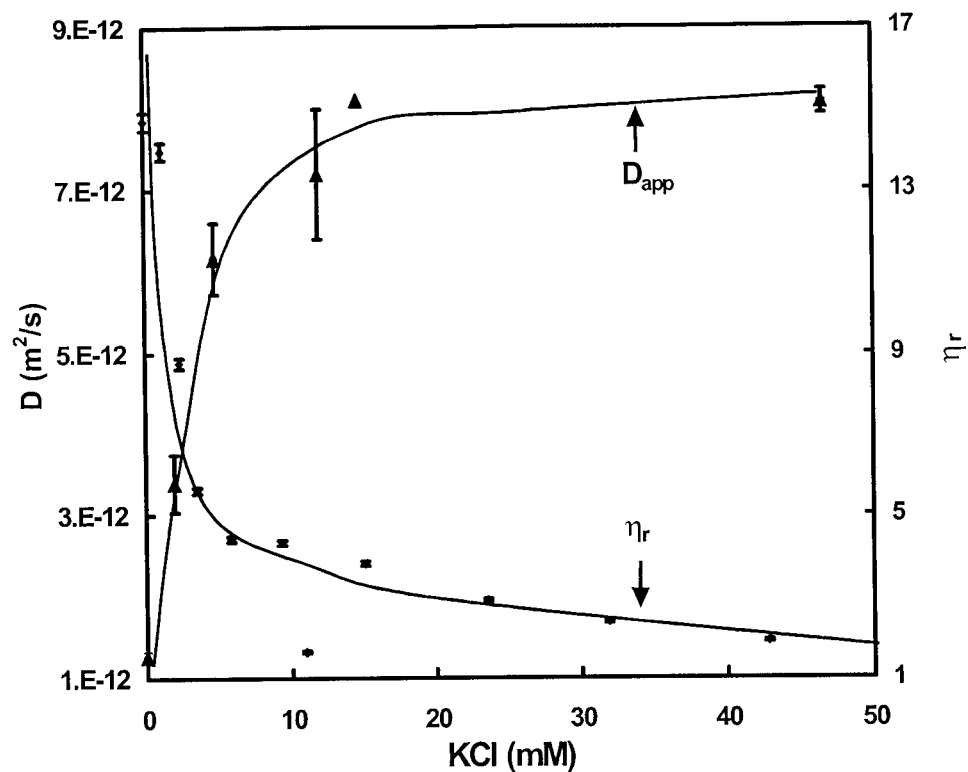


Figure 7. Effect of ionic strength on apparent diffusion coefficient and viscosity of PKS.48/PEO mixture. PKS.48 concentration:  $1.06 \pm 0.01$  g/L; PKS.48/PEO (w/w) =  $1.167 \pm 0.04$ ; PEO MW  $1 \times 10^6$  Da;  $25.00 \pm 0.02^\circ\text{C}$ , shear rate:  $37.32 \text{ s}^{-1}$



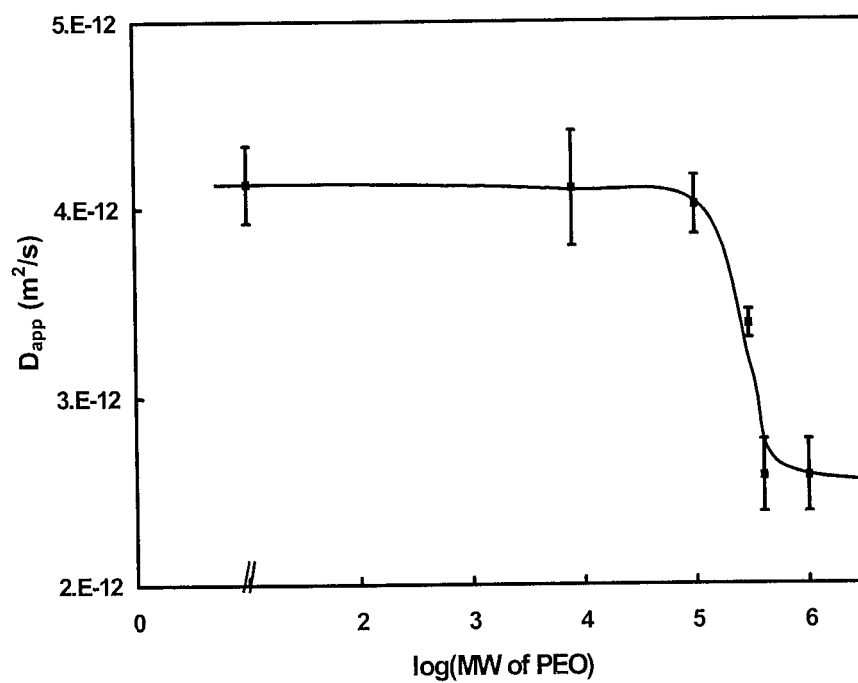


Figure 8. The Effect of MW of PEO on the apparent diffusion coefficient ( $D_{app}$ ) of PKS.48/PEO mixture at 25°C. PKS.48/PEO (w/w)=1.15, PEO concentration 1.18g/L.

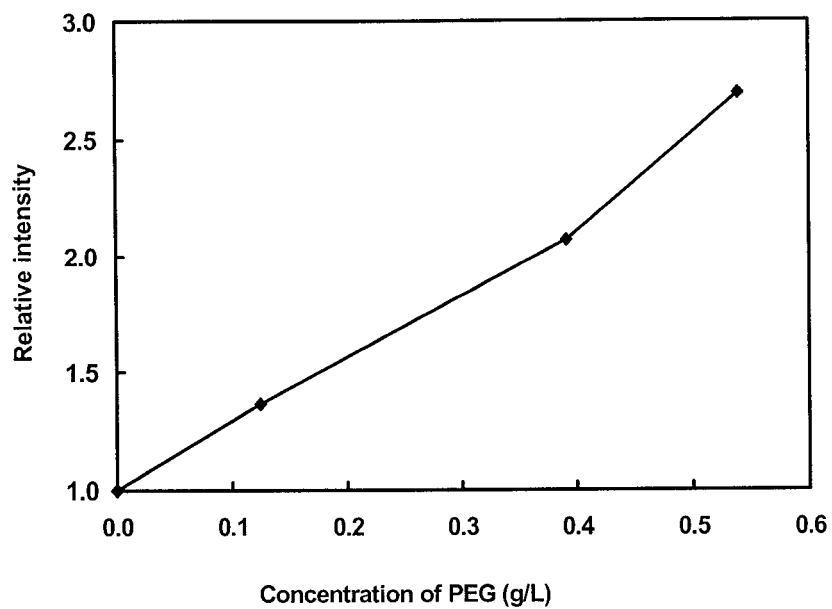


Figure 9. The effect of PEO (Mw  $8 \times 10^3$  Da) on the emission intensity of labeled PKS.48 at 498 nm. [PKS.48] = 1.0 g/L

## References

- 
- <sup>1</sup> Pelton, R. H.; Allen, L. H.; Nugent, H. M. *Pulp and Paper Canada* **1980**, *81*, T9.
  - <sup>2</sup> Pelton, R. H.; Xiao, H.; Brook, M. A.; Hamielec, A. *Langmuir* **1996**, *12*, 5756.
  - <sup>3</sup> Carignan, A.; Garnier, G.; van de Ven, T. G. M. *J Pulp Paper Sci.* **1998**, *24*, 94.
  - <sup>4</sup> Stack, K. R.; Dunn, L. A.; Roberts, N. K. *Colloids and Surfaces* **1991**, *61*, 205.
  - <sup>5</sup> Sedlak, M. *Langmuir* **1999**, *15*, 4045.
  - <sup>6</sup> Stack, K. R.; Dunn, L. A.; Roberts, N. K. *Colloids and Surfaces* **1991**, *61*, 205.
  - <sup>7</sup> Devanand, K.; Selser, J. C. *Macromolecules* **1991**, *24*, 5943.
  - <sup>8</sup> Polverari, M.; van de Ven, T. G. M. *J. Phys. Chem.* **1996**, *100*, 13687.
  - <sup>9</sup> Devanand, K.; Selser, J. C. *Nature* **1990**, *343*, 739.
  - <sup>10</sup> Porsch, B.; Sundelöf, L. O. *Macromolecules* **1995**, *28*, 7265.
  - <sup>11</sup> Bloomfield, V. A. *Biopolymer* **2000**, *54*, 168.
  - <sup>12</sup> Lanni, F.; Ware, B. R. *Rev. Sci. Instrum.* **1982**, *53*, 907.
  - <sup>13</sup> Ware B. R. *American Laboratory* **1984**, 18.
  - <sup>14</sup> Fong, B.; Stryjewski, W.; Russo, P. S. *J. Colloid Interface Sci.*, **2001**, *239*, 374.
  - <sup>15</sup> Johnson, C. S. Jr. *Progr. NMR Spectrosc.* **1999**, *34*, 203.
  - <sup>16</sup> Blum, F. D. *Spectroscopy* **1986**, *1*, 32.
  - <sup>17</sup> Jerschow, A.; Müller, N. *Macromolecules* **1998**, *31*, 6573.
  - <sup>18</sup> Van Gorkom, L. C. M.; Hancewicz, T. M. *J. Magn. Reson.* **1998**, *130*, 13.
  - <sup>19</sup> Morris, K. F.; Johnson, C. S. Jr. ; Wong, T. C. *J. Phys. Chem.* **1994**, *98*, 603.
  - <sup>20</sup> Chen, A.; Wu, D. H.; Johnson, C. S. Jr. *J. Phys. Chem.* **1995**, *99*, 828.
  - <sup>21</sup> Gibbs, A.; Yang, Z.; Xiao, H.; Pelton, R. H. *Transactions of 4th Fundamental Resource Conference, PIRA International, Leatherhead, UK* **1997**, 1135.
  - <sup>22</sup> Cong, R.; Bain, A.; Pelton, R. H. *J. Poly. Sci Part B* **2000**, *38*, 1276.
  - <sup>23</sup> Molecular Probe, Inc. *Handbook of Fluorescent Probes and Research Products*, Chapter 6
  - <sup>24</sup> Mustafa, M. B.; Tipton, D.; Russo, P. S. *Macromolecules* **1989**, *22*, 1500.
  - <sup>25</sup> Bu, Z.; Russo, P. S. *Macromolecules* **1994**, *27*, 1187.

- 
- <sup>26</sup> Longworth, L. G. *J. Phys. Chem.* **1960**, *64*, 1914.
- <sup>27</sup> Hara, M. *Polyelectrolytes: Science and Technology*; Marcel Dekker, Inc., New York, **1992**
- <sup>28</sup> Brown, W.; Stilbs, P.; Johnson, R. M. *J. Polym. Sci. Part B* **1983**, *21*, 1029.
- <sup>29</sup> Zero, K.; Ware, B. R. *J. Chem. Phys.* **1984**, *80*, 1610.
- <sup>30</sup> Brown, W. *Macromolecules* **1984**, *17*, 66.
- <sup>31</sup> Cox, R. A. *J. Polym. Sci.*, **1960**, *47*, 441.
- <sup>32</sup> Reed, W. F.; Ghosh, S.; Medjahdi, G.; Francosi, J. *Macromolecules* **1991**, *24*, 6189.
- <sup>33</sup> Xiao, H.; Pelton, R. H.; Hamielec, A. *J. Poly. Sci.* **1995**, *33*, 2605.
- <sup>34</sup> van de Ven, T. G. M.; Alince, B. *J. Pulp Paper Sci.* **1996**, *22*, J257.
- <sup>35</sup> Lindström, T.; Glad-Nordmark, G. *Colloids Surface* **1984**, *8*, 337.
- <sup>36</sup> Xia, J.; Dubin, P. L.; Dautzenberg, H. *Langmuir* **1993**, *9*, 2015.
- <sup>37</sup> Tsuchida, E.; Osada, Y.; Ohno, H. *J. Macromol. Sci.-Phy.* **1980**, *B17*, 683.
- <sup>38</sup> Bailey, F. E.; Lundberg, R. D.; Callard, R. W. *J. Polym. Sci. Part A* **1964**, *2*, 845.
- <sup>39</sup> Osada, Y.; Sato, M. *Polym. Lett. Edi.* **1976**, *14*, 129.

## **Chapter IV A model colloid for flocculant testing**

### *Abstract*

This paper proposes dextran sulfate-modified precipitated calcium carbonate particles (DS-PCC) as a new colloidal model. Negatively charged dextran sulfate (DS) adsorbs on positively charged PCC surfaces, changing the surface charge from positive to negative, and sterically stabilizing the PCC particles. The characterization of this new model is given and its utility as a colloidal model in wet-end retention is demonstrated by its flocculation behaviour in the presence of cationic polyacrylamide, and poly (ethylene oxide) (PEO) in conjunction with commercial cofactor, added as retention aids.

### ***Introduction***

Water-soluble polymers are employed in papermaking to enhance the deposition of colloidal filler particles onto the fibers and to improve the physical properties of the resulting paper. Polymeric flocculants, or retention aids, are required to incorporate colloidal material. More recently there has been much interest in using retention aids in the processing of mechanical pulps. Mechanical pulping processes produce high concentrations of a mixture of dissolved and colloidal substances (DCS). They are sometimes referred to as anionic trash.<sup>1,2,3</sup> They bind with cationic charged flocculants, leading in a high cationic demand. Some of them interfere with the retention of filler, for example by adsorption onto the filler surfaces.<sup>4</sup> This changes the surface properties of the particles involved, sterically stabilizing them and making them more difficult to flocculate. In order to understand retention aid mechanisms, highly hydrophobic and negatively charged polystyrene,<sup>5,6,7</sup> and positively charged precipitated calcium carbonate (PCC)<sup>8,9</sup> have been widely used in laboratories as model fillers. Research using these compounds is invaluable for determining mechanisms, but has a very limited ability to predict the behavior of retention aids in commercial mechanical pulp suspensions.

In order to narrow the gap between practice and bench, some research groups have used white water from mills containing DCS to dilute fillers.<sup>10</sup> Although

effective, white waters from mills are continuously changing composition so it is impossible to compare results from day to day.

Commercial PCC was chosen as the target colloidal filler. However PCC in water is not ideal because the pH of a PCC suspension is about 9.5 at equilibrium at ambient atmosphere, and its surface is slightly negatively charged and sensitive to the carbon dioxide concentration.<sup>11</sup>

This paper describes the characterization of the surface properties of a new colloidal model produced by the adsorption of dextran sulfate (DS) onto PCC, and the flocculation behavior of the model system with a variety of flocculants. This well-defined new model is expected to have similar surface properties to PCC suspended in actual pulp furnish.

## *Experimental*

### *Materials*

Precipitated calcium carbonate (PCC) was a gift from Mineral Research Centre (Bethlehem, PA), with a reported average diameter of 1.22  $\mu\text{m}$  and a specific surface area of 12.0  $\text{m}^2/\text{g}$ . PEO (Polyox 309), MW=9,000,000, and cofactor ACS (trade name OXIREZ)<sup>12</sup> were gifts from Union Carbide (Danbury, CT) and Allied Colloids (Bradford, UK) respectively. DS, MW=10,000, was purchased from Sigma (Oakville, ON) as the sodium salt with 2.3 sulfate groups per glucosyl residue. 1mM potassium polyvinyl sulphate (PVSK) and 1 mM polybrene were purchased from

Testing Machines Inc. (Islandia, NY). 0.1 M HCl was prepared using Acculute® concentrate from Anachemia (Rouses Point, NY). Superfloc® C-496, C-494, C-492 and C-491 are high molecular weight (5-7 million) copolymers of polyacrylamide and trimethylaminoethyl acrylate chloride with cationicities of 35, 20, 10 and 5 % respectively and are referred to in the text as CPAM35, CPAM20, CPAM10 and CPAM5. Superfloc N-300 is polyacrylamide with a molecular weight above 10 million Da and is referred to as PAM. They were obtained as a gift from Cytec Industries (West Paterson, NJ).

### *Procedures*

#### *Preparation of DS-modified PCC (DS-PCC)*

PCC stock solutions with varying DS content were prepared from 0.625g PCC and an aliquot (0 – 8 mL) of 10 g/L DS, then made up to 12.5 g. The solutions were gently mixed for 24 hours on a rotating mixer. Standard DS-PCC stock solution was prepared from 0.125 g of DS and 6.25 g of PCC made up to 125 g with water to give a PCC concentration of 50 g/kg.

Stock solutions were diluted fifty-fold before use. The pH after such a dilution was 9.5. The pH of the suspensions were generally adjusted by including 1.8 mL of 0.1 M HCl in the 250 mL volume prepared for flocculation measurements, giving a pH of ~7.7. The pH of one such suspension was monitored for 10 days.



### *Colloidal characterization*

#### *Adsorption isotherm of DS on PCC*

The isotherm adsorption of DS on PCC surface was obtained using a Rank Brothers Charge- Analyzer II to measure residual DS concentrations.

A calibration curve was prepared as follows: 300 mL 1 g/L PCC suspension at pH 7.7 was filtered with suction and then passed through a 0.45  $\mu\text{m}$  milli-pore filter. The filtrate was used to prepare standard solutions containing 0, 13.33, 24.28, 15.26 and 36.11 mg/L DS. Standard solution (20.00 g) was added to the titration beaker containing 50-60 ml water. Polybrene (3.000 or 6.000 mL of 0.001M) was added to give an excess positive charge and the solution was back titrated with 0.001M PVSK to neutral charge. A linear regression line was obtained with  $R=0.9995$ .

PCC suspensions (1g/L) at pH 7.5 containing 0.00, 5.73, 9.33, 12.11, 16.73, 22.60 and 33.45 mg/L DS were prepared with vigorous shaking, then kept overnight to reach adsorption equilibrium. The suspensions were filtered with a 0.45  $\mu\text{m}$  milli-pore filter and the filtrate (20.00 g) was back-titrated as described above.

#### *Desorption experiment*

DS solution (2.911g of 1.000g/L) was added to 120.0 ml of 1.000g/L PCC suspension, giving a final DS concentration of 23.68 mg/L. The suspension was kept at room temperature overnight to reach the adsorption equilibrium, after which time

most of the particles had precipitated and the supernatant was decanted. An amount of 30.00 mL PCC supernatant without DS (prepared in a similar fashion but from a suspension of unmodified PCC ) was added to the PCC precipitate. The suspension was well shaken and kept at room temperature for 41 hours. The suspension was then filtered with a 0.45  $\mu\text{m}$  millipore filter and back-titrated (excess polybrene then PVSK) in duplicate, to determine if any free DS was present. In order to improve the titration sensitivity, 43.82 g instead of 20.00g of the supernatant was used in the back titration.

*Determination of concentration of ions in the supernatant.*

Suspensions of 1g/L PCC containing 1.8 mL 0.1 M HCl and either no DS or 20 mg/L DS were prepared. After 3 hours they were filtered through 0.45  $\mu\text{m}$  Millipore filters, the pH was measured and the concentration of calcium was determined using inductively coupled plasma (ICP, Wetland Biogeochemistry Institute, Louisiana State University, Baton Rouge, LA 70803, USA)

*Electrophoretic mobility*

The electrophoretic mobility of PCC dispersions was measured with a Coulter Delsa 440SX using 1 g/L PCC at pH 7.7. Mobilities were calculated from the analysis of the parabolic curve.<sup>13</sup>

### *Sedimentation experiment*

Well-shaken 1g/L PCC suspension at pH 7.7 was added to a 1 cm optical cell. The absorbance was read against water at 300, 400, 450 and 500 nm with a Hewlett 8452A Packard Diode Array Spectrophotometer. PCC particles settled over time as shown by decreased absorbance readings. The result was converted to turbidity by taking  $A/A_{t=0}$ , so that results were comparable to those obtained from the PDA, although in this case they were obtained in the absence of shear.

### *Dynamic light scattering (DLS)*

The average diameter of DS- PCC particles was measured by dynamic light scattering measurements with a Brookhaven Model BI-9000AT with digital correlation, a BI-2000SM goniometer and a Lexel (25 mw) argon laser with an incident wavelength of 514 nm. The data was processed by CONTIN with exponential sampling. Several drops of 1000 ppm DS-PCC at pH 7.7 were added to a vial containing 0.001 M NaCl. It was impossible to measure the average diameter of unmodified PCC particles by dynamic light scattering because of sedimentation of the particles.

### *Disc centrifugation*

The average diameters and cumulative particle size distributions of DS- PCC and unmodified PCC were also measured by disc centrifugation with a Brookhaven Disc Centrifuge Particle Sizer. PCC suspension (15.0 ml of 1000 ppm adjusted to pH

7.7) was added into the disc at 1500 rpm and measured with homogeneous start mode operation at room temperature.

### *Flocculation Experiments*

Flocculations of DS-PCC suspensions (5 mL stock DS-PCC made up to 250 mL after pH adjustment) were followed using a Photometric Dispersion analyzer, the operation of which has been described previously.<sup>14</sup>

When PEO and the commercial cofactor ACS were used to initiate flocculation, the PEO dosage was 2 g/kg of solid content; the ratio of cofactor/PEO (w:w) was 2.

PCC suspensions with variable concentrations of DS were flocculated using 1 mL 5.0 g/L CPAM10 or 1 mL 5.0 g/L CPAM35. After the flocculation was complete (the turbidity remained constant) an aliquot of the suspension was allowed to spread out in a petri dish. Pictures of flocs were obtained using a microscope (M420, Wild), with a camera (Panasonic CCTV) interfaced to a computer using Asymetrix DVP Capture 4.0 software.

Standard DS-PCC suspensions were flocculated using various aliquots of 1.0 g/L or 5.0 g/L suspensions of CPAM5, CPAM10, CPAM20, CPAM35 and PAM.

## **Results**

### *Adsorption of DS*

The isotherm for the adsorption of DS onto PCC is shown in Fig. 1. No obvious desorption of DS from DS-PCC particle surfaces was detected when DS-PCC was resuspended in the supernatant from unmodified PCC.

### *The effect of DS concentration on flocculation*

The propensity of this system to undergo flocculation was then studied as a function of the amount of DS present in a 1.0 g/L aqueous suspension of PCC. Initially, increasing the DS content dramatically increased the ability of 20 mg/L CPAM10 to initiate flocculation of the suspended PCC, in terms of both flocculation rate and final relative turbidity while the concentration of DS above 16  $\mu\text{g/mL}$  caused decreased flocculation efficiencies (Figs 2 and 3). Repeating these experiments with CPAM35 as flocculant gave identical results (Figure 3). It was also noted that the flocs produced in the systems varied in size as a function of the amount of DS present in the PCC suspension. Increasing flocculation is reflected in an increase in the height of the RMS signal from the PDA, which parallels the decrease in turbidity. An increase in the amplitude of the oscillations in both the relative turbidity and RMS signal reflects the presence of many large flocs (Figs 2 and 4). The addition of DS changed the flocs from small finely divided flocs (Figure 5a) to larger flocs (Figure 5b), to small elongated or string-like flocs (Figure 5c) and finally to large flocs (Figs.

5d and 5e) which seemed to be clumps of those seen previously. Some of the long stringy clumps were several centimeters long and half centimeter across. The production of sticky strings of precipitate was also seen when solutions of the cationic polyacrylamide copolymers were titrated with solutions of DS. Although a few large flocs were formed with the higher concentrations of DS, the flocculations were incomplete, as evidenced by the many small particles seen in the background of Figs 5d and 5e. The presence of 100 mg/L DS (Figs 2 and 4) acted to stabilize the PCC in suspension. Subsequent experiments were carried out using 1.0 g/L PCC containing 20 mg/L DS, which is referred to below as DS-PCC.

#### *Characterization of DS-PCC*

##### *Ion content and pH*

The pH of a PCC suspension was not altered by the addition of DS. The pH of a DS-PCC suspension was shown to remain constant after adjustment for at least 10 days. Adjustment of the pH to values lower than 7 caused significant dissolution of the PCC. The calcium concentration (27 mg/L) was not changed by the addition of DS.

##### *Electrophoretic mobility*

The mobility of PCC at pH 7.5 was  $+1.32 \times 10^{-8} \text{ m}^2/\text{Vs}$ .<sup>14</sup> Treatment with 20 mg/L DS caused a dramatic decrease in mobility to  $-(2.17 \pm 0.16) \times 10^{-8} \text{ m}^2/\text{Vs}$ .

### *Sedimentation*

Figure 6 shows the turbidity of both a PCC and a DS-PCC suspension as a function of time as determined by measurements of transmitted light of 400 nm. Results using 300, 450 and 500 nm were similar. For the unmodified PCC, the turbidity dropped dramatically in the first hour, indicating that unmodified PCC particles were easy to sediment. The DS-PCC suspension exhibited only a slight change in turbidity over the same time period, and even after 5 hours a significant fraction of the particles had still not settled out.

### *DS-PCC particle size*

Figure 7 shows the cumulative distribution of particle diameter for PCC and DS-PCC, as obtained from disc centrifugation measurements. Surprisingly, for every cumulative percentage, DS-PCC had a relatively smaller diameter than that of unmodified PCC. In addition, there were no particles of DS-PCC with a diameter larger than 2.1  $\mu\text{m}$ , although the unmodified PCC suspension contained some particles as large as 4.0  $\mu\text{m}$ . Measurements using disc centrifugation and dynamic light scattering also indicated that the average diameter of DS-PCC particles was smaller than that of unmodified PCC (Table 1). Our measurement for the latter was in close agreement with that of the manufacturer (1.22  $\mu\text{m}$ ).

### *Flocculation*

Figure 8 shows the flocculation results for DS-PCC and PCC itself after the addition of ACS and PEO retention aid. Untreated PCC was completely flocculated with PEO in the presence of ACS cofactor. In contrast, the DS-PCC was poorly flocculated by the PEO/ACS combination and was completely unaffected by PEO alone.

Figure 9 shows the flocculation results for DS-PCC with PAM and a suite of CPAMs of varying cationicity. The flocculation behaviour of the CPAMs was quite distinct from that of polyacrylamide, but the actual degree of cationicity of the CPAM seemed to be unimportant. At low concentrations, PAM was somewhat more effective than CPAM in producing flocculation.

Flocculations involving DS-PCC where the supernatant contained no DS were much more efficient in terms of the amount of flocculant required (Fig 9), and produced only small flocs.



### *Discussion*

DS is a good model compound for dissolved colloidal substances (DCS). It is a negatively charged, hydrophilic polymer. When DS was mixed with positively charged PCC particles, the electrostatic attraction resulted in adsorption of the DS onto the PCC surface (Figure 1). Electrophoresis measurements provided additional evidence for the adsorption of DS onto PCC surfaces, with the particle-charge becoming extremely negative after the addition of DS.

The effect of the adsorption of the DS on the propensity of the PCC to be flocculated by a cationic copolymer of polyacrylamide was quite dramatic. Optimal flocculation occurred when 16 mg/L DS were present in the 1 g/L PCC suspension. At this point, coverage of the PCC with DS was almost complete and 8 mg/L were free in solution. Our results suggest that the DS adsorbed onto the positive surface of the PCC, producing regions of negative charge onto which the cationic flocculant could adsorb. As more adsorbed, more flocculation resulted.

When more than the optimum amount of DS was added to a PCC suspension, the concentration of free DS was significantly increased, causing a decrease in the flocculation rate. We attributed this to the sequestering of much of the polymer by the free DS. This mimics the effect of the DCS that is present in pulp furnish. It was also noted that the size and nature of the flocs produced varied with the amount of DS present in the PCC suspensions. At low concentrations of DS, the flocs were small with no evidence of unflocculated material, but as the concentration of DS was

increased, a significant amount of PCC was left unflocculated (note the small particles in the background of Figs 6d and 6e). This indicates that the CPAM reacts preferentially with the DS, as it is assumed to do with DCS in pulp furnish [84]. As more DS was added, the flocs also became larger and stringier. This is also attributed to the direct interaction between DS and the flocculant, as the production of sticky strings of insoluble complex was also seen when DS was titrated into solutions of the cationic polymers, while flocculation of DS-PCC in the absence of free DS produced only small flocs.

For our model system, we did not wish to choose that which gave the best flocculation with a particular type of polymer, but rather one that most closely resembled a real furnish. The amount of DCS varies from pulp to pulp, and in fact we could, if desired, tailor our system to mimic a particular pulp furnish by changing the DS:PCC ratio. However, for our model system we chose to use 1 g/L of PCC with 20 mg/L of DS. In this particular system, 9 mg of the DS was adsorbed ( $0.75 \text{ mg/m}^2$ ) and reversed the surface charge of the PCC particles. The adsorption of the DS onto the PCC was irreversible under the experimental conditions, which is not surprising in light of the multiple attachment sites available on DS. The addition of 20 mg/L DS to the 1 g/L PCC suspension did not change the concentration of free calcium ions. This suggests that there is no interaction of the ions with the DS, and that surface adsorption does not take place by displacement of calcium ions. DS-PCC could be used immediately after preparation or after standing for a week, making it a convenient laboratory standard.

The measurements of particle diameter, and the greater stability of DS-PCC as compared to PCC suspensions, suggests that the adsorption of DS onto PCC acts to help disperse the PCC, leading to a greater preponderance of smaller particles. (Figure 7 and Table 1). It also acts to sterically stabilize the particles, as indicated by their staying suspended for much longer than their unmodified PCC counterparts (Figure 6).

Theoretically, the thickness of the adsorbed layer could be obtained from the difference in the diameters between DS-PCC and unmodified PCC. However, it was impossible to obtain this thickness either from disc centrifugal measurements (the DS-PCC showed a smaller diameter because of drag force or better dispersion as mentioned above) or dynamic light scattering (it was impossible to measure the average diameter for unmodified PCC because of quick sedimentation (Figure 7)).

Having characterized the system, we proceeded to more fully demonstrate its use with various retention aids. When the initial flocculation experiment, using PCC with varying DS content, and CPAM10 as flocculant, was repeated using CPAM35, the effects on the turbidity changes were the same. We had expected that polymers of different charge density might react to different extents with the DS, and our results prompted further flocculation experiments using these polymers.

The charge density of the flocculant was found to have very little effect on the efficiency of the flocculation, as long as there was some cationic character. Polyacrylamide itself was also able to flocculate the DS-PCC to a limited extent. At

low concentrations, polyacrylamide was more effective than CPAM in producing flocculation. Presumably the flocculation of the DS-PCC was a result of bridging by the polyacrylamide. When suspensions of DS-PCC with no free DS were flocculated, the polymers were much more efficient at initiating flocculation and the flocs formed were uniformly small. This confirms the suggestion above that the CPAMs interact with the DS in solution, preventing the polymer itself from flocculating the PCC. The complexes so formed can participate in bridging, and form big stringy flocs. Such flocs were not seen in the absence of free DS.

Another flocculant which is commonly used with pulp furnishes is PEO/ACS. This retention aid gave much poorer flocculation of DS-PCC than did unmodified PCC (Figure 8). The surface of DS-PCC is negatively charged. There should be no electrostatic attraction between negatively charged PCC surface and negatively charged cofactor, while unmodified PCC bears positive a charge, ensuring strong electrostatic interactions between the surface of the PCC and the negatively charged cofactor ACS. This suggests that such an electrostatic attraction may be an important factor in the flocculation process. The steric stabilization of the PCC particles by the DS may also be a contributing factor.

Thus flocculation results further confirmed that DS-PCC could serve as a better colloidal model than unmodified PCC to predict the behavior of retention aids in mechanical pulp furnish.

### ***Conclusions***

A colloidal DS-PCC model has been proposed with the following characteristics:

- Hydrophilic, negatively charged surface
- Electro-sterically stabilized
- Relatively better dispersed than PCC itself
- Easily prepared
- The amount of excess DS can be adjusted to mimic different pulp furnishes
- DS-PCC can be flocculated using cationic polyacrylamides, PAMs or PEO/cofactor. The presence of the DS moderates the effects of these flocculants just as DCS are thought to.

These properties indicate that DS-PCC may serve as a better colloidal model than PCC itself for studying the retention mechanism of filler in mechanical pulp furnish. DS-PCC has similar surface properties to those expected for PCC filler that has been covered with DCS.

**Table 1. The average diameter of PCC particles**

<b>Method</b>	<b>Particle</b>	<b>Average diameter (<math>\mu\text{m}</math>)</b>
<b>Disc centrifugal particle sizer</b>	<b>PCC</b>	<b>1.21<math>\pm</math>0.74</b>
	<b>DS-PCC</b>	<b>1.12<math>\pm</math>0.66</b>
<b>Dynamic light scattering</b>	<b>DS-PCC</b>	<b>1.12</b>
<b>Manufacturer</b>	<b>PCC</b>	<b>1.22</b>

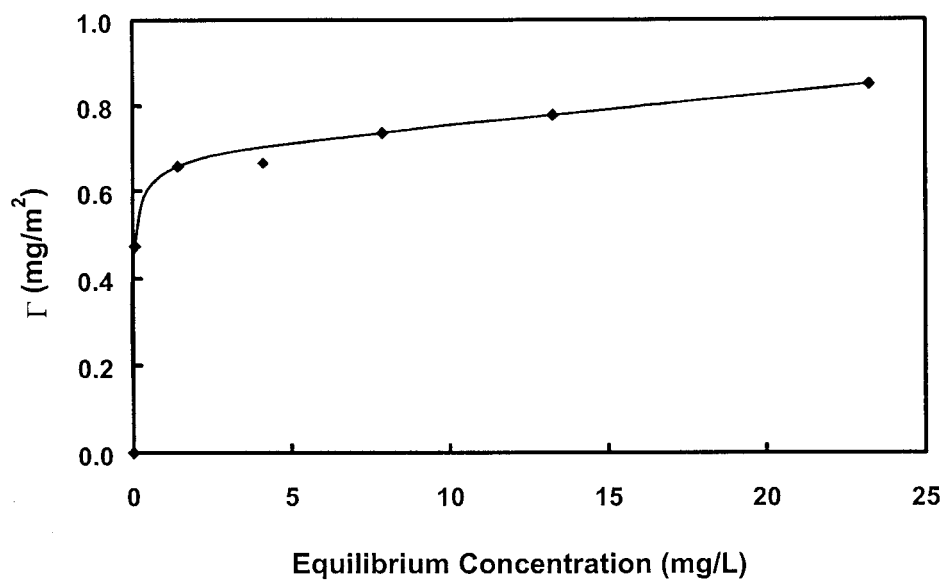


Figure 1. The adsorption isotherm of DS on 1.0 g/L PCC at pH 7.7.

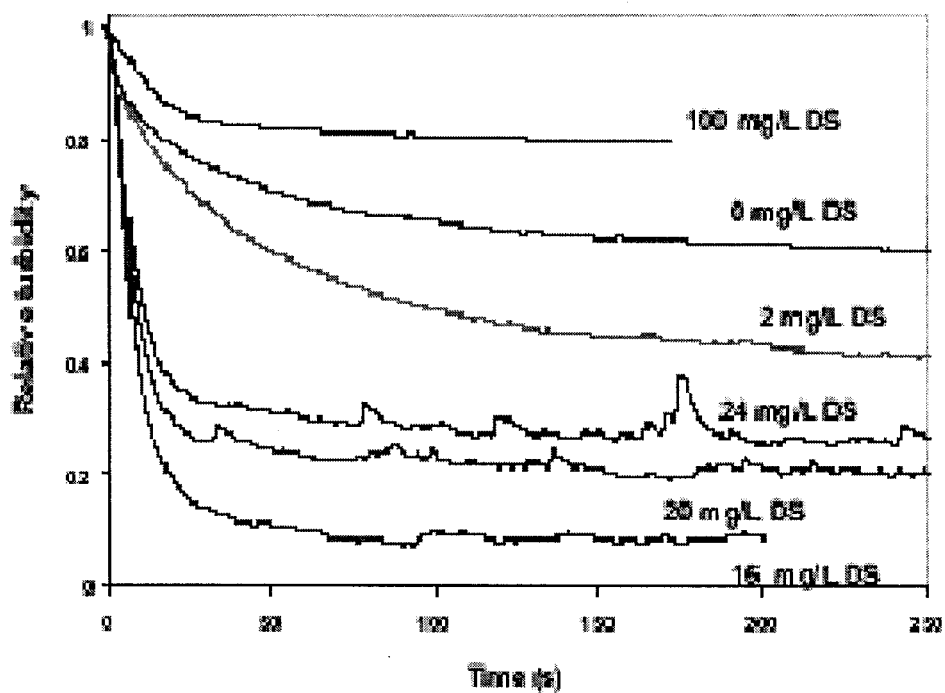


Figure 2. Relative turbidities of 1.0 g/L suspensions of PCC as a function of time after the addition of 4 mg/L CPAM10. The solutions contained 0  $\mu\text{g}/\text{mL}$  DS, 2  $\mu\text{g}/\text{mL}$  DS , 16  $\mu\text{g}/\text{mL}$  DS , 20  $\mu\text{g}/\text{mL}$  DS, 24  $\mu\text{g}/\text{mL}$  DS and 100  $\mu\text{g}/\text{mL}$  DS.



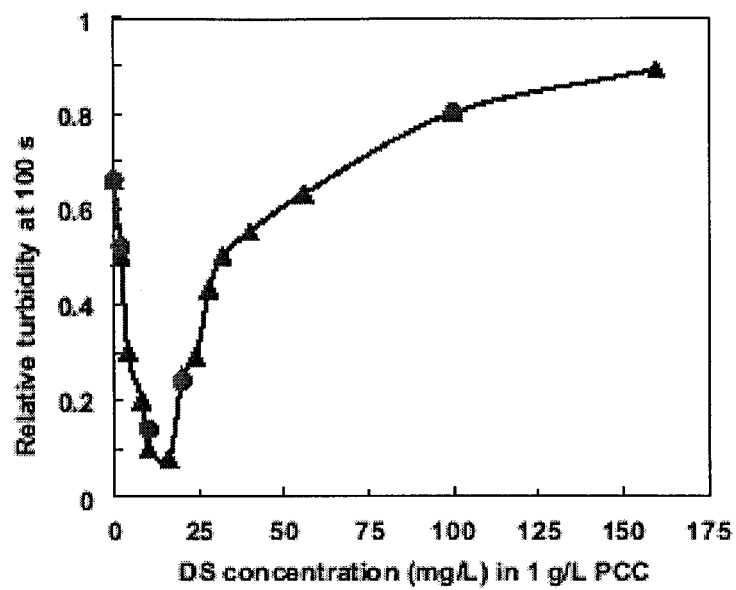


Figure 3. Relative turbidities of 1.0 g/L suspensions of PCC as a function of [DS], 100 s after the addition of 20 mg/L CPAM10 (▲) or CPAM35 (●).

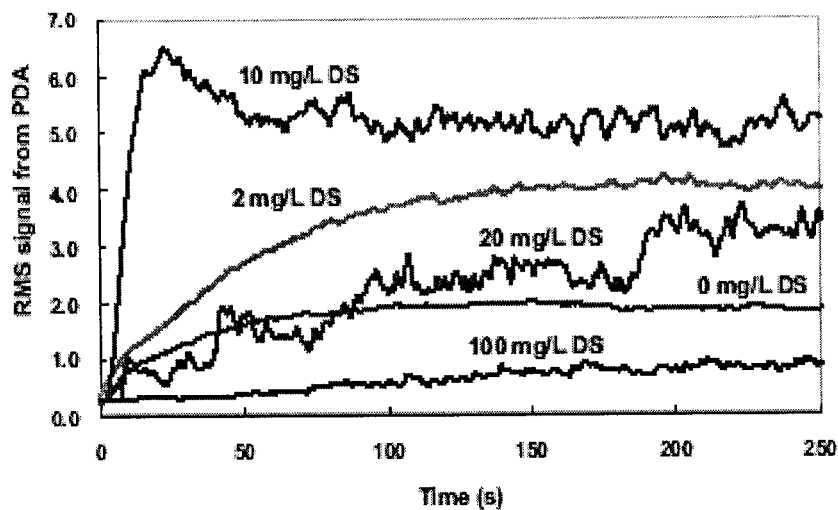
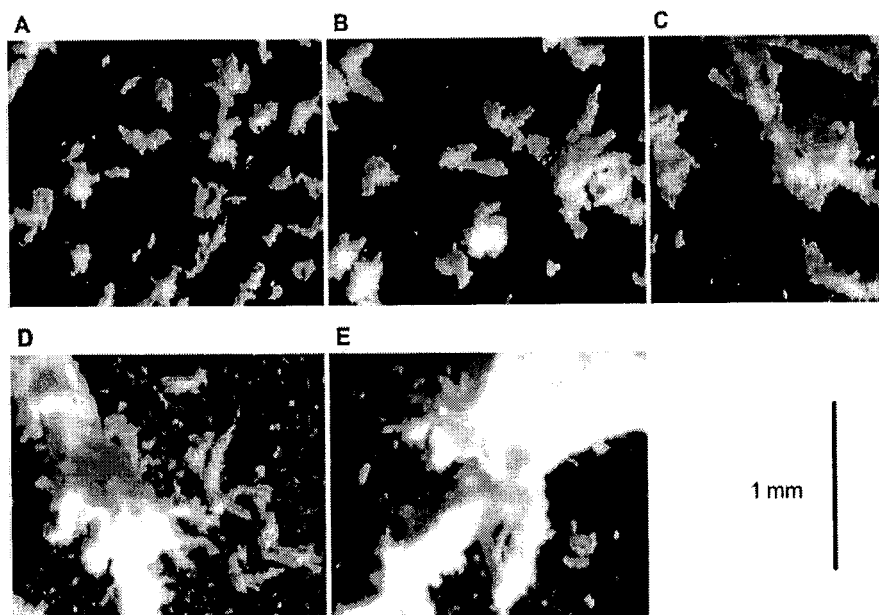


Figure 4. RMS signal from PDA for 1.0 g/L suspensions of PCC as a function of time after the addition of 20 mg/L CPAM10. The solutions contained 0  $\mu\text{g/mL}$  DS, 2  $\mu\text{g/mL}$  DS, 10  $\mu\text{g/mL}$  DS, 20  $\mu\text{g/mL}$  DS and 100  $\mu\text{g/mL}$  DS.



**Figure 5.** Pictures of flocs formed after the addition of 20 mg/L CPAM10 to suspensions of 1 g/L PCC containing 2 µg/mL DS, 8 µg/mL DS, 16 µg/mL DS, 24 µg/mL DS and 28 µg/mL DS.

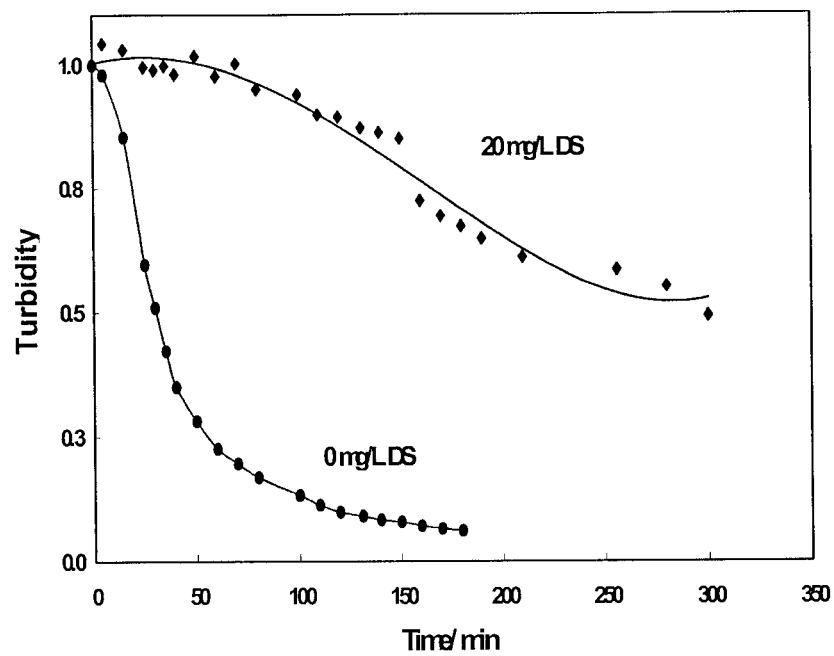
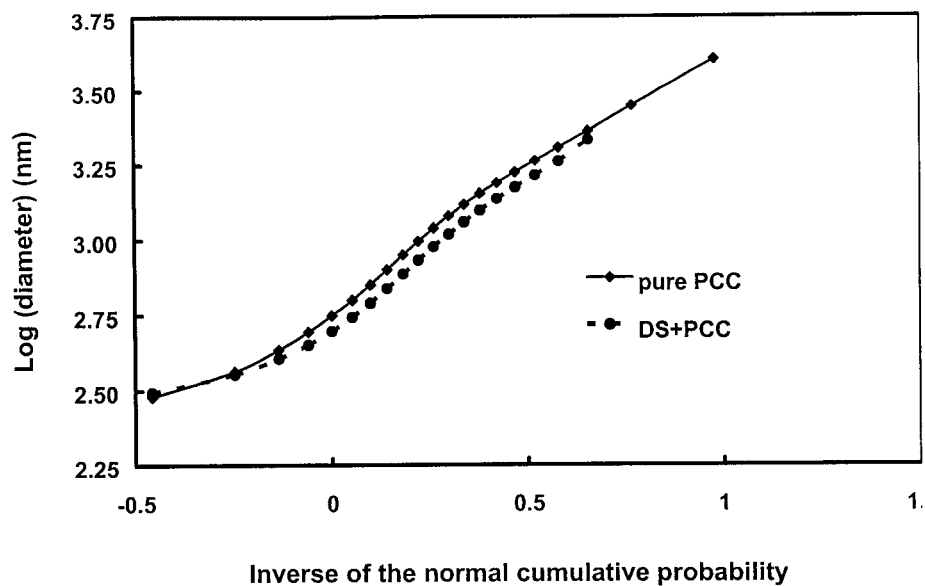
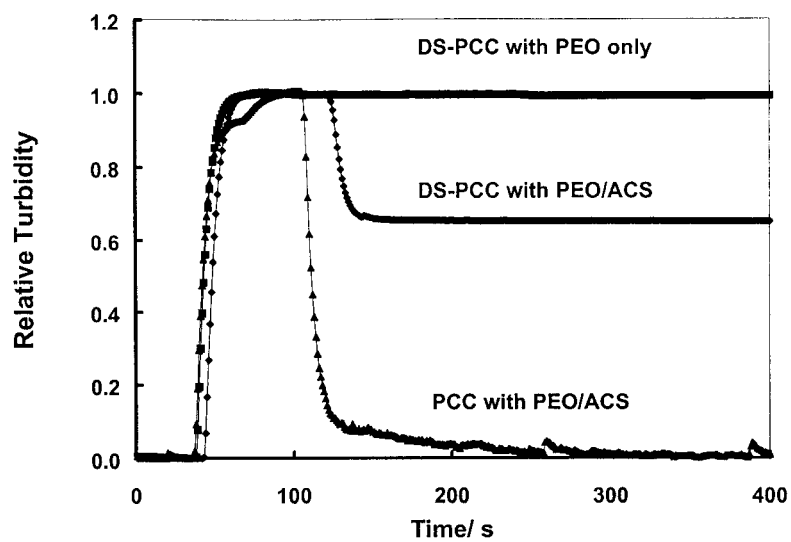


Figure 6. Relative turbidities of 1 g/L PCC and DS-PCC suspensions as a function of time as calculated from absorbance measurements in a 1 cm cell at 400 nm.



**Figure 7.** Distribution of particle size for PCC (◆) and DS-PCC (●) shown as log diameter (measured in nm) versus the inverse of the normal probability as determined using a disc centrifuge particle sizer.



**Figure 8.** Relative turbidity of 1 g/L suspensions of -DS-PCC after the addition of 2 mg/L PEO or 2 mg/L PEO with 4 mg/L ACS cofactor, and 1 g/L PCC after the addition of 2 mg/L PEO with 4 mg/L ACS cofactor.

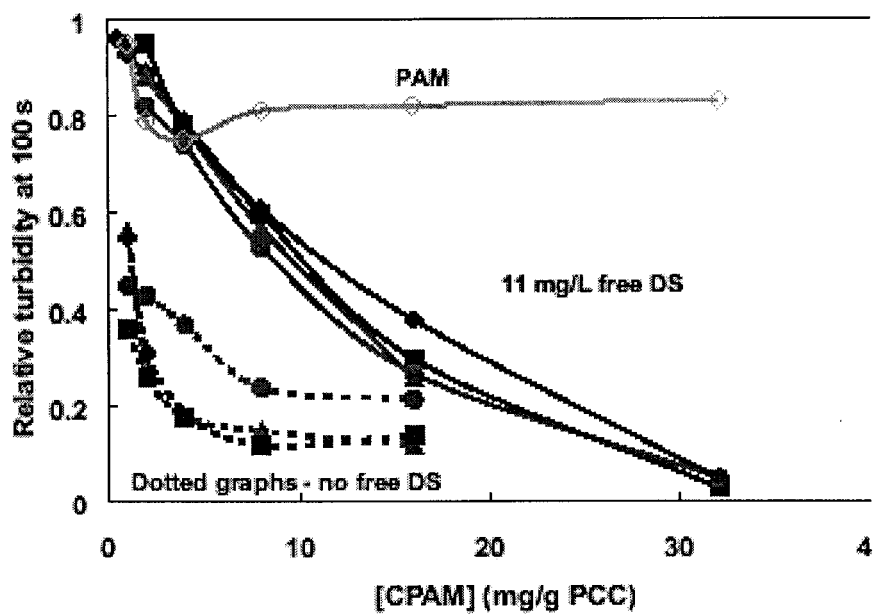


Figure 9. Relative turbidity of 1.0 g/L suspensions of DS-PCC 100s after the addition of CPAM5 (◆), CPAM10 (▲), CPAM20 (■), CPAM35 (●) and PAM (◇) with free DS (11 mg/L) present (solid lines) or absent (dotted lines).

## References

---

- <sup>1</sup> Penniman, J. G. *Pap. Trade J.* **1978**, April, 36.
- <sup>2</sup> Pelton, R. H.; Allen, L. H.; Nugent, H. M. *Svensk Papperstidning*, **1980**, 83, 251.
- <sup>3</sup> Sundberg, K.; Thornton, J. ; Holmbom, B.; Ekman, R. *J. Pulp Paper Sci.* **1996**, 22, J226.
- <sup>4</sup> Cechova, M.; Alinec, B.; van de Ven, T. G. M. *Colloids Surf.* **1998**, 141, 153.
- <sup>5</sup> Lindström, T.; Glad-Nordmark, G. *J. Colloid Interface Sci.*, **1984**, 97, 62.
- <sup>6</sup> Xiao, H.; Pelton, R. H.; Hamielec, A. *J. Pulp Paper Sci.*, **1996**, 22, 475.
- <sup>7</sup> van de Ven , T.G.M.; Alinec, B. *J. Pulp Paper Sci.*, **1996**, 22, J257.
- <sup>8</sup> Gibbs, A.; Xiao, H.; Deng, Y.; Pelton, R. H. *Tappi J.* **1997**, 80, 163.
- <sup>9</sup> Alinec, B.; Porubska, J.; van de Ven, T. G. M. *Paper Technology* , **1997**, 38, 51.
- <sup>10</sup> Allen, L.; Polverari, M.; Levesque, B. Francis, W. *Tappi J.* **1999**, 82,188.
- <sup>11</sup> Thompson, D. W.; Pownall, P. G. *J. Colloid Interface Sci.* **1989**, 131, 74.
- <sup>12</sup> Satterfield, B. F.; Stockwell, J. O. European Patent WO95/21296 **1995**.
- <sup>13</sup> Pelton, R. H.; Miller, P. McPhee, W.; Rajaram, S. *Colloids Surf. A* **1993**, 80, 181.
- <sup>14</sup> Gibbs, A.; Pelton, R. H.; Cong, R. *Colloids Surf. A* **1999**, 159, 31.



## **Chapter V The influence of PEO/poly (vinyl phenol-co-styrene sulfonate) aqueous complex structure on flocculation**

### *Abstract*

Colloidal suspensions were flocculated with high molecular weight polyethylene oxide (PEO) in conjunction with polystyrene sulfonate copolymers, poly (vinyl phenol-co-potassium styrene sulfate) (PKS) and poly(styrene-co-styrene sulfonate) (PS-co-SSS) as cofactors. The phenolic groups appear to be the primary active component of PKS driving complex formation and flocculation. Phenolic-free PS-co-SSS/PEO flocculated hydrophobic bare polystyrene (PS) latex, precipitated calcium carbonate (PCC) and dextran sulfate coated PCC (DS-PCC), casting doubt about the widely proposed mechanism of hydrogen bonding between phenolic OH and ether oxygen of PEO as the sole interaction for cofactor/PEO bridging flocculation.

The role of cofactor/PEO complex size in flocculation was investigated. Factors resulting in decreased PEO size, such as increased temperature or ionic strength, diminished flocculation. Neither PKS/PEO nor pure PEO or pure PKS could effectively flocculate poly (N-isopropylacrylamide) grafted hydrophilic PS latex (PS-g-PNIPAM), while PKS/PEO flocculated about 60% PS latex. This high stability of PS-g-PNIPAM was attributed to the lack of strong interaction between PKS/PEO

complexes and PNIPAM.  $\text{Ca}^{2+}$  induces phase separation of PKS/PEO complexes and greatly promoted flocculation.

### ***Introduction***

High molecular weight poly (ethylene oxide) (PEO) is a flocculant used in papermaking.<sup>1</sup> Interestingly, the presence of a second component, usually water-borne phenolic polymer, called a cofactor, greatly improve the PEO performance in many colloidal systems.<sup>2,3,4</sup> Examples of the cofactors are water dispersible phenolic resins,<sup>2,3</sup> tannic acid,<sup>5</sup> lignin derivatives<sup>6</sup> and poly (vinyl phenol).<sup>4,7</sup>

The PEO/cofactor system is believed to operate by some variation of bridging flocculation. One of the key features in bridging flocculation is that polymeric flocculant has to sequentially adsorb on two particles. Therefore, the size of flocculant, must be greater than the distance of closest approach between particles in a suspension.

The early literature contains much speculation about the structure of PEO/cofactor complexes usually inferred from flocculation studies<sup>8,13</sup> or molecular modeling.<sup>9</sup> Carignan et al. employed dynamic light scattering to estimate the size of complexes formed between PEO and some commercial cofactors.<sup>9</sup> They showed that PEO coils contracted when they formed complexes with charged phenolic polymers. There are, however, more hydrophobic phenolic resins, which display syneresis when complexed with PEO solutions.<sup>10, 13</sup> Unfortunately these unstable systems are much more difficult to characterize.

Recently, we reported the use of poly (vinyl phenol-co-potassium styrene sulfonate) (PKS) as a model cofactor.<sup>11,22</sup> The advantage of using PKS instead of commercial cofactors is that PKS has a well-defined structure and forms water-soluble complexes with PEO. The interaction between PEO and PKS has been investigated with <sup>1</sup>H NMR, fluorescence photobleaching recovery and diffusion-ordered NMR. This work showed that the driving forces for complex formation between PKS/PEO were: 1) mainly the hydrogen bonding between the polyether oxygens and phenolic hydroxyls of cofactors as proposed by others;<sup>1, 5, 12, 13</sup> and, 2) the hydrophobic interactions between aromatic ring of PKS and PEO.<sup>14, 15</sup> Upon complex formation, the conformation of PKS collapsed, therefore, PKS/PEO complexes were found to be more sensitive to ionic strength than PKS itself.

The sizes of PKS/PEO complexes were measured by fluorescence photobleaching recovery and diffusion-ordered NMR studies using PEO Mw  $1 \times 10^6$  Da which is smaller than the PEO used for flocculation ( $8 \times 10^6$  Da). The average PKS/PEO complex was an aggregate of about 6 PEO coils. Increasing either temperature or ionic strength resulted in a decrease in the apparent size of complexes. Non phenolic poly(styrene-co-styrene sulfonate) (PS-co-SSS) formed water-soluble complexes with PEO with similar binding mechanism as PKS/PEO. A goal of this chapter is to link our knowledge about complex size to flocculation performance.

A well-known observation is that extremely high molecular weight (i.e.  $> 2 \times 10^6$  Da) PEO is required for good flocculation. One reason was proposed that

PEO/phenolic resin complex collapses to an inactive (with respect to flocculation) coacervate and only with very high molecular weight PEO does this collapse occur slowly enough for flocculation to occur.<sup>10</sup> A second possibility may be that only the flocs formed with very high molecular weight PEO can be robust enough to resist the hydrodynamic forces existing during flocculation. Direct measurement of tensile strength for flocs showed that the strength of flocs increased with PEO MW.<sup>16</sup> A third possibility is related to the formation of networked PEO/cofactor complexes. It is possible that only very high MW of PEO will form networked complex with cofactors. Thus, it is worthy to explore the different behavior of PEO Mw  $1 \times 10^6$  Da and PEO Mw  $8 \times 10^6$  Da in forming complexes with PKS.

Hydrodynamic forces can contribute to both floc formation and floc disruption.<sup>17, 18</sup> Initially, flocs grow rapidly, however, with increasing size they become vulnerable to breakage by fluid-particle interactions. At long times, the particle-size distribution is invariant.<sup>17,19</sup> By direct measuring rupture strength of precipitated calcium carbonate (PCC) flocs with micromechanics, Gibbs et al. reported that the strength of PCC flocs was related to molecular weight of PEO.<sup>16,20</sup> The strongest flocs formed with PEO Mw  $8 \times 10^6$  Da, which is the highest MW of commercially available PEO.<sup>16</sup> A direct linkage between flocs strength and laboratory flocculation was found for PCC flocculation, good flocculation gives strong flocs. Both the tensile strength and elongation also depended on the structure of cofactors. Branched cofactor gave stronger tensile strength but lower elongation than linear

cofactor.<sup>21</sup> No other details about how the structure of cofactors affects the strength of flocs have been reported in literature.

In this chapter we report the result of a series of flocculation experiments using PKS/PEO as flocculants. Flocculation was measured as a function of temperature and ionic strength to extract the relationships between cofactor/PEO size and flocculation performance.

### ***Experimental***

#### *Materials*

Scalenohedral precipitated calcium carbonate (PCC) was a gift from Specialty Minerals (Bethlehem, PA) with a number-averaged diameter of 1.22  $\mu\text{m}$  and a specific surface area of 12.0  $\text{m}^2/\text{g}$ . Polyethylene oxide (PEO) (Polyox 309  $M_w=8\times 10^6$  Da and Polyox N-12K  $M_w=1\times 10^6$  Da) were gifts from Union Carbide (Danbury, CT).  $\text{K}_2\text{S}_2\text{O}_8$ ,  $\text{NaHSO}_3$ ,  $\text{FeCl}_3$ , styrene and dextran sulfate sodium salt (DS) with 2.3 sulfate groups per glucosyl residue ( $M_w=10,000$  Da) was from Sigma (Oakville, ON). Styrene was purified by vacuum distillation. N-isopropylacrylamide (NIPAM) was obtained from Kodak Co. with twice recrystallized from toluene/hexane.

### *Procedure*

Poly(vinyl phenol-co-potassium styrene sulfate) (PKS) was synthesized by free radical polymerization of 4-acetoxystyrene with sodium 4-styrene sulfonate followed by extensive hydrolysis in alkaline solution.<sup>22</sup> The detailed procedure for purification and characterization was reported previously.<sup>11,14</sup> Five PKS copolymers with phenolic mole fractions ranging from 0.34 to 0.82 were synthesized. Table 1 summarizes the properties of the polystyrene sulfonate polymers.

Polystyrene (PS) latex was synthesized by surfactant-free emulsion polymerization.<sup>23</sup> The PS latex was purified by extensive dialysis (10,000 Da cutoff) against a steady flow of milli-Q water for one week. PS coated with poly (N-isopropylacrylamide) (PS-g-PNIPAM) was synthesized by the polymerization of NIPAM in the presence of the well-defined PS latex.<sup>24</sup> 162.2 g of 2.89% solid content of PS latex suspension (diameter  $504 \pm 4$  nm, polydispersity 1.02) was further purified by 3 cycles of ultra centrifugation, decantation and redispersion before grafting. PS latex suspension was added into a 500 ml 3-neck round-bottom flask fitted with a mechanical stirrer (400 RPM) containing 36.0 g milli-Q water with 2.2 g NIPAM. The suspension was purged with ultra-pure N<sub>2</sub> for 30 minutes. 0.32 g K<sub>2</sub>S<sub>2</sub>O<sub>8</sub>, 0.12 g NaHSO<sub>3</sub> and 0.2 mg FeCl<sub>3</sub> was added into PS latex suspension to initiate the polymerization of NIPAM. The mixture was allowed to polymerize at 25°C for 18 hours. After the polymerization, a white suspension was obtained. PS-g-PNIPAM was purified by five cycles of ultra centrifugation at 40,000 rpm for 30 min at 20°C, decantation and re-dispersion. Re-dispersion process of PS-g-PNIPAM was much

easier than bare PS latex. The presence of PNIPAM on the latex was confirmed by  $^1\text{H}$  NMR (Data was not shown here). The size of the PS-co-PNIPAM was measured by disc centrifugation with a Brookhaven Disc Centrifuge Particle Sizer. The electrophoretic mobility of PCC dispersions was measured with a Coulter Delsa 440SX using 1 mM NaCl as the supporting electrolyte. The details for the mobility<sup>25</sup> and size measurements<sup>27</sup> were reported previously. Table 2 shows the properties of PS and PS-g-PNIPAM latex.

The surface properties for colloidal calcium carbonate (PCC) were modified by adsorbing dextran sulfate (DS) onto bare PCC surface using methods developed in Chapter IV.<sup>26</sup>

Flocculation was conducted by using a Photometric Dispersion analyzer (PDA) (Rank Brothers, Cambridge, UK).<sup>27, 28</sup> In a typical flocculation experiment, PEO was added 60 seconds later after the addition of colloidal particles. The suspension was stirred at 400 rpm using a three-bladed propeller (55-mm diameter) and the extent of flocculation was monitored by circulating the suspension through PDA detector at a rate of 60 ml/min. The DC output was converted to relative turbidity by the following relationshi



$$\tau_r = \ln\left(\frac{V_w}{V_t}\right) / \ln\left(\frac{V_w}{V_{t=0}}\right) \quad (1)$$

where  $V_w$  is the output voltage for water,  $V_{t=0}$  is the output voltage for colloidal suspension before the addition of PEO and  $V_t$  is the output voltage at time  $t$ . It is assumed that the relative turbidity is roughly proportional to the concentration of unflocculated particles. The higher the relative turbidity, the lower the flocculation extent.

Flocculation at different temperatures was done by incubating PDA sample beaker in a water bath controlled with an accuracy of  $\pm 0.2^\circ\text{C}$ . All the solutions and colloidal suspensions were incubated for a sufficient time to reach thermal equilibrium.

The efficiency of premixed PKS/PEO complexes as flocculants was also evaluated by the PDA. PEO and PKS solutions were premixed in PDA sample beaker first. The concentration of PEO was 2 ppm, a typical concentration used in most of flocculation experiments. 5.00 ml 50 g/L PCC suspension was added later into the premixed PKS/PEO, giving the typical PEO dosage 2g/kg of solid content of colloidal particles. All the other experimental conditions were unchanged.

The flocculation of PS-co-PNIPAM at different  $\text{CaCl}_2$  concentrations was determined by adding 0.50 ml 5.96% PS-co-PNIPAM suspension into 167 ml water

containing 1 mM NaCl first. The addition procedure for PEO and cofactors were same as the other flocculation experiments mentioned above.

### ***Results***

The flocculating ability of PKS/PEO complexes was measured using a number of target colloidal suspensions. One of them, scalenohedral precipitated calcium carbonate (PCC), was used to study the mechanism of water-soluble polymers in flocculation. PCC is not a good model for fillers in mechanical pulps which contain high concentrations of a mixture of dissolved colloidal substances (DCS) in pulp suspension. Most of DCS are negatively charged.<sup>29,30</sup> Some of them interfere with the retention, for example, by adsorption on the surfaces of the fillers, change the surface properties of fillers and sterically stabilize the filler particles, making them more difficult to be flocculated. Dextran sulfate treated PCC has been proposed to be a new colloidal model particle with negatively charged and sterically stabilized surface. Excess dextran sulfate in solution mimics the effect of dissolved colloidal substances in the papermaking process.

Both bare PCC and DS-PCC contain 0.7 mM  $\text{Ca}^{2+}$  in solution.  $\text{Ca}^{2+}$  complicates the flocculation because of the strong interaction with negatively charged PEO/cofactor complex. Thus, well-defined monodispersed polystyrene (PS) latex was used as another colloidal target. The only possible driving force for interactions between PEO/cofactor and PS latex are hydrophobic interactions. PS-g-PNIPAM has hydrophilic surface, resulting in a decrease in the hydrophobic interaction between

complexes and PS surface. Therefore, it is possible to use PS-g-PNIPAM to study the importance of hydrophobicity and  $\text{Ca}^{2+}$  on flocculation.

The major properties of these four colloidal targets are summarized in Table 2.

#### *Effect of phenolic content on the flocculation and the robustness of flocs*

Figure 1 shows the result of a typical flocculation experiment of DS-PCC suspension with PKS/PEO. DS-PCC is dextran sulfate treated PCC model colloid with negatively charged and sterically stabilized surfaces. At time  $t = 0$  s, water was pumped through the turbidity detector, the relative turbidity was equal to zero. At  $t = 30$  s, DS-PCC was added and the relative turbidity increased to 1 (by definition). At  $t = 60$  s, PKS was added to the DS-PCC suspension to give a concentration of 4 ppm. No change in turbidity was observed indicating no flocculation. At  $t = 100$  s, PEO was added and the turbidity rapidly decreased due to the flocculation of DS-PCC particles. The minimum turbidity, corresponding to maximum flocculation, herein is referred to as “maximum flocculation”. At longer times the relative turbidity climbed to a steady-state value referred to as “steady-state flocculation”. The difference between maximum flocculation and steady-state flocculation is taken as an index for the robustness of flocs. In this case (Figure 1), the fact that the steady-state turbidity was nearly one indicates that the flocs formed with PKS.34/PEO were completely redispersed by being stirred at 400 rpm during flocculation experiments. This result

indicated that PEO/cofactor/DS-PCC particles tethers were not strong enough to withstand the hydrodynamic forces.

For a reversible flocculation process, shear-induced flocculation consists of floc formation and floc breakup.<sup>31,32</sup> At the beginning, the particles rapidly grow. As the particles grow larger, they become vulnerable to breakage by fluid-particle interactions. After a certain time, the particle-size distribution no longer changes with time.<sup>33</sup> The result shown in Figure 1 suggests that the flocculation of DS-PCC with PKS/PEO is irreversible meaning one some polymer/particle bonds are broken, they do not reform.

Neither pure PEO nor pure PKS caused any decrease in relative turbidity in DS-PCC suspension. Only the addition PEO in the conjunction with PKS caused the flocculation of DS-PCC, which indicated that PKS was necessary for PEO to flocculate DS-PCC particles.

Figure 2 shows the maximum turbidity and the corresponding steady-state turbidity values of DS-PCC particles as functions of the PKS phenolic molar content. The relative turbidity for maximum flocculation increased (i.e. flocculation got worse) from 0.45 to 0.67 with increasing phenolic content from 0.34 to 0.82. By contrast, the relative turbidity for steady-state flocculation decreased from 0.97 to 0.69. The large difference between maximum flocculation and steady-state flocculation for low phenolic content indicated that the flocs formed by PKS/PEO at low phenolic content were most sensitive to hydrodynamic forces. No substantial

difference between maximum and steady-state flocculation was observed for PKS.82, indicating that the flocs formed by PKS.82/PEO were not sensitive to the shear rate, although in this case the extent for flocculation was not very good - about 67% DS-PCC was not flocculated.

#### *The influence of temperature*

PKS.34/PEO and PKS.82/PEO were chosen to study the effect of temperature on maximum flocculation. Figure 3 shows the temperature effect of maximum flocculation of DS-PCC by PKS.34/PEO and by PKS.82/PEO. The maximum extent of flocculation decreased with increasing temperature. For PKS.34/PEO, at 25°C, the maximum flocculation was 0.44. By contrast, at 50°C, the relative turbidity was about 1, indicating that no flocculation was induced by PKS.34/PEO. This effect was found less profound than PKS.34/PEO system.

Pure PEO has a cloud point of temperature of about 98°C and the presence of 50 mM CaCl<sub>2</sub> decreases this phase separation temperature to 97°C.<sup>34,35</sup> All the experiments summarized in Figure 3 were below the cloud point temperature of the PEO/electrolyte solutions.

#### *The influence of ionic strength on flocculation*

The electrostatic repulsion existing between negatively charged PS latex particles keeps them from aggregating. Increasing the ionic strength by electrolyte addition screens the electrostatic repulsion. Therefore, the extent of flocculation is

expected to increase with ionic strength. Figure 4 shows the effects of ionic strength on the flocculation of PS latex with PKS.67/PEO. The ionic strength was adjusted by sodium phosphate buffer solution at pH 7.5. Increasing ionic strength from 0.0032M to 0.043M, the flocculation did not increase as expected from electrical double layer theory. On the contrary, the flocculation was substantially weakened, although the repulsion forces between particles were suppressed by the increase in ionic strength. The effect of ionic strength on flocculation at 300 s is shown in Figure 5. Also shown in Figure 5 is the apparent size of complexes (formed with PEO molecular weight  $1 \times 10^6$  Da) at different ionic strength reported in Chapter 3.

#### *Flocculation with non-phenolic cofactor*

PEO forms complexes through hydrophobic interaction with poly (styrene-co-sodium styrene sulfonate) (PS-co-SSS), a simple linear polymer without phenolic groups.<sup>11</sup> Figure 6 shows the flocculation results using untreated PCC, DS-PCC and PS latex at stirring rate 400 rpm by using PS-co-SSS/PEO as flocculants. The decrease in relative turbidity for bare PCC, or PS or DS-PCC suspension upon adding PS-co-SSS/PEO confirmed that PS-co-SSS worked as cofactor for PEO. However, compared to other cofactors this performance is poor (see below). The DS-PCC in particular showed only transient flocculation.

Figure 7 shows the influence of stirring rate on the flocculation behavior DS-PCC in the presence of the non-phenolic cofactor. The relative turbidity of DS-PCC

suspension climbed to about 1 (Figure 7), suggesting the formed flocs were shear-sensitive. Furthermore, the rate of floc redispersion was greater at the higher stirring speeds.

Table 3 summarizes the flocculation performance of PKS.71/PEO and PS-co-SSS/PEO on bare PCC, DS-PCC and PS latex. The reason for choosing PKS.71 for comparison is because PKS.71 has a similar molar fraction of styrene sulfonate group as PS-co-SSS. PS-co-SSS/PEO only flocculated about 60% of PCC particles and 40% of PS particles, while PKS.71/PEO flocculated more than 95% of PCC particles and 43% of PS latex. This indicates that without phenolic group in structure, PS-co-SSS/PEO less effectively flocculated PCC and PS particles than PKS/PEO with phenolic groups. The difference between steady-state flocculation and maximum flocculation was 0.52 for PS-co-SSS/PEO, while the difference was  $<0.1$  much less for PKS.71/PEO, suggesting that non-phenolic PS-co-SSS/PEO/DS-PCC flocs was much less robust than phenolic PKS/PEO/DS-PCC flocs.

One role of the styrene sulfonate groups in PKS or PS-co-SSS is to make polymers water-soluble. Homopolymer poly(styrene sulfonate)/PEO was added to DS-PCC and untreated PCC particles. No improvement in PCC flocculation compared with PEO alone was observed. Furthermore, no flocculation of DS-PCC was observed, as PEO alone will not flocculate DS-PCC. Thus, it appears that the main active components for PKS or PS-co-SSS were phenolic OH group of PKS or styrenic group on PS-co-SSS.

### *Flocculation with premixed PKS/PEO*

Many researchers have reported that premixing commercial cofactors with PEO results in a complete loss of flocculation ability.<sup>1, 5, 12, 13</sup> The main reason is that most of commercial cofactors form unstable complexes with PEO which quickly precipitate from aqueous solution.

Adding PCC particles into premixed PKS.67/PEO resulted in a decrease in the relative turbidity to 0.02. This result shows that premixed PKS.67/PEO did induce excellent flocculation for PCC. More than 95% of PCC particles were flocculated. Premixed PKS.67/PEO also induced flocculation for DS-PCC particles, but the formed flocs were not robust enough to withstand the hydrodynamic forces during the flocculation experiments. The key point here was that PKS/PEO was mixed first in very dilute solution. Under this condition, loose complexes (large tethers) were formed first. When adding positively charged PCC particles into dilute complex solution, the strong electrostatic attractions between PKS/PEO complexes and the particle surfaces resulted in a good flocculation. On the other hand, if 0.7 mM  $\text{Ca}^{2+}$  was added to the premixed solution, more compact complexes were formed, therefore, no flocculation was obtained. This result suggested that  $\text{Ca}^{2+}$  actually was involved in the complex formation, resulting in compact complexes which could not promote bridging flocculation.



### *Importance of hydrophobicity of PS surface*

In order to identify the importance of hydrophobicity of colloidal particles on flocculation performance, monodispersed polystyrene (PS) latex with and without a hydrophilic coating were used as target colloidal particles. Figure 8 shows the flocculation performance by using PKS/PEO on PS-g-PNIPAM. Neither pure PEO, pure PKS, commercial phenolic resin (FPR), nor PKS/PEO or PEO/FPR could flocculate PS-g-PNIPAM colloidal particles, which have highly hydrophilic surfaces. The fluctuation in turbidity curves was due to the bubbles generated by propellers and circulated through PDA detector by pump. On the other hand, as shown in Figure 4, the relative turbidity of bare PS latex decreased to 0.5 by adding PKS.67/PEO at ionic strength 0.0032 M, indicating that ca 50% PS latex was flocculated by PKS.67/PEO. This large difference in flocculation performance indicated the importance of hydrophobicity on colloidal surfaces. The high hydrophobicity on PS surface resulted in a strong interaction between PEO/cofactor retention aid and colloidal particle surface. Once PS was grafted with hydrophilic PNIPAM, PS-g-PNIPAM has a highly sterically stabilized surface than bare PS latex. PNIPAM does not interact with PEO in aqueous solution;<sup>36</sup> therefore, no obvious flocculation was achieved.

### *Flocculation of PS-g-PNIPAM in the presence of $Ca^{2+}$*

PS grafted with poly (N-isopropylacrylamide) (PS-g-PNIPAM) was more stable than bare PS latex with higher critical coagulation concentration (Table 2) at room temperature. Flocculation with premixed PKS/PEO showed that  $Ca^{2+}$  resulted

in an increase in hydrophobicity of PKS/PEO complexes. Therefore, the flocculation of PS-g-PNIPAM should be improved in the presence of  $\text{Ca}^{2+}$ .

Figure 9 shows that the effect of  $\text{Ca}^{2+}$  on the flocculation of PS-g-PNIPAM. The flocculation was greatly enhanced by adding  $\text{Ca}^{2+}$ , even at a concentration as low as 0.18 mM. This result suggested that increasing the hydrophobicity of PKS/PEO complexes could strengthen the interactions between PKS/PEO complexes with colloidal surfaces, therefore resulting in a better flocculation performance.

#### *Viscosity measurement for PKS/PEO mixtures*

In order to understand the effect of  $\text{Ca}^{2+}$  on PS-co-PNIPAM flocculation, viscosity measurement was used to explore  $\text{Ca}^{2+}$  effect on the viscosity of PKS.67/PEO complexes.

Figure 10 shows the relative viscosity measurement for PKS.67/PEO mixture at PKS.67/PEO(w/w)=2 and [PEO]=23.7 mg/L. The relative viscosity ( $\eta_r$ ) is defined as the viscosity of PKS.67/PEO mixture to the viscosity of pure water at same experimental conditions. There are three important features in Figure 10. The  $\eta_r$  of PKS.67/PEO decreased with time at shear rate= $37.12 \text{ s}^{-1}$ , while pure PEO at same concentration did not show strong shear-sensitivity.  $\eta_r$  of PKS.67/PEO was about 198 times higher than pure PEO indicating that the involvement of multiple polymer chains.  $\text{Ca}^{2+}$  increased the hydrophobicity of PKS.67/PEO complexes, resulting in a collapse of complexes over a short period of time (less than 20 s).

Note that the  $\eta_r$  of PKS.67/PEO was strongly related to the molecular weight of PEO. Our early studies on dynamic viscosity measurement with PEO Mw  $1 \times 10^6$  Da showed that  $\eta_r$  of PKS.67/PEO was several times higher than pure PEO at same experimental condition. Fluorescence photobleaching recovery and diffusion-ordered NMR measurement showed that only several PEO coils existed in each complex. But when using PEO Mw  $8 \times 10^6$  Da, the relative viscosity of PKS/PEO was 198 times higher than pure PEO at  $[\text{PEO}] = 23.7$  mg/L. This may suggest a possibility of forming networked complexes.

Another difference between PEO Mw  $8 \times 10^6$  Da and PEO Mw  $1 \times 10^6$  Da was the shear-thinning behavior. As shown in Figure 10, the relative viscosity of PKS/PEO complexes decreased with time at shear rate of  $37.12 \text{ s}^{-1}$ . Our early study showed that with PEO Mw  $1 \times 10^6$  Da, PKS.67/PEO complexes did not show the shear-thinning behavior at same shear rate  $37.12 \text{ s}^{-1}$ .<sup>11</sup>

### ***Discussion***

Water-soluble polystyrene sulfonate copolymers work effectively as cofactors in combination with high molecular weight PEO to flocculate bare scalenohedral precipitated calcium carbonate (PCC), dextran sulfate treated PCC, polystyrene (PS) latex and poly (N-isopropylacrylamide) grafted hydrophilic PS latex (PS-g-PNIPAM). By investigating the change of flocculation performance of cofactor/PEO flocculants with structures of cofactors, temperature, ionic strength and surface properties of colloidal particles, we obtained information about the role of cofactors.

Our results address the importance of aromatic rings in cofactors, the size of PEO/cofactor complexes, the interactions between PEO/cofactor complexes and colloidal surfaces and the relationship between the rate of floc breakage and phenolic content in cofactor.

Phenolic groups are the PEO binding sites in PKS cofactors. The interactions are likely to involve both hydrogen bonding and hydrophobic effects.<sup>11</sup> Increasing the phenolic molar content increases the number of PEO binding sites while lowering the molar content of styrene sulfonate. Low molar content of styrene sulfonate results in a weak electrostatic repulsion. Both effects promote the stronger interactions between PEO and PKS at high phenolic content, pull the interacting polymer chains closer, therefore, result in a less flocculation efficiency and lower sensitivity of DS-PCC flocs to shear force in flocculation. The sensitivity of flocculation performance at different phenolic content is unlikely to be due to the change in molecular weight of PKS, because there is no clear trend in molecular weight for PKS at different phenolic content (Table 1). By substituting phenolic group with styrene group, poly(styrene-co-styrene sulfonate) sodium salt (PS-co-SSS) is impossible to interact with PEO through hydrogen bond. PS-co-SSS works as cofactor with PEO on various colloidal particles (Figure 6 and 7). This shows that hydrogen bonding between phenolic OH of cofactors and PEO ether oxygen is not the only driving force for phenolic polymer to work as cofactors.<sup>11,14</sup>

Without hydrogen bonding, PS-co-SSS/PEO complexes are even weaker. At 400 rpm stirring rate, flocs formed in PS-co-SSS/PEO/DS-PCC system were completely disrupted (Figure 7). As a comparison (Table 3), for PKS.71/PEO having similar molar content of styrene sulfonate as PS-co-SSS, the difference between maximum flocculation and steady-state flocculation was ca 0.1, indicating that most of PKS.71/PEO/DS-PCC flocs were not disrupted by hydrodynamic force at stirring rate 400 rpm. This suggests that hydrogen bonding make some contributions to the strength of flocs.

The apparent size of PEO increases in the presence of PKS.<sup>11</sup> The relative viscosity of PEO ( $M_w=8 \times 10^6$  Da) at  $[PEO]=23.5$  mg/L was found about 198 times higher than pure PEO at the same experimental conditions (Figure 10). This gives clear evidence that multiple polymer chains were involved. PEO/cofactor/PCC flocs show substantial elasticity suggesting that complex is a crosslinked network.<sup>37</sup>

PEO/cofactor flocculation system is believed to operate by some variation of bridging flocculation. Thus, factors resulting in a decrease in apparent size of PKS/PEO complexes lower PEO/cofactor flocculation performance. Increasing temperature and ionic strength, promotes the hydrophobic interactions between PEO and PKS,<sup>11</sup> therefore, the compact complexes cause the poor flocculation performance (Figure 3 and 4).

The size of PKS/PEO complexes decreased with the increase in ionic strength through two mechanisms.<sup>11</sup> The increase in the ionic strength partly screens off the

electrostatic repulsion force between charged styrene sulfonate groups. Secondly, some of counter ions condense on polymer chains by changing the conformation of PKS from extended conformation to more compact conformation. Stronger and more compact complexes were formed with an increase in ionic strength. For bridging flocculation, the tether must be long enough to connect two colloidal particles together. A dramatic change in the apparent size may result in a loss in the ability as bridging flocculant. Further increasing ionic strength to 0.15M, which was close to the critical coagulation concentration of PS latex, the flocculation was improved once again.

Accordingly to the theory of flocculation kinetics,<sup>38,39,40</sup> protruding part of the adsorbed polymer on the colloidal surface increases the collision frequency. The maximum flocculation rate is related to the size of the colloidal particles,  $k_f \propto (r_i + r_j)^3$ , where  $r_i$  and  $r_j$  were the radius of size of colloidal particle and the size of the colloidal particles with the adsorbed tether respectively. The maximum flocculation rate can be estimated from the slope of  $\ln(N_t/N_0)$  versus time, where  $N_t$  is the number concentration of primary particle.<sup>39</sup> Rough calculation showed that the maximum flocculation rate at 0.0032M was about 8 times faster than the flocculation rate at “Salt-out” ionic strength. This result supported the conclusion in literature.<sup>19, 39,</sup>

40

Most commercially important cofactors usually undergo coacervation when forming complexes with PEO, while both PKS and PS-co-SSS form water-soluble

complexes with PEO in the absence of  $\text{Ca}^{2+}$ . The interactions between PKS/PEO or PS-co-SSS/PEO were weak compared with the interactions between most commercial cofactors and PEO. This weak interaction resulted in an interesting sensitivity of flocs to hydrodynamic forces. Flocs formed from DS-PCC particles can be disrupted by the hydrodynamic force in flocculation experiment.

The relationship between flocs strength and laboratory flocculation has been reported for bare PCC system: good flocculation gives strong flocs.<sup>16,21</sup> For DS-PCC, our experimental results showed that high maximum flocculation does not necessarily result in strong flocs (Figure 1 and 2). During the initial stages of shear-induced flocculation, particle growth is dominant and the average particle (flocs) size increases rapidly by shear-induced flocculation. As the flocs grow and become comparable to the size of fluid eddies, the significance of fragmentation (breakage) increases.<sup>17</sup> Thus the rate of the change of primary particle  $N_i$  concentration by coagulation and fragmentation is given by:<sup>17,18</sup>

$$dN_i / dt = -\text{Rate of flocculation} + \text{Rate of floc breakage} \quad (2)$$

Photometric dispersion analysis (PDA) mainly monitors the relative turbidity for primary particles. Thus under this experimental condition, mainly the breakage of flocs through erosion can contribute the change in relative turbidity. Thus, the breakage of flocs of size of  $i$  produces  $i$  primary particle  $N_i$ .

$$\text{Rate of floc breakage} = k_d \sum_{i=2}^{\max} iN_i \quad (3)$$

Where  $k_d$  is defined as the apparent flocs breakage rate.  $N_i$  is the number concentration of flocs of size  $i$ . The index "max" represents the largest particle size that forms at time  $t$ .

Smellie and La Mer proposed that the probability of building flocs is proportional to the product of the particle collision frequency and the fraction of the collisions which produce bridging ( $E$ ).<sup>41</sup>

$$\text{Rate of flocculation} = \frac{1}{2} E \sum_{i=1}^{\text{max}-1} k_{i1} N_i N_1 \quad (4)$$

Where  $k_{i1}$  is the collision frequency between particle  $N_i$  and primary particle  $N_1$ .

Chen et al. recently proposed that for PEO bridging flocculation  $E$  is proportional to the fractional surface coverage of one particle by adsorbed active polymers.<sup>42</sup> Due to fast collapse of PEO/PKS complexes in the presence of  $\text{Ca}^{2+}$  (Figure 10), it is reasonable to assume the concentration of active tether close to zero after maximum flocculation. Therefore,

$$dN_1 / dt = -k_d \sum_{i=2}^{\text{max}} iN_i \quad (5)$$

The conservation of the number of particles at time  $t$  requires

$$N_o = N_1 + \sum_2^{\text{max}} iN_i \quad (6)$$



Where  $N_0$  is the initial number concentration of primary particles.

$$dN_1 / dt = k_d \sum_{i=2}^{\max} iN_i = k_d(N_0 - N_1) \quad (7)$$

During the PDA flocculation experiments, the extent to which particle suspension was flocculated was monitored by measuring suspension relative turbidity ( $\tau$ ).

$$\tau = \frac{N_1}{N_0} \quad (8)$$

The solution of Eqn (7) is

$$\ln(1 - \tau) = -k_d t + C \quad (9)$$

The apparent rate of the floc breakage,  $k_d$ , can be obtained by plotting  $\ln(1 - \tau)$  versus time  $t$ . Herein, time  $t$  at zero second is defined as the moment at maximum flocculation. The plots are shown in Figure 11. The straight line indicates that the proposed model for DS-PCC floc breakage is reasonable. Table 3 summarizes the results for  $k_d$  for PKS with different phenolic content. The high maximum flocculation resulted in a high flocs breakage rate.

Flocculation performance of PEO/PKS depends on the surface properties of target particles (Table 5). The first factor is the sign of charge. The strong electrostatic attraction between negatively charged PKS/PEO tether and positively

charged bare PCC surface resulted in a better flocculation on bare PCC than dextran sulfate treated PCC. The second factor is the hydrophobic property of colloidal particle. Grafting PNIPAM onto hydrophobic surface of bare PS latex, results in a complete lost of flocculation performance of PKS/PEO, due to decreased hydrophobic interaction between tether and PS-g-PNIPAM. The third factor is the presence of low concentrations of  $\text{Ca}^{2+}$  (0.7 mM). The addition of  $\text{Ca}^{2+}$  lowers the charge of the complexes and hydrophilic properties of PEO/cofactor complexes at a short time scale (less than 20s) (Figure 10), making them easier to adsorb onto negatively charged particles. PKS/PEO thus more effectively flocculated negatively charged hydrophilic DS-PCC than negatively charged hydrophilic PS-g-PNIPAM. Another evidence is that  $\text{Ca}^{2+}$  greatly enhanced flocculation for PS-co-PNIPAM (Figure 9).

A broader implication of this work is that cofactor structure affected flocculation and any factors resulting in compact complexes deteriorated PEO bridging flocculation. Taking into account that most flocculation of colloidal particles occurs at very high shear force in modern papermaking machine, it would be better to use cofactors with high phenolic contents while maintaining water solubility. This may impact the future development of effective cofactors and optimization of the use of PEO as flocculant in papermaking industry.

### ***Conclusions***

The main conclusions of this chapter are:

1. Phenolic and styrenic groups are the active bonding moieties in the PEO complexes. The higher the phenolic content, the stronger are the flocs formed by the complexes.
2. Complexes formed with phenolic cofactors are more effective flocculants than are styrenic cofactors.
3. Complex formation is driven by both hydrogen bonding and hydrophobic interactions.
4. The optimum phenolic content is a compromise between two effects. High phenolic content gives strong, compact complexes which in turn give shear resistant flocs. On the other hand, high styrene sulfonate contents give larger more highly charged complexes that give greater initial flocculation efficiencies.
5. Calcium ion effects are complicated. On one hand, calcium ions cause complex shrinkage that inhibits flocculation. On the other hand, calcium ions lower the electrostatic repulsion between negatively charged complex and negatively charged particles.
6. Non-phenolic poly (styrene-co-styrene sulfonate) functions as a cofactor for PEO retention aid on PS, PCC and DS-PCC. Thus, the widely proposed hydrogen bonding between phenolic group and ether oxygen in literature is not the sole mechanism for cofactor/PEO bridging flocculation.

Table 1. Characterization of poly(styrene sulfonate) copolymers

Sample	Phenolic/Styrenic Content * (Molar fraction)	Mw (Da)**	Polydispersity**
PKS.34	0.34	141,000±8000	1.4±0.1
PKS.48	0.48	158,000±5000	1.6±0.1
PKS.67	0.67	211,000±7000	1.5±0.1
PKS.74	0.74	41,000±1000	1.6±0.1
PKS.82	0.82	99,237±1780	1.9±0.1
PS-co-SSS	0.71	127,000±3000	2.7±0.1

\*Measured by  $^1\text{H}$  NMR.

\*\*Measured by GPC-LS. The standard deviation was calculated by 3 ~5  
repeat measurements

Table 2. Properties of particles used for flocculation studies

Particle	Diameter (nm)*	Mobility** (m <sup>2</sup> /v•s)	[Ca <sup>2+</sup> ] (mM)****	Surface	Critical Coagulation Concentration (of CaCl <sub>2</sub> )
PS latex	504±3.8	-(4.84±0.10)×10 <sup>-8</sup>	0	Hydrophobic	0.003- 0.005M
PS-g- PNIPAM	479±4.7	-(4.39±0.23)×10 <sup>-8</sup>	0	Sterically stabilized	>0.20M
PCC	1,210±740	1.32×10 <sup>-8</sup> Ref***	0.7	Hydrophobic	
DS-PCC	1,120±660	-(2.17±0.16)×10 <sup>-8</sup>	0.7	Sterically stabilized	

\*Number averaged diameter by a BI-DCP (Disc Centrifuge

Photosedimentometer) Particle Sizer (Brookhaven Instrument Co.)

\*\*Measured with a Coulter Delsa 440SX. Mobility was calculated from the analysis of the parabolic curve.

\*\*\* Gibbs, A.; Pelton R. and Cong, R. *Colloids Surfaces A*. 1999, 159, 31.

\*\*\*\*Cong, R.; Smith-Palmer, T.; Pelton, R. H. *J. Pulp Paper Sci.*, 2001, 27, 379.

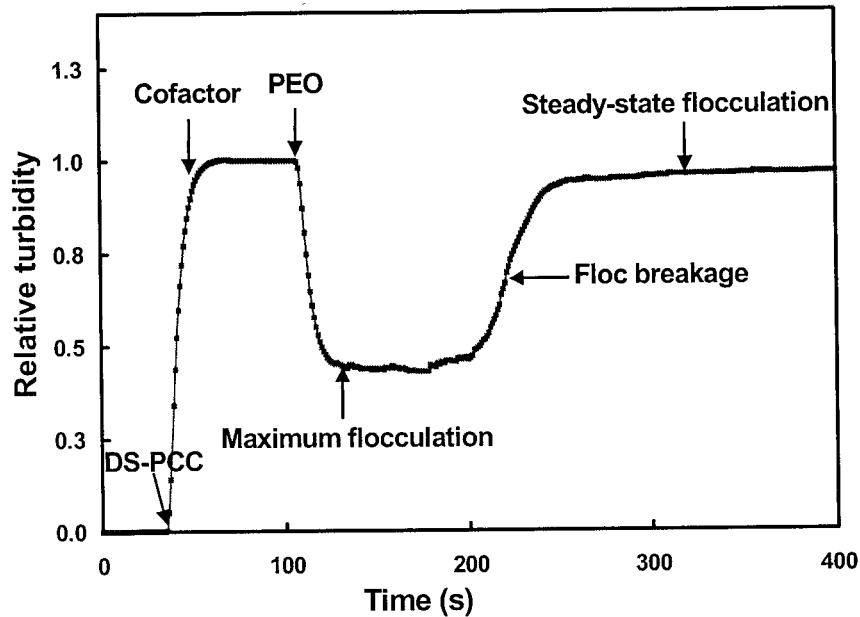


**Figure 1.** The output from a typical flocculation experiment. The instrument as initially filled with water and the labels indicate the times as which the various components were added. The lower the relative turbidity, the higher the extent of DS-PCC agglomeration. The lowest turbidity is defined as maximum flocculation. The relative turbidity increase at long mixing times to a steady state value indicating that the initially formed flocs partially redispersed with continual mixing. Flocculant: PKS.34/PEO.

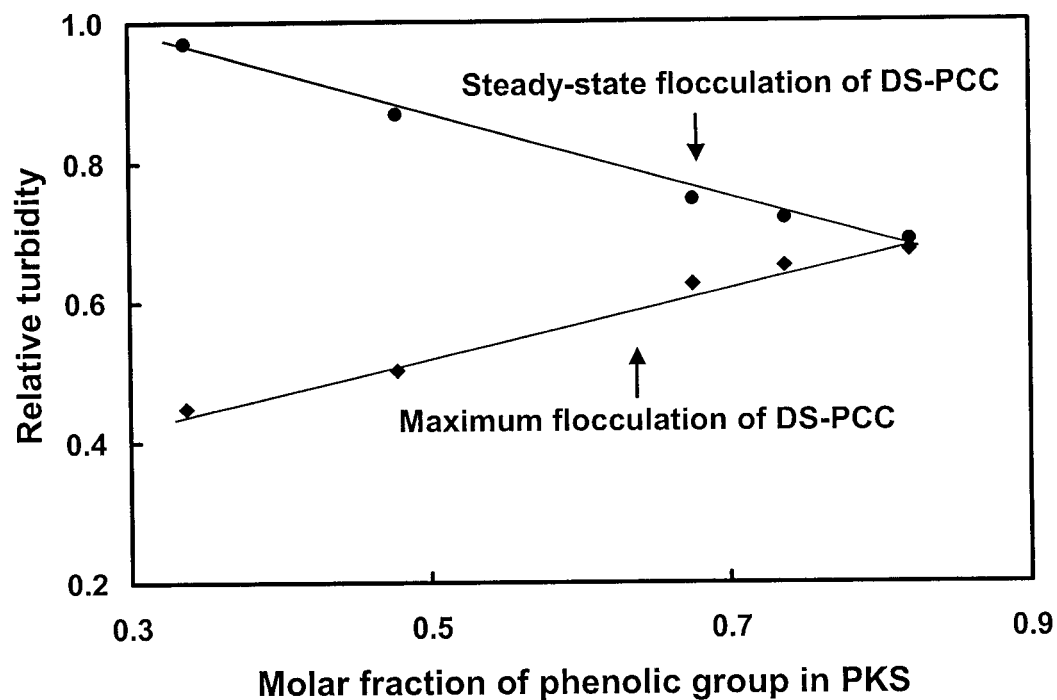


Figure 2. Initial and steady state relative turbidity values as functions of the phenolic content in PKS. (●) Steady-state flocculation; (◆) Maximum flocculation. Experimental conditions: [DS-PCC]=1000ppm; 400rpm, PKS/PEO (w/w)=2; PEO Mw  $8 \times 10^6$  Da; [PEO]= 2ppm; pH 7.7; room temperature.

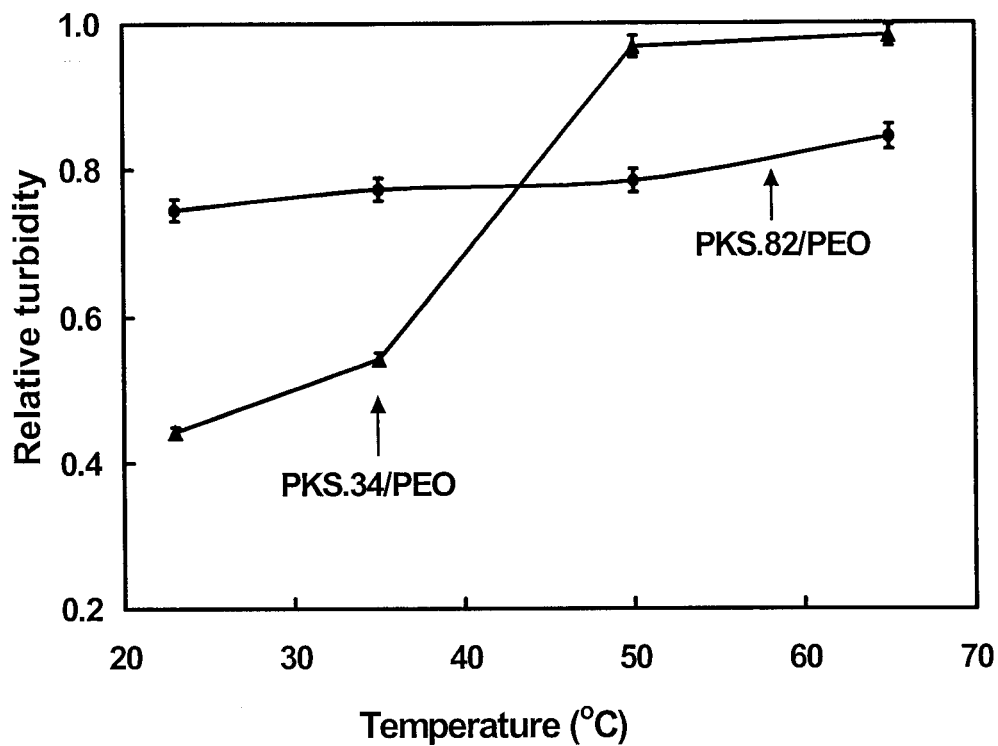


Figure 3. Temperature effect on maximum flocculation of DS-PCC ( $\blacktriangle$ ) PKS.34/PEO; ( $\bullet$ ) PKS.82/PEO. Flocculation conditions: [DS-PCC]=1000ppm; 400rpm; PKS/PEO (w/w)=2; PEO MW  $8 \times 10^6$  Da; [PEO]=2ppm; pH 7.7. The experimental error range is based on duplicate measurements at each temperature.



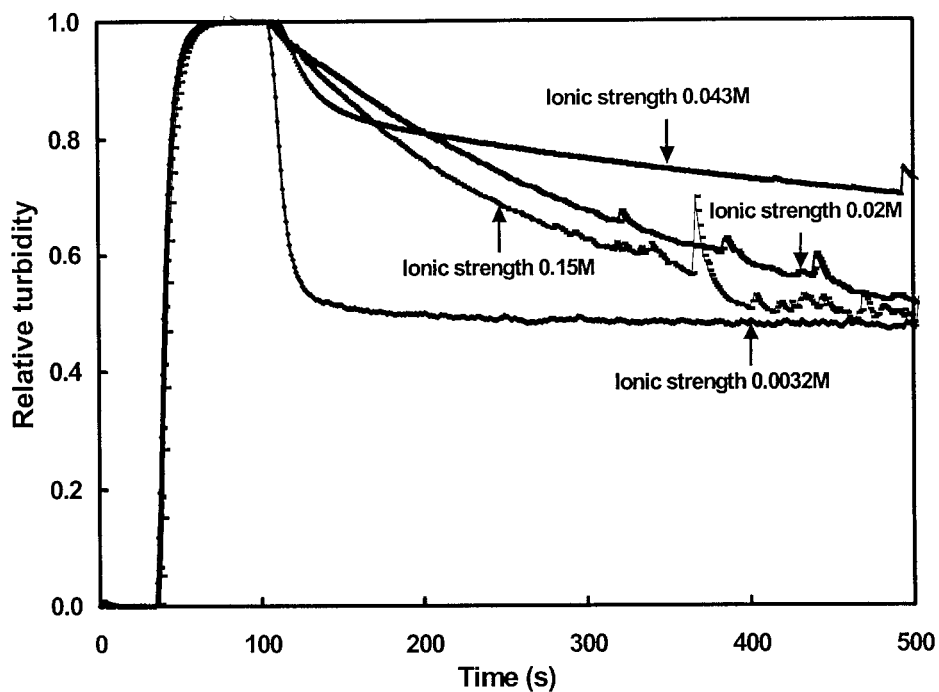
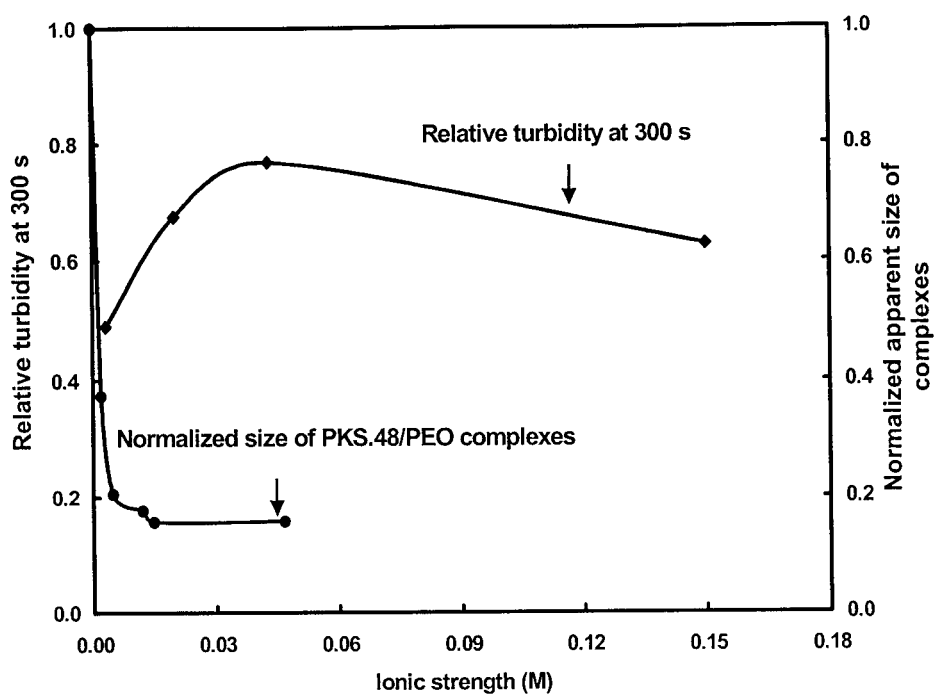
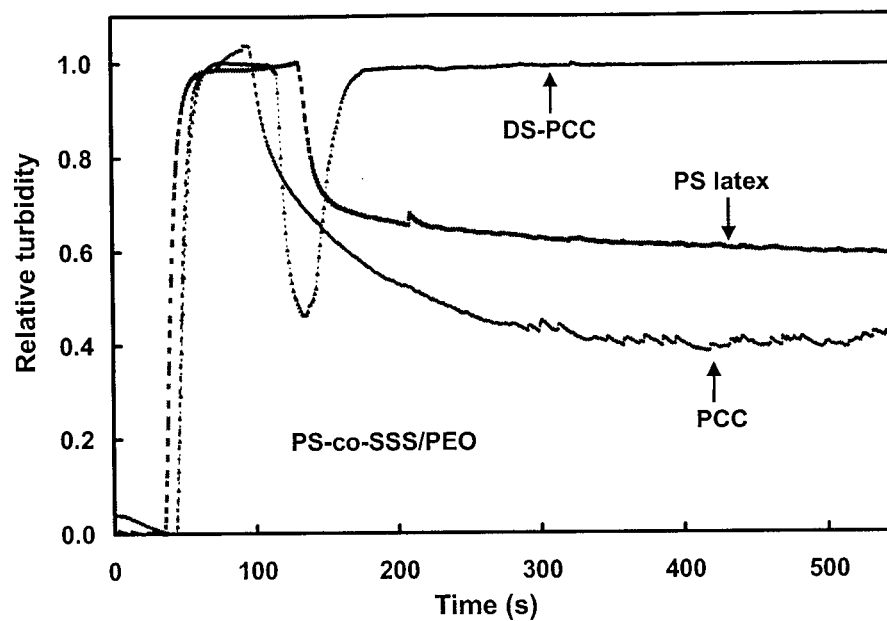


Figure 4. Effect of ionic strength on flocculation of PS latex. Experimental conditions: [PS latex]=150 ppm; PKS.67/PEO (w/w)=2; PEO Mw  $8 \times 10^6$  Da; [PEO]=5 ppm; 400 rpm; room temperature. The experimental error was estimated about 5% based on two repeat measurements.



**Figure 5. Relative turbidity at 300 s and apparent hydrodynamic radius versus ionic strength. (♦) Relative turbidity at 300 s; (●) Apparent hydrodynamic radius of PKS.48/PEO( $M_w 1 \times 10^6$  Da) complexes with respect the radius of complexes at zero ionic strength. Flocculation conditions: [PS latex]= 150 ppm; PKS.67/PEO (w/w)=2; PEO  $M_w 8 \times 10^6$  Da; [PEO]=5 ppm; 400 rpm; room temperature.**



**Figure 6.** Flocculation of PS-co-SSS/PEO for polystyrene latex (PS), precipitated calcium carbonate (PCC) and dextran sulfate treated PCC (DS-PCC) at pH 7.5. PEO dosage for PS: 3.5kg/ton of PS solid; PEO dosage for PCC: 2kg/ton of PCC solid. Stirring rate: 400 rpm, 0.001M NaCl solution, PS-co-SSS/PEO (w/w)=2.

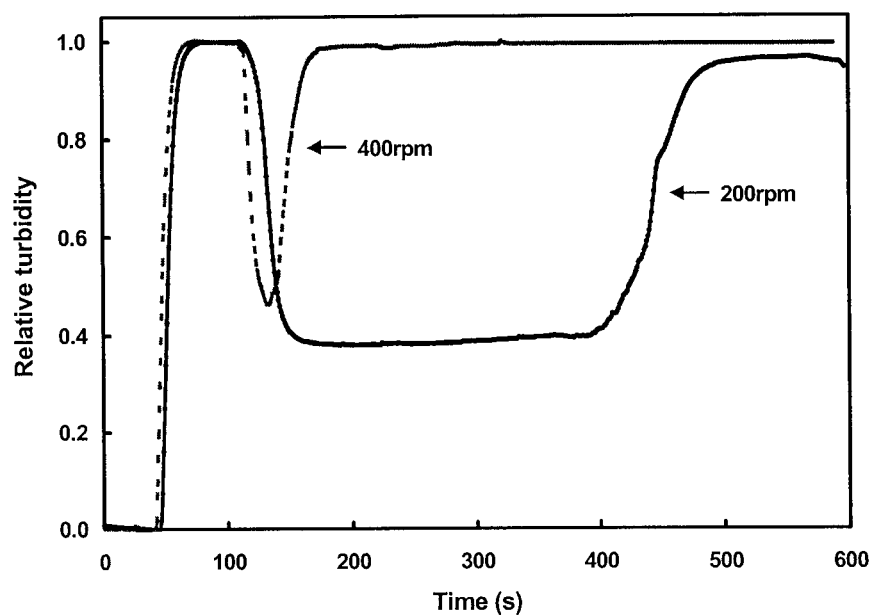


**Figure 7. Flocculation of PS-co-SSS/PEO for dextran sulfate modified precipitated calcium carbonate (DS-PCC) at pH 7. PEO dosage: 2kg/ton of PCC solid; 400 rpm; 0.001M NaCl solution; PS-co-SSS/PEO (w/w)=2; [DS-PCC]= 1000 ppm.**

**Table 3. Comparison of flocculation performance of non-phenolic PS-co-SSS/PEO with phenolic PKS/PEO on various colloidal particles**

Flocculant	Relative turbidity			
	Maximum flocculation for untreated PCC	Maximum flocculation for PS latex	Maximum flocculation for DS-PCC	Steady-state flocculation for DS-PCC
PKS.71/PEO	0.04	0.57	0.65	0.72
PS-co-SSS/PEO	0.40	0.60	0.47	1.0

\* Relative turbidity was used here. Thus, the large relative turbidity indicates the poor flocculation performance

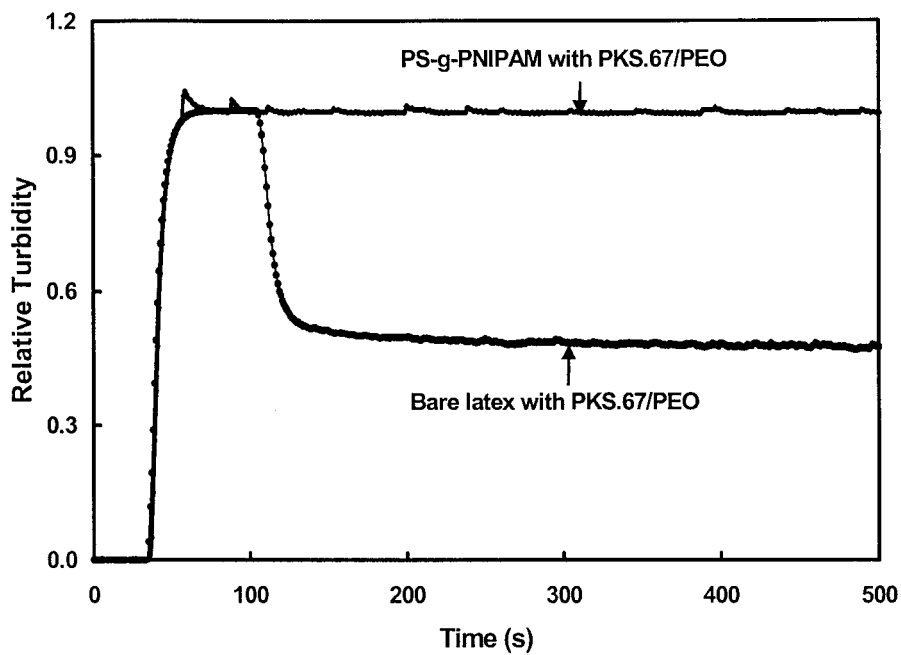


**Figure 8.** PKS.67/PEO flocculation on PS latex and PS-g-PNIPAM latex  
Experimental conditions: PEO Mw  $8 \times 10^6$  Da; [PEO]=5 ppm; [latex]=150 ppm; PKS.67/PEO (w/w)=2; ionic strength 0.0032M; 400 rpm; room temperature.

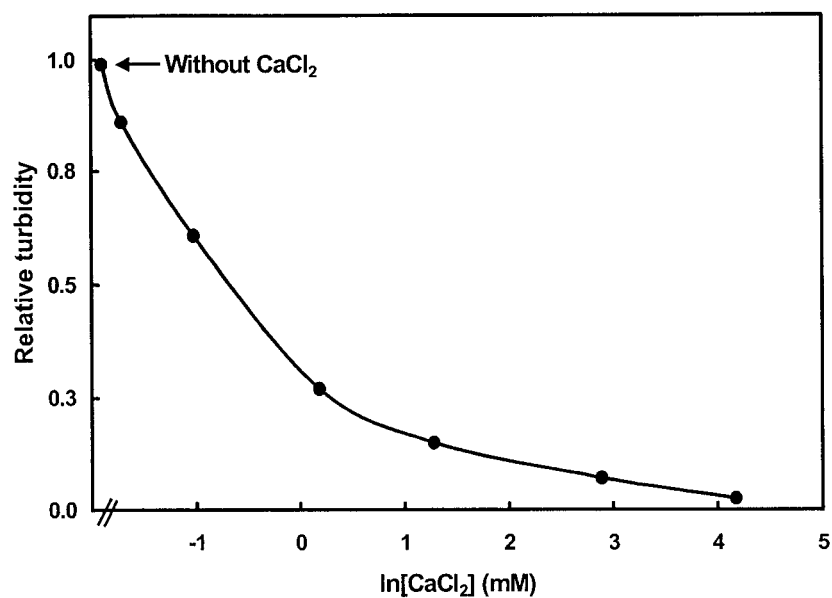


Figure 9. The effect of CaCl<sub>2</sub> on PS-g-PNIPAM flocculation PEO dosage: 5g/kg of solid content; PKS.67/PEO (w/w)=2; PEO Mw  $8 \times 10^6$  Da; [PEO]=5 ppm; temperature 25°C; shear rate  $37.12 \text{ s}^{-1}$

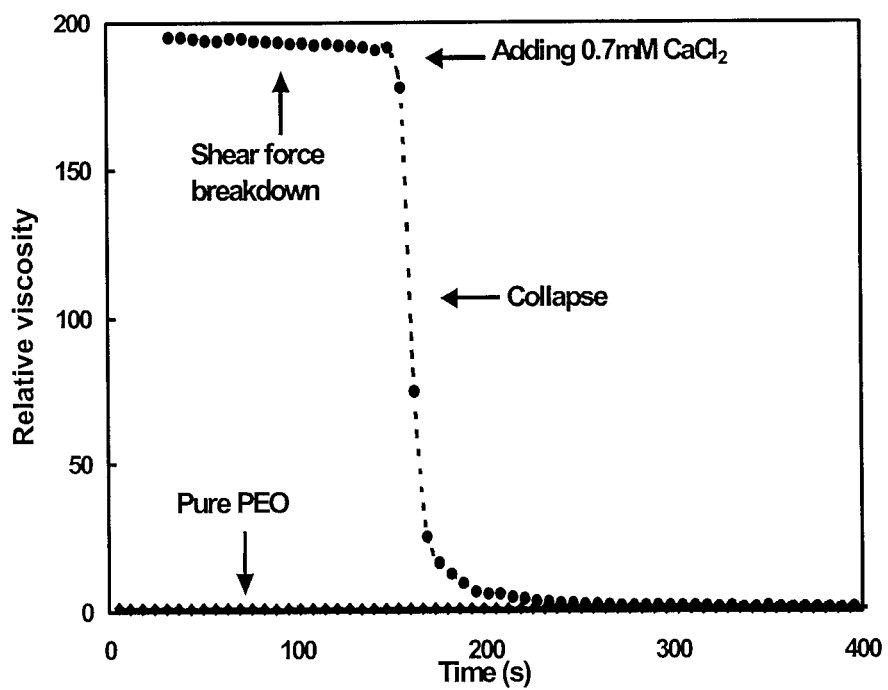


Figure 10. The effect of  $\text{Ca}^{2+}$  on relative viscosity of PKS.67/PEO mixture.  $[\text{CaCl}_2]=0.7 \text{ mM}$ ;  $[\text{PEO}]=23.8 \text{ mg/L}$ ; PKS.67/PEO(w/w)=2; PEO Mw  $8 \times 10^6 \text{ Da}$ ; temperature  $25^\circ\text{C}$ ; shear rate  $37.12 \text{ s}^{-1}$ .



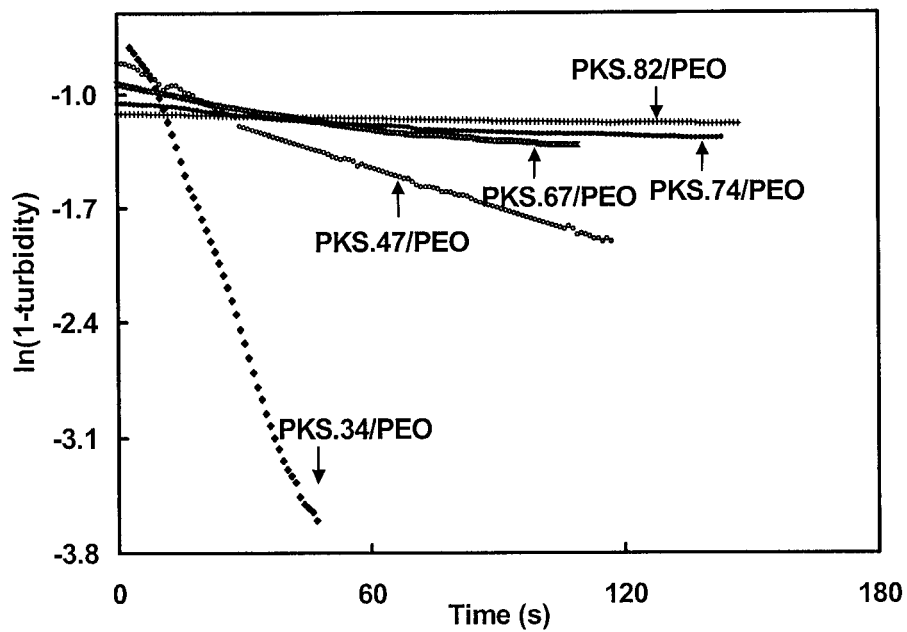


Figure 11. Plot of  $\ln(1-\text{turbidity})$  versus time for PKS/PEO/DS-PCC system. The apparent rate for DS-PCC floc breakage can be calculated from the slope of each line.  $t=0$  represents the moment at the maximum flocculation.

**Table 4. Apparent rate of DS-PCC floc breakage for various PKS/PEO flocculant**

Flocculant	$k_d$ (s <sup>-1</sup> ) Apparent rate of DS-PCC floc breakage*	Relative turbidity for maximum flocculation
PKS.34/PEO	$(5.62 \pm 0.51) \times 10^{-2}$	0.45
PKS.47/PEO	$7.39 \times 10^{-3}$	0.50
PKS.67/PEO	$(1.62 \pm 0.06) \times 10^{-3}$	0.62
PKS.74/PEO	$(1.57 \pm 0.07) \times 10^{-3}$	0.65
PKS.82/PEO	$(3.85 \pm 0.07) \times 10^{-4}$	0.67

\* Data was based on duplicate measurements.

## References

---

- <sup>1</sup> Pelton, R.H., Allen, L.H., and Nugent, H. M. *Tappi* **1981**, 64, 89.
- <sup>2</sup> Carrard, J. P.; Pummer, H. *US Patent* 4,070,236, **1978**.
- <sup>3</sup> Stockwell, J. O. *WO Patent* 95/21296, **1995**
- <sup>4</sup> Ech, E. *US Patent* 5,472,570, **1995**
- <sup>5</sup> Lindström, T.; Glad-Nordmark, G. *Colloids and Surfaces* **1984**, 8, 337.
- <sup>6</sup> Pelton, R. H.; Allen, L.; Nugent, H *US Patent* 4,313,790, **1980**.
- <sup>7</sup> Pelton, R. H; Xiao, H.; Brook, M. A.; Hamielec, A. *Langmuir* **1996**, 12, 5756.
- <sup>8</sup> van de Ven, T. G. M.; Alice, B. *J. Pulp Paper Sci.* **1996**, 22, J257.
- <sup>9</sup> Carignan, A.; Garnier, G.; van de Ven , T. G. M. *J. Pulp Paper Sci.* **1998**, 24, 94.
- <sup>10</sup> Xiao, H.; Pelton, R. H.; Hamielec, A. *J. Pulp Paper Sci.* **1996**, 22, J475.
- <sup>11</sup> Cong, R. Ph.D. Dissertation, McMaster University, Chapter 2. Canada, **2002**
- <sup>12</sup> Xiao, H.; Pelton, R. H.; Hamielec, A. *J. Poly. Sci.* **1995**, 33, 2605.
- <sup>13</sup> Stack, K. R.; Dunn, L. A.; Roberts, N. K. *Colloids and Surfaces* **1991**, 61, 205.
- <sup>14</sup> Cong, R.; Bain, A. D.; Pelton, R. H. *J. Poly. Sci. Part B* **2000**, 38, 1276.
- <sup>15</sup> Pelton, R. H. *Colloid-Polymer Interactions: from Fundamentals to Practice*; Wiley: New York, **1999**
- <sup>16</sup> Gibbs, A.; Pelton, R. H. *J. Pulp Paper Sci.*, **1999**, 25, 267.
- <sup>17</sup> Spicer, P. T.; Pratsinis, S. R. *AIChE J.* **1996**, 42, 1612.
- <sup>18</sup> Lu, C. F.; Spielman, L. A. *J. Colloid Interface Sci.*, **1985**, 103, 95.
- <sup>19</sup> Kobayashi, M.; Adachi, Y.; Ooi, S. *Langmuir* **1999**, 15, 4351.
- <sup>20</sup> Yeung, A.; Gibbs, A.; Pelton, R. H. *J. Colloid Interface Sci.*, **1997**, 196, 113.
- <sup>21</sup> Goto, S.; Pelton, R. H. *Tappi J.*, **2000**, 82, 1.
- <sup>22</sup> Gibbs, A.; Yang, Z.; Xiao, H.; Pelton, R. H. *Transactions of 4th Fundamental Resource Conference, PIRA International*, Leatherhead, UK **1997**, 1135
- <sup>23</sup> Goodwin, J. M.; Hearn, J.; Ho, C. C.; Ottewill, R. H. *Br. Polym .J.*, **1973**, 5, 347.

- 
- <sup>24</sup> Pelton, R. H. *J. Polym. Sci. A: Polym. Chem.*, **1988**, *26*, 9
- <sup>25</sup> Pelton, R. H.; Miller, P.; McPhee, W.; Rajaram, S. *Colloids and Surfaces*. **1993**, *80*, 181.
- <sup>26</sup> Cong, R.; Smith-Palmer, T.; Pelton, R. H. *J. Pulp Paper Sci*, **2001**, *27*), 379.
- <sup>27</sup> Gibbs, A.; Pelton, R. H.; Cong, R. *Colloids and Surfaces*.**1999**, *159*, 31.
- <sup>28</sup> Gregory J. *J. Colloid Interface Sci.*, **1985**, *105*, 357.
- <sup>29</sup> Dunham, A. J.; Tubergen, K. R.; Govoni, S. T.; Alfano, J. C. *J. Pulp Paper Sci.*, **2000**, *26*, 95.
- <sup>30</sup> Zhang, X.; Stebbing, D. W.; Saddler, J.N.; Beatson, R. P.; Kruus, K. *J. Wood Chem. Tech.*, **2000**, *20*, 321.
- <sup>31</sup> Spicer, P. T.; Pratsinis, S. R. *AIChE J.* **1996**, *42*, 1612.
- <sup>32</sup> Lu, C. F.; Spielman, L. A. *J. Colloid Interface Sci.* **1985**, *103*, 95.
- <sup>33</sup> Kobayashi, M.; Adachi, Y.; Ooi, S. *Langmuir* **1999**, *15*, 4351.
- <sup>34</sup> Pang, P.; Engiezos, P. *Nordic Pulp Paper Res. J.* **2000**, *15*, 387.
- <sup>35</sup> Bailey, F. E., Jr.; Koleske, J. V. *Poly(ethylene oxide)*; Academic Press : **1976**.
- <sup>36</sup> Xia, H. Ph.D. Dissertation, McMaster University, Canada, **1995**.
- <sup>37</sup> Goto, S. and Pelton, R. H. *Colloids Surf. A* **1999**, *155*, 231.
- <sup>38</sup> Vold, R. D.; Vold, M. J. *Colloid and interface chemistry*; Addison-Wesley Publishing Company. Inc: **1983**.
- <sup>39</sup> Adachi, Y.; Wada, T. *J. Colloid Interface Sci.*, **2000**, *229*, 148.
- <sup>40</sup> Wales, W. E. *J. Colloid Interface Sci.* **1968**, *27*, 797.
- <sup>41</sup> Smellie, R. H., Jr.; La Mer, V. K. *J. Colloid Interface Sci.*, **1958**, *23*, 589.
- <sup>42</sup> Lu, C.; Pelton, R. H. *Langmuir*, **2001**, *17*, 7770.

## Chapter VI Concluding Remarks

Canada's largest single export is newsprint. Canadian newsprint manufacturers are confronted with the challenge of manufacturing a better product at lower cost. This thesis deals with one aspect of improving newsprint manufacture – the use of water-soluble polymers to enhance fines retention. High molecular weight PEO is an effective flocculant for newsprint and the efficiency of PEO as flocculant can be dramatically enhanced in the presence of second polymeric component called a cofactor.

It is generally agreed that PEO/cofactor complexes are the key flocculating agents and that PEO binds with cofactors presumably through hydrogen bonding between phenolic OH and ether oxygens of PEO. The real challenge is to obtain the details about the mechanisms of complex formation, the complex structures and the links with flocculation efficiency.

Unfortunately, commercial cofactors are condensation polymers. The complicated structures make them unsuitable for some fundamental studies. Our strategy is to use well-defined PKS as a model cofactor. In this work the complex formation between PEO and PKS both at microscopic and macroscopic scales has been extensively investigated with various 1D and 2D NMR techniques, fluorescence photobleaching recovery (FPR) and viscosity measurement. Based on the knowledge of PEO/PKS complex formation, the links between the complex structures and flocculation are demonstrated with various colloidal targets, such as precipitated

calcium carbonate (PCC), dextran-sulfonate modified PCC (DS-PCC),  
polystyrene latex

The major contributions of this work include:

1. Hydrogen bonding between the phenolic OH and ether oxygens of PEO is important, but is not the sole mechanism. Hydrophobic interactions between the aromatic rings of PKS and the ethylene groups of PEO also contribute to complex formation.
2. Upon complex formation, ethylene groups of PEO locate above or below the aromatic rings in less than 5 Å, at least for the part of the times. The conformation of the phenolic cofactors is more collapsed after complex formation, as evidenced by increased sodium counterion binding.
3. Phenolic groups of PKS are the major interacting sites. They serve as the sites both for hydrophobic interactions and hydrogen bonding.
4. Complex formation is irreversible in the macroscopic sense – that is, the complexes are not destroyed by dilution or temperature change. By contrast, NMR indicates that at a microscopic scale, PEO/cofactor binding is reversible. This behaviour is analogous to that of high molecular weight polymers adsorbed on a solid – the adsorption of individual segments is usually reversible whereas desorption does not occur with dilution.

5. The complex formation between phenolic group-free poly(styrene-co-styrene sulfonate) with PEO indicates that the hydrogen bonding is not required for the complex formation.
6. PKS acts as a crosslinker. PEO/PKS complexes range from single PEO coils with bound cofactor molecules, to large complex species containing many PEO chains.
7. The sizes of the complexes depend on the molecular weight of PEO, the phenolic content, temperature and ionic strength. Increase in temperature, phenolic content and ionic strength result in compact complexes.
8. Flocculation efficiency is directly linked to the sizes of the complexes. The larger the complexes, the better the flocculation. Factors such as increasing temperature or ionic strength, which give smaller complexes, also give poorer flocculation.
9. Cofactors performance is sensitive to the balance of hydrophobic phenolic groups and hydrophilic styrene sulfonates.
10. Both phenyl and phenol groups are effective hydrophobic component in the cofactor. The hydrogen bonding potential of phenolic cofactors offer some advantages relative to phenyl groups.

11. A crucial step in the flocculation is the adsorption of PEO/cofactor complex onto the target colloids. Thus, flocculation is sensitive to the target colloid surface chemistry.
12. The flocculation of highly negatively charged, dextran sulfate coated, DS-PCC and poly (N-isopropylacrylamide) grafted hydrophilic PS latex seems to be stimulated by the presence of soluble  $\text{Ca}^{2+}$  which makes the complex less soluble and more likely to adsorb.
13. A newly developed model colloid, DS-PCC, shares the similar surface properties as the fillers in real papermaking furnishes. With this new model colloid, it is possible to mimic the effect of dissolved colloidal substances on flocculation in real papermaking process.